Thermoresponsive Microgels as Functional Draw Agents for Forward Osmosis Desalination

by

Yusak Hartanto

Bachelor of Engineering (Hons.)

Thesis Advisors:

A/Prof. Sheng Dai & A/Prof. Bo Jin

A thesis submitted for the degree of Doctor of Philosophy

School of Chemical Engineering

Faculty of Engineering, Computer and Mathematical Sciences

The University of Adelaide

January 2016

“If I have seen further, it is by standing upon the shoulders of giants”

Isaac Newton

Table of Contents

List of Figures

List of Tables

To my family,

Tan Ka Hing, Tjiong Lisa Mariana & Tan Andreas Arifin

Abstract

Forward osmosis (FO) process has recently been viewed as a low energy membrane separation technology for desalination process due to the absence of high hydraulic pressure. Typical FO desalination is a two-step process: water separation and water recovery, where the water recovery stage currently consumes more energy than the reverse osmosis (RO) process. There has been surge of interest to lower the energy requirement during water recovery process by finding suitable draw materials. One of the potential draw agents proposed for FO desalination is the thermoresponsive polymer hydrogel, which is able to absorb and release water reversibly by a slight change in the operational temperature. Unfortunately, the performance of these hydrogels as FO draw agents was very poor compared to other types of draw agents such as thermolytic solutes and linear polymers. As a result, further work in developing thermoresponsive polymer hydrogels as practical FO draw agent is necessary.

In this thesis, thermoresponsive copolymer microgels were proposed and applied as FO draw agent for the first time. A series of copolymer microgels of N-isopropylacrylamide and acrylic acid was synthesized and evaluated as FO draw agent. The microgels show significantly improved performance than the previously synthesized bulk hydrogels due to their large surface areas. The microgels could generate high water flux up to 23.8 LMH and water recovery up to 55% depending on the concentration of acrylic acid in the microgels. The subsequent study investigated the effect of different acidic comonomers in the copolymer microgels on the FO water flux and water recovery performance. The results show that microgel

with itaconic acid had the best overall performance among other acidic microgels due to the strong ionization of this comonomer as indicated by its pK_a. The water flux and water recovery for this microgel are 44.8 LMH and 47.2 %, respectively. The apparent water flux of this microgel is 3.1 LMH. Thermoresponsive cationic copolymer microgels with different chemical structures of cationic comonomers were then synthesized and applied as FO draw agent to overcome long equilibrium swelling times of the acidic copolymer microgels. It was shown that microgel with *2*-(diethylamino) ethyl methacrylate as a comonomer had the best performance among other cationic copolymer microgels. Furthermore, the shortest equilibrium swelling time, 30 minutes, among other microgels was achieved when this microgel was applied as FO draw agent. The water flux and water recovery for this microgel are 45.6 LMH and 44.8 %, respectively. The apparent water flux of this microgel is 5.5 LMH which is higher than the previously synthesized acidic microgels. In this study, Hansen solubility parameter was also proposed as a tool to predict the performance of the microgels as FO draw agents. The solubility parameters of the comonomers and the dissociation constants of the comonomers correlated well with the experimental results. Finally, different non-ionic copolymer microgels were synthesized and applied as FO draw agent. The microgel with acrylamide as a comonomer shows enhanced water recovery performance while maintaining relatively high water flux when used as FO draw agent. The water flux and water recovery for this microgel are 24.7 LMH and 78.7 %, respectively. The apparent water flux of this microgel is 6.1 LMH. This work will pave the way to design functional polymer materials as draw agent for FO desalination application.

Declaration

I certify that this work contains no material which has been accepted for the award of any other degree or diploma in my name, in any university or other tertiary institution and, to the best of my knowledge and belief, contains no material previously published or written by another person, except where due reference has been made in the text. In addition, I certify that no part of this work will, in the future, be used in a submission in my name, for any other degree or diploma in any university or other tertiary institution without the prior approval of the University of Adelaide and where applicable, any partner institution responsible for the joint-award of this degree.

I give consent to this copy of my thesis when deposited in the University Library, being made available for loan and photocopying, subject to the provisions of the Copyright Act 1968.

The author acknowledges that copyright of published works contained within this thesis resides with the copyright holder(s) of those works.

I also give permission for the digital version of my thesis to be made available on the web, via the University's digital research repository, the Library Search and also through web search engines, unless permission has been granted by the University to restrict access for a period of time.

Name : Yusak Hartanto

Signature : _____ Date : 27/01/2016

Acknowledgement

First, I would like to express my deep gratitude to my advisor, Associate Professor Sheng Dai, for his continuous guidance and enthusiasm on this project during my candidature. I have gone from ‘zero to hero’ during the past three years when I compare myself to the beginning of this journey. I do not regret at all pursuing PhD degree in this area under your guidance. In fact, I feel that my passion in polymer research is growing day by day. There is a lot of interesting thing I found and learned during these past years that would be useful for my future. Furthermore, I would also like to thank to my co-advisor, Associate Professor Bo Jin, for his invaluable support, both academically and mentally, throughout my journey here in School of Chemical Engineering, The University of Adelaide.

I would also like to extend my gratitude to all group members, Dr. Hu Zhang, Associate Professor Jingxiu Bi, Dr. Amir Mellati, Dr. Bingyang Shi, Dr. Konggang Qu, Xiaolin Cui, Dr. Masoumeh Zargar, Mailin Misson, Aabhash Shrestha, Umar Azhar, Qi Bi, Huzairy Hassan, Cornelius Ngau, Seonho Yun, Hesamoddin Rabiee, Wenwen Liu, Jiabin Zhang, Bingyang Zhang and Wanxia Zhao, for their support and friendship during my study at The University of Adelaide.

I am also grateful for my family, mom, dad, my brother and my extended family for their sacrifice, support and encouragement in the past three years. This thesis would not be possible without their love and support

Lastly, I would like to thank The University of Adelaide for providing me an opportunity and scholarship to study Doctor of Philosophy degree. Also, I would like to acknowledge Australian Research Council for supporting this research project.

Chapter 1. Introduction

1.1 Background

Membrane-based desalination process offers lower energy consumption than conventional thermal desalination process due to the absence of water evaporation which consumes considerable amount of energy. The reverse osmosis (RO) membrane separation process currently accounts for more than 50 % of installed desalination plants around the world [1]. However, current RO desalination plants which operate at 50 % water recovery have higher average energy consumption than its theoretical prediction [2]. In addition, severe membrane fouling is one of the major disadvantages of this process due to the application of high pressure to overcome the osmotic pressure of seawater [3].

Recently, forward osmosis (FO) process has gained a lot of attention from researchers and is viewed as a low energy membrane separation option due to the absence of highly applied pressure in the operation process [4-8]. The absence of highly applied pressure also makes the fouling propensity in FO process less severe than the RO process [9]. The real application of FO for desalination, however, does not necessarily mean lower energy consumption than RO process due to the thermodynamics involved [2, 10-13]. As a result, FO as desalination process is only viable if the energy used during water recovery process comes from low-grade energy such as waste heat. This inspires the use of thermolytic solutes as draw agents for FO desalination where the diluted thermolytic solution can be distilled at mild temperature to recover water [14, 15], and waste heat can be used in the distillation process to reduce the absolute energy cost of this process [16]. However, there are

some problems associated with the use of these thermolytic solutes such as high reverse solute flux [17], incomplete separation of these solutes from water product [18] and their corrosive properties [19].

Various synthetic materials have been recently developed and proposed as draw agents for FO desalination process to overcome the inherent drawbacks of thermolytic solutes [5, 7, 17, 18, 20, 21]. Some of these synthetic materials, especially polymer-based materials, have comparable performance to the thermolytic solutes and thus have promising application as draw agent materials. However, several drawbacks applying polymers as draw agents such as high viscosity [22] and reverse solute flux [23] still hinder the application of these polymers as practical FO draw agents. Recently, thermoresponsive hydrogels have been proposed as the semi-solid draw agents [24] because these hydrogels could generate high osmotic pressure [25]. Unfortunately, the current performance of these hydrogels is still poor compared to thermolytic solutes, though different strategies have been applied to improve their performance [26-29]. As a result, further development of high performance thermoresponsive hydrogels as FO draw agent is necessary. In this thesis, we propose thermoresponsive microgels, a sub-micrometer hydrogel which has large surface areas, to improve the performance of hydrogel-driven FO desalination process. We hypothesize that the large surface area of the microgel might significantly improve its performance as the FO draw agent. A series of experimental design focusing on material optimization has been designed and presented in this thesis to confirm our hypothesis.

1.2 Objectives and scopes

This thesis aims to achieve the following objectives:

1. To improve FO water flux by using thermoresponsive copolymer microgels synthesized using surfactant-free emulsion polymerization process.
2. To further improve the FO performance of weak acidic-based thermoresponsive copolymer microgels. The effect of different acidic comonomers on water flux, water recovery and overall performance on microgel-driven FO desalination was investigated.
3. To further improve the water flux and the equilibrium swelling time of the thermoresponsive microgels. The effect of different cationic comonomers and their chemical structures on water flux, water recovery and overall performance on microgel-driven FO desalination was investigated.
4. To improve the performance of water recovery in microgel-driven FO desalination by using non-ionic copolymer microgels.

This thesis focuses primarily on the design of microgel materials to improve the water flux and water recovery in microgel-driven FO desalination. Thus, the following experimental scopes have also been defined:

1. N-isopropylacrylamide was used for thermoresponsive moiety in microgels throughout this thesis.
2. Feed concentration used in this study was 2000 ppm NaCl as a model for saline solution.

3. Membrane orientation used in this study was active layer facing draw solute (AL-DS) or PRO mode to compare the performance of our materials with the published results.
4. The FO water evaluation study was conducted in batch mode using a simple homemade FO cell.
5. The water recovery study was conducted using centrifugation process for laboratory evaluation purpose.
6. The microgel loading was fixed to 100 mg dried microgel throughout the study.

1.3 Thesis outline

This thesis is prepared by paper-based format. The following provides a short summary of of the thesis:

Chapter 1 (Introduction) introduces forward osmosis desalination concept, the current research gaps in the development of thermoresponsive hydrogels as draw agent for FO desalination process, the objectives and outlines of the thesis.

Chapter 2 presents a literature review on the recent development of draw agent materials for FO desalination. The challenges associated in applying thermoresponsive hydrogels as draw agents for FO desalination are also analyzed and discussed.

In Chapter 3, a series of thermoresponsive microgels of N-isopropylacrylamide and different acrylic acid concentration synthesized using surfactant-free emulsion polymerization were evaluated as draw agents for FO desalination. The microgels

were characterized using dynamic light scattering to measure the change in hydrodynamic diameter against temperature. The exact amount of acrylic acid in the microgels was determined using pH and conductivity titration. The FO performance was evaluated in terms of initial water flux, water recovery and overall water production rate. In addition, a new approach to evaluate water flux was presented to minimize the error associated with gravimetric approach.

In Chapter 4, a series of acidic copolymer microgels with different acidic comonomers were synthesized using surfactant-free emulsion polymerization and evaluated as FO draw agents. The microgels were characterized using dynamic light scattering, Fourier transform infrared spectroscopy and pH and conductivity titration. The effect of different strength of acidic comonomers on water flux, water recovery, equilibrium swelling time and apparent water flux was investigated. Theoretical energy consumption for water recovery process was also presented in this chapter.

In Chapter 5, thermoresponsive cationic copolymer microgels having tertiary amines group from different cationic comonomers were synthesized and evaluated as FO draw agents. The microgels were characterized using dynamic light scattering and the amount of tertiary amines group was determined using pH and conductivity titration. The effect of different strength and chemical structures of cationic comonomers and their solvation behavior on water flux, water recovery, equilibrium swelling time and apparent water flux were investigated. The analysis of Hansen solubility parameters for each monomer was introduced in this chapter to further our understanding on the molecular interaction between water molecules and monomers.

In Chapter 6, we choose three non-ionic comonomers with different degree of solvation behavior based on their Hansen solubility parameters and copolymerized

them with N-isopropylacrylamide. The microgels were characterized using dynamic light scattering and Fourier transform infrared spectroscopy. The FO performance was evaluated in terms of water flux, water recovery, equilibrium swelling time and apparent water flux. The effect of acrylamide loading on the copolymer microgels on FO performance was also evaluated.

Chapter 7 is the conclusion of this thesis, where key scientific contributions are summarized and future development of microgel-based draw agents for FO desalination is recommended.

1.4 Key contributions of this thesis

This thesis initiates the development of microgel-based FO draw agents for desalination process and to advance our understanding on designing thermoresponsive microgel to improve its performance as FO draw agent. The research outcomes have direct impact on the development of FO process as an energy-efficient desalination process. The following summarizes specific contributions of this thesis:

1. **The development of thermoresponsive microgels as high performance draw agents for FO desalination process.** This study demonstrates for the first time that significant improvement in water flux in FO process can be achieved by using microgels instead of bulk hydrogels. This is due the large surface areas of the microgels, which enhances the contact between membrane surface and microgel particles.

2. **The development of a new approach to evaluate water flux in microgel-driven FO processes.** This approach demonstrates that monitoring

conductivity of feed solution and using mass balance principle to calculate water flux in microgel-driven FO systems proved to have better accuracy than gravimetric approach.

3. **The effect of different strength of acidic comonomers and its concentration in the microgels on FO performance.** This study compares different strength of acidic comonomers on the FO performance in terms of water flux, water recovery, equilibrium swelling time and apparent water flux. The results show that copolymer microgels with double carboxylic acid comonomers generate more water flux than single carboxylic acid comonomers. This is due to the stronger ionization of the carboxylic acid groups in double carboxylic acid comonomers than single carboxylic acid comonomers as indicated by their acid dissociation constants (pK_a). In addition, the concentration of acidic comonomers plays an important role in water recovery stage. Increasing the concentration of the comonomers reduces the amount of water recovered when the microgel is heated above its volume phase transition temperature.

4. **The effect of positive charge and hydrophilicities of cationic comonomers on FO performance.** This study demonstrates cationic copolymer microgels show improved FO performance in terms of water flux and equilibrium swelling time. The cationic copolymer microgels with aromatic ring-containing comonomers have less water flux than aliphatic comonomers due to the hydrophobicity of the ring structure.

5. **Hansen solubility parameter analysis as a tool for designing thermoresponsive microgels as FO draw agents.** The analysis provides an

insight on the solvation behavior of a monomer by examining the water affinity towards the monomers. This analysis helps to predict the degree of solvation behavior of a monomer or comonomer which would be useful in designing optimized microgel materials for FO draw agents.

6. **The effect of hydrophilicities of non-ionic comonomers on water recovery performance.** The study demonstrates that hydrogen-bonding interaction between hydrophilic non-ionic copolymer microgels leads to better water recovery performance than ionic copolymer microgels. The presence of ionic moieties in the microgels reduces the water recovery performance due to stronger interaction of water molecules with ionic moieties than non-ionic moieties.

1.5 References

1. Shannon, M. A.; Bohn, P. W.; Elimelech, M.; Georgiadis, J. G.; Marinas, B. J.; Mayes, A. M., Science and technology for water purification in the coming decades. *Nature* **2008,** *452*, (7185), 301-310.

2. Semiat, R., Energy Issues in Desalination Processes. *Environmental Science & Technology* **2008,** *42*, (22), 8193-8201.

3. Xie, M.; Lee, J.; Nghiem, L. D.; Elimelech, M., Role of pressure in organic fouling in forward osmosis and reverse osmosis. *Journal of Membrane Science* **2015,** *493*, 748-754.

4. Qin, J. J.; Lay, W. C. L.; Kekre, K. A., Recent developments and future challenges of forward osmosis for desalination: a review. *Desalination and Water Treatment* **2012,** *39*, (1-3), 123-136.

5. Klaysom, C.; Cath, T. Y.; Depuydt, T.; Vankelecom, I. F., Forward and pressure retarded osmosis: potential solutions for global challenges in energy and water supply. *Chem Soc Rev* **2013,** *42*, (16), 6959-89.

6. Chekli, L.; Phuntsho, S.; Kim, J. E.; Kim, J.; Choi, J. Y.; Choi, J.-S.; Kim, S.; Kim, J. H.; Hong, S.; Sohn, J.; Shon, H. K., A comprehensive review of hybrid forward osmosis systems: Performance, applications and future prospects. *Journal of Membrane Science* **2016,** *497*, 430-449.

7. Chung, T. S.; Zhang, S.; Wang, K. Y.; Su, J. C.; Ling, M. M., Forward osmosis processes: Yesterday, today and tomorrow. *Desalination* **2012,** *287*, 78-81.

8. She, Q.; Wang, R.; Fane, A. G.; Tang, C. Y., Membrane fouling in osmotically driven membrane processes: A review. *Journal of Membrane Science* **2016,** *499*, 201-233.

9. Lee, S.; Boo, C.; Elimelech, M.; Hong, S., Comparison of fouling behavior in forward osmosis (FO) and reverse osmosis (RO). *Journal of Membrane Science* **2010,** *365*, (1-2), 34-39.

10. McGovern, R. K.; Lienhard V, J. H., On the potential of forward osmosis to energetically outperform reverse osmosis desalination. *Journal of Membrane Science* **2014,** *469*, 245-250.

11. Shaffer, D. L.; Werber, J. R.; Jaramillo, H.; Lin, S.; Elimelech, M., Forward osmosis: Where are we now? *Desalination* **2015,** *356*, 271-284.

12. Semiat, R.; Sapoznik, J.; Hasson, D., Energy aspects in osmotic processes. *Desalination and Water Treatment* **2010,** *15*, (1-3), 228-235.

13. Shaffer, D. L.; Arias Chavez, L. H.; Ben-Sasson, M.; Romero-Vargas Castrillón, S.; Yip, N. Y.; Elimelech, M., Desalination and Reuse of High-Salinity Shale Gas Produced Water: Drivers, Technologies, and Future Directions. *Environmental Science & Technology* **2013,** *47*, (17), 9569-9583.

14. McCutcheon, J. R.; McGinnis, R. L.; Elimelech, M., A novel ammonia—carbon dioxide forward (direct) osmosis desalination process. *Desalination* **2005,** *174*, (1), 1-11.

15. Boo, C.; Khalil, Y. F.; Elimelech, M., Performance evaluation of trimethylamine–carbon dioxide thermolytic draw solution for engineered osmosis. *Journal of Membrane Science* **2015,** *473*, 302-309.

16. Mazlan, N. M.; Peshev, D.; Livingston, A. G., Energy consumption for desalination — A comparison of forward osmosis with reverse osmosis, and the potential for perfect membranes. *Desalination* **2016,** *377*, 138-151.

17. Ge, Q. C.; Ling, M. M.; Chung, T. S., Draw solutions for forward osmosis processes: Developments, challenges, and prospects for the future. *Journal of Membrane Science* **2013,** *442*, 225-237.

18. Zhao, S.; Zou, L.; Tang, C. Y.; Mulcahy, D., Recent developments in forward osmosis: Opportunities and challenges. *Journal of Membrane Science* **2012,** *396*, 1-21.

19. Zhong, Y.; Feng, X.; Chen, W.; Wang, X.; Huang, K.-W.; Gnanou, Y.; Lai, Z., Using UCST ionic liquid as a draw solute in forward osmosis to treat high-salinity water. *Environmental Science & Technology* **2015**.

20. Chekli, L.; Phuntsho, S.; Shon, H. K.; Vigneswaran, S.; Kandasamy, J.; Chanan, A., A review of draw solutes in forward osmosis process and their use in modern applications. *Desalination and Water Treatment* **2012,** *43*, (1-3), 167-184.

21. Qasim, M.; Darwish, N. A.; Sarp, S.; Hilal, N., Water desalination by forward (direct) osmosis phenomenon: A comprehensive review. *Desalination* **2015,** *374*, 47-69.

22. Zhao, D.; Chen, S.; Wang, P.; Zhao, Q.; Lu, X., A Dendrimer-Based Forward Osmosis Draw Solute for Seawater Desalination. *Industrial & Engineering Chemistry Research* **2014,** *53*, (42), 16170-16175.

23. Tian, E.; Hu, C.; Qin, Y.; Ren, Y.; Wang, X.; Wang, X.; Xiao, P.; Yang, X., A study of poly (sodium 4-styrenesulfonate) as draw solute in forward osmosis. *Desalination* **2015,** *360*, 130-137.

24. Li, D.; Zhang, X.; Yao, J.; Simon, G. P.; Wang, H., Stimuli-responsive polymer hydrogels as a new class of draw agent for forward osmosis desalination. *Chemical Communications* **2011,** *47*, (6), 1710-1712.

25. Wack, H.; Ulbricht, M., Effect of synthesis composition on the swelling pressure of polymeric hydrogels. *Polymer* **2009,** *50*, (9), 2075-2080.

26. Li, D.; Zhang, X.; Yao, J.; Zeng, Y.; Simon, G. P.; Wang, H., Composite polymer hydrogels as draw agents in forward osmosis and solar dewatering. *Soft Matter* **2011,** *7*, (21), 10048-10056.

27. Cai, Y.; Shen, W.; Loo, S. L.; Krantz, W. B.; Wang, R.; Fane, A. G.; Hu, X., Towards temperature driven forward osmosis desalination using Semi-IPN hydrogels as reversible draw agents. *Water Research* **2013,** *47*, (11), 3773-3781.

28. Razmjou, A.; Barati, M. R.; Simon, G. P.; Suzuki, K.; Wang, H., Fast Deswelling of Nanocomposite Polymer Hydrogels via Magnetic Field-Induced Heating for Emerging FO Desalination. *Environmental Science & Technology* **2013,** *47*, (12), 6297-6305.

29. Razmjou, A.; Liu, Q.; Simon, G. P.; Wang, H., Bifunctional Polymer Hydrogel Layers As Forward Osmosis Draw Agents for Continuous Production of Fresh Water Using Solar Energy. *Environmental Science & Technology* **2013,** *47*, (22), 13160-13166.

Chapter 2. Emerging Draw Solute Materials in Forward Osmosis Desalination: Recent Development and Challenges

Yusak Hartanto, Xiaolin Cui, Bo Jin, Sheng Dai

School of Chemical Engineering, The University of Adelaide, SA 5005, Australia

Graphical Abstract:

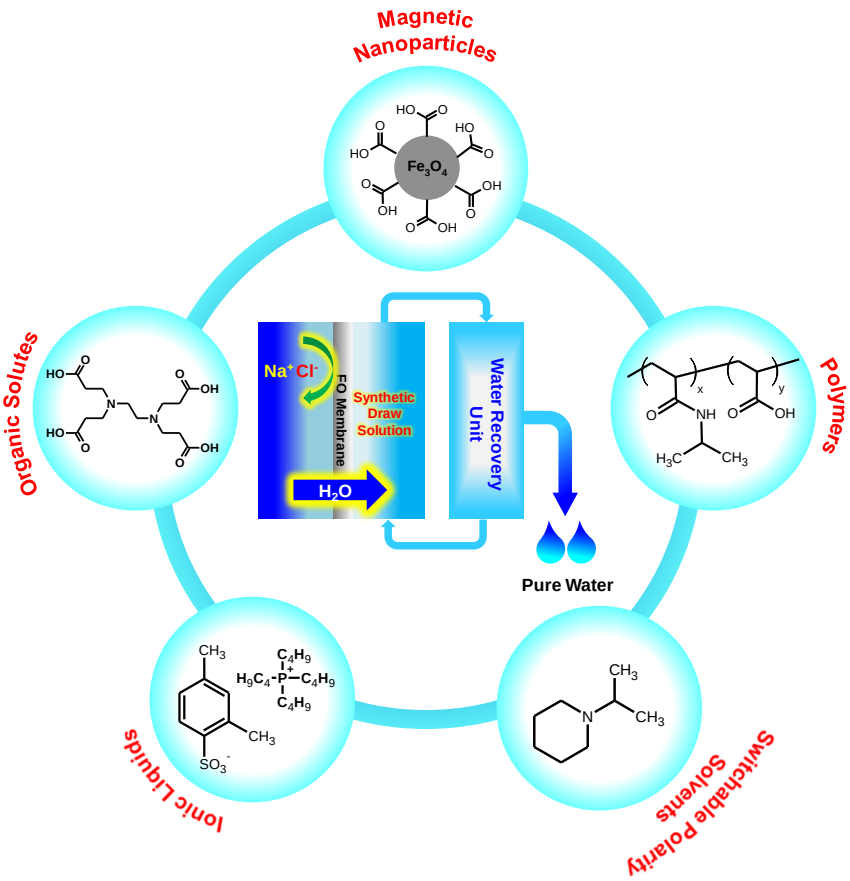

Statement of Authorship

Title of Paper	Emerging Draw Solute Materials in Forward Osmosis Desalination: Recent Development and Challenges
Publication Status	☐ Published ☐ Accepted for Publication ☐ Submitted for Publication ☑ Unpublished and Unsubmitted work written in manuscript style
Publication Details	In preparation for Advances in Colloid and Interface Science

Principal Author

Name of Principal Author (Candidate)	Yusak Hartanto		
Contribution to the Paper	Reviewed the research papers, structured and wrote the manuscript.		
Overall percentage (%)	70 %		
Certification:	This paper reports on original research I conducted during the period of my Higher Degree by Research candidature and is not subject to any obligations or contractual agreements with a third party that would constrain its inclusion in this thesis. I am the primary author of this paper.		
Signature		Date	

Co-Author Contributions

By signing the Statement of Authorship, each author certifies that:

i. the candidate's stated contribution to the publication is accurate (as detailed above);

ii. permission is granted for the candidate in include the publication in the thesis; and

iii. the sum of all co-author contributions is equal to 100% less the candidate's stated contribution.

Name of Co-Author	Xiaolin Cui		
Contribution to the Paper	Proof read the manuscript and giving feedback		
Signature		Date	

Name of Co-Author	Bo Jin		
Contribution to the Paper	Proof read the manuscript and giving feedback		
Signature		Date	

Name of Co-Author	Sheng Dai		
Contribution to the Paper	Proof read the manuscript and giving feedback		
Signature		Date	27/01/2016

2.1 Abstract

Forward osmosis (FO) desalination is an emerging membrane-based desalination process that has the potential to be a low energy desalination technology and to treat high salinity feed solution. The driving force of this separation process is the osmotic gradient between the feed and draw solution. As a result, exploring suitable draw solute materials is important besides designing suitable membrane for this process. During the past years, there has been significant development on various classes of draw solute materials to improve FO process efficiency and to lower the energy cost of the process. Here, we systematically review the performance of different draw solute materials for FO desalination – synthetic organic solutes, polymers, switchable polarity solvents and ionic liquids – and discuss the associated challenges for practical FO desalination. We also highlight the thermodynamics involved in dissolution of small molecules and polymers is different and thus polymer-based draw solute materials have potential to lower the energy consumption during water recovery stage as observed in some recent experimental work.

Keywords: forward osmosis; draw solute; polymers; ionic liquids; organic; switchable polarity solvents

2.2 Introduction

Forward osmosis (FO) process is an osmotic-driven membrane separation process that has a wide range of applications such as desalination [1-4], wastewater treatment [5-7], food processing [8, 9], protein and DNA enrichment [10-12] and energy generation [13, 14]. The absence of high applied pressure during the process [15], low membrane fouling propensity [16, 17] and high rejection of wide range of contaminants [6] make this process more interesting than reverse osmosis (RO) process. Different from RO process, desalination using FO process includes both water absorption and water recovery. In the literature, the application of FO in desalination process is particularly being heavily researched due to its potential to reduce the overall energy consumption to produce potable water [18].

There are two main aspects in the FO desalination process, the FO membranes and the draw solute materials. Design on suitable FO membranes is different from RO membranes in terms of the support layer structure due to the presence of internal concentration polarization (ICP) [19] and reverse solute flux [20]. As a result, different strategies to modify the FO membrane support layer have been used to mitigate the aforementioned issues [21-29]. The draw solution aspect is also an important factor in determining the FO performance although there has been a debate whether optimized draw solute materials would lower the energy consumption in water recovery stage [30-32].

In the past years, various draw solute materials such as synthetic organic solutes [33-35], polyelectrolytes [36, 37], magnetic nanoparticles [38], polymer hydrogels [39, 40], switchable polarity solvents [41] and ionic liquids [42-44] have been developed to overcome the inherent drawbacks of inorganic or thermolytic solutes

[45-49]. These materials are also able to generate relatively high osmotic pressure compared to traditional draw solute materials [50]. As a result, there is possibility to tune the generated osmotic pressure through materials engineering which would extend the application of FO desalination process to treat high salinity feed water such as oil and gas wastewater [51]. In addition, near complete separation can be achieved due to the large molecular size of these materials. Therefore, the advancement of novel draw solute materials is an important field of research to make FO desalination process competitive with other desalination technology.

In this paper, we systematically review various draw solute materials – synthetic organic solutes, inorganic nanoparticles, polymer-based materials, switchable polarity solvents and ionic liquids – on the FO desalination process. The challenges in applying these materials as draw solutes are analyzed in detailed. Finally, we discuss the future research direction in the development of future draw solute materials.

2.3 Synthetic organic solutes

Thermolytic solutes such as ammonium bicarbonate [1] and trimethylamine – carbon dioxide [49] have been proposed as FO draw solute materials due to their ease of separation at moderate temperature. The heating energy can be provided by low grade heat to reduce the overall energy cost of the process. However, there are several drawbacks on using thermolytic solutes such as high reverse solute flux [47], corrosive [43], membrane degradation [34], toxicity [52] and incomplete separation of the draw solutes [45] which hinder the practical application of these materials as FO draw solutes. Synthetic organic solutes having thermoresponsive properties

and/or abundant ionic moieties were developed to overcome the issues of using thermolytic solutes as draw materials. The large molecular size of these synthetic materials also minimizes reverse solute flux which is the major problem in using thermolytic solutes or inorganic salts. These organic solutes can be divided into three broad categories – thermoresponsive solutes, ionic solutes and surfactant materials. Table 2.1 summarizes the recent development in synthetic organic solutes as FO draw solute materials.

Table 2.1 FO performance of various synthetic organic solutes

Draw Solute (DS)	FO Membrane Type	DS concentration	FO Performance	Water Recovery Process	Ref.
Thermoresponsive solutes					
*n*Bu-TAEA	Cellulose trifluoroacetate	2 M	Water flux: ~ 4.2 LMH	-	[34]
Di(ethylene glycol) *n*-hexyl ether	Commercial CTA membrane	12 M	Water flux: ~ 1.4 LMH	-	[53]
Ionic Solutes					
2-Methylimidazole compounds	Commercial CTA FO membrane	2 M	Water flux: 0.1 – 20 LMH Reverse flux: 5–80 g/m^{2}h	Membrane Distillation	[33]
Hydroacid complexes	Commercial CTA FO membrane	2 M	Water flux: 10 – 30 LMH Reverse flux: 0.09–0.19 g/m^{2}h	Nanofiltration	[35]
Hexavalent phosphazene salts	Commercial CTA FO membrane	0.067 M	Water flux: 6 – 8.5 LMH Reverse flux: 0.09–0.19 g/m^{2}h	-	[54]
Ethylenediamine Tetrapropionic (EDTP)	Commercial CTA FO membrane	0.8 M	Water flux: 22.69 LMH Reverse flux: 0.32	Nanofiltration	[55]

Salt			g/m^2h		
Ethylenediamine Tetraacetic acid (EDTA) complexes	Commercial CTA FO membrane	1 M	Water flux: ~ 7 – 30 LMH Reverse flux: 0.32 g/m^2h	Nanofiltration	[56]
Surfactants					
SDS	Commercial CTA FO membrane	0.5 M	Water flux: ~ 0.8 – 1.3 LMH Reverse flux: 5.25 x 10^{-4} g/m^2h	Ultrafiltration	[57]
TEAB	Commercial CTA FO membrane	0.5 M	Water flux: ~ 4 – 8 LMH Reverse flux: 7.88 x 10^{-5} g/m^2h	Ultrafiltration	[57]
Triton X-100 and EDTA-2Na	Commercial CTA FO membrane	Triton X-100: 0.5 mM EDTA-2Na: 1 M	Water flux: 9.6 LMH Reverse flux: ~ 0.01 g/m^2h	Nanofiltration	[58]

2.3.1 Thermoresponsive solutes

Thermoresponsive solute, *n*-butyryl tris(*2*-aminoethyl) amine (*n*Bu-TAEA), having a lower critical solution temperature (LCST) has been proposed as thermoresponsive draw solute for FO desalination process [34]. *n*Bu-TAEA contains tertiary amines which impart weak basic properties when dissolved to form aqueous solution. This material might offer better membrane stability when used as draw solute than the thermolytic solutes which usually have strong basic characteristic in solution [43]. Although the idea of using thermo-sensitive solute is great to assist in regeneration process, the water flux generated by this compound was still low compared to most inorganic salts [45]. Recently, di(ethylene glycol) *n*-hexyl ether (DEH) was proposed as draw solute materials [53]. This material had relatively low phase separation temperature compared to *n*Bu-TAEA (~30 ^{o}C). Although it can further reduce the

energy consumption during the water recovery stage, its low LCST values indicates that this material is more hydrophobic than *n*Bu-TAEA, and thus drop the water flux.

2.3.2 Ionic solutes

Synthetic ionic solutes are able to generate high water flux when employed as draw solutes due to the multivalent ionic nature of these materials. Most of them have carboxylic acid and tertiary amine functional groups which are hydrophilic and ionizable in aqueous solution. The weak acidic and basic properties of these functional moieties also provide better membrane compatibility than thermolytic solutes which are usually strong acids or strong bases. Due to the large size of these solutes compared to inorganic salts, minimal reverse solute flux can also be achieved [45].

2-Methylimidazole-based compounds having tertiary amine group were previously synthesized and applied as FO draw solutes [33]. The quaternized form of these materials was able to generate very high osmotic pressure, and thus enhancing their water flux performance. However, the rate of reverse solute diffusion of quaternized 2-methylimidazole compounds were higher than their uncharged forms due to the imbalanced charges in the feed and draw solution [59]. On the other hand, anionic solutes having multiple carboxylic groups such as hexavalent phosphazene salts [54], hydroacid complexes [35, 60], carbon quantum dots [61], ethylenediamine tetrapropionic (EDTP) salts [55] and ethylenediamine tetraacetic acid (EDTA) complexes were also evaluated as potential FO draw solute materials. However, concentration polarization might exist if the size of these materials is larger than the pore size of support layer of FO membranes, which might result in the significant decrease in water flux [54]. For example, the water flux generated by hexavalent

phosphazene salts was not as high as other multi-carboxylic salts due to the large molecular size of these materials causing severe concentration polarization. Another drawback of using organic ionic solutes as draw solutes is the separation cost might not be as low as thermoresponsive solutes when pressure-driven membrane process is used since relatively high pressure proportional to the osmotic pressure of draw solution is always needed to perform draw solute recovery process [62]. As a result, these ionic solutes are more suitable to be applied to treat challenging feed water with high salinity where RO process is not capable to operate at this range of hydraulic pressure [4].

2.3.3 Surfactants

Surfactant materials have also been proposed as draw solute materials for forward osmosis desalination due to their ability to form micelle in solution which assists in draw solute separation and minimizing reverse solute flux [57]. Various surfactant materials have been evaluated as draw solutes such as sodium dodecyl sulphate (SDS), *1*-octane sulfonic acid sodium salt (1-OSA), meristyltrimethyl ammonium bromide (MTAB), trimethyloctylammonium bromide (TMOAB), tetraethyl ammonium bromide (TEAB), Triton X-100 and nonylphenol ethoxylate (Tergitol NP9) [57, 58, 63, 64]. In terms of FO performance, cationic surfactants could generate higher water flux than anionic surfactant [57]. However, the osmotic pressures of these materials are relatively low which limit their applications to treat low salinity feed water. Interestingly, combining synthetic ionic solutes or inorganic salts and surfactants has dramatically improved the FO performance, especially the reverse solute flux issue [58, 63]. For example, Triton X-100 was coupled with sodium ethylenediamine tetraacetic acid where the surfactants act as an additional

barrier by interacting with the surface of FO membrane preventing the reverse permeation of the ionic solutes [58].

2.4 Polymer-based draw materials

2.4.1 Polymers

Polymers are another class of material which have been proposed as the draw solutes for FO desalination due to their relatively large molecular size and ease of separation [36]. In addition, some functionality such as thermal, pH , magnetic, gas and electric responsive properties can be introduced to these materials to further assist in water recovery [46].

Currently, there has been a continuous debate whether finding suitable draw solute materials will reduce the energy consumption during water recovery process [30]. This is due to the energy required to bring the entropy of the system to its initial state during draw solute recovery is always higher than the RO process. However, the entropy changes of small molecules such as inorganic salts and macromolecules such as polymers are different thermodynamically. According to Flory – Huggins theory, the change of entropy caused by polymer dissolution is much smaller than that of small molecules due to less configurational possibilities than dissolution of small molecules [65, 66]. This phenomenon is illustrated using two-dimensional lattice model shown in Figure 2.1. As a result, a diluted polymer solution can be reconcentrated with lower energy than a small molecule solution. This theory explains the possibility to recover water from polymer solutions using lower energy process such as low pressure ultrafiltration [36, 67].

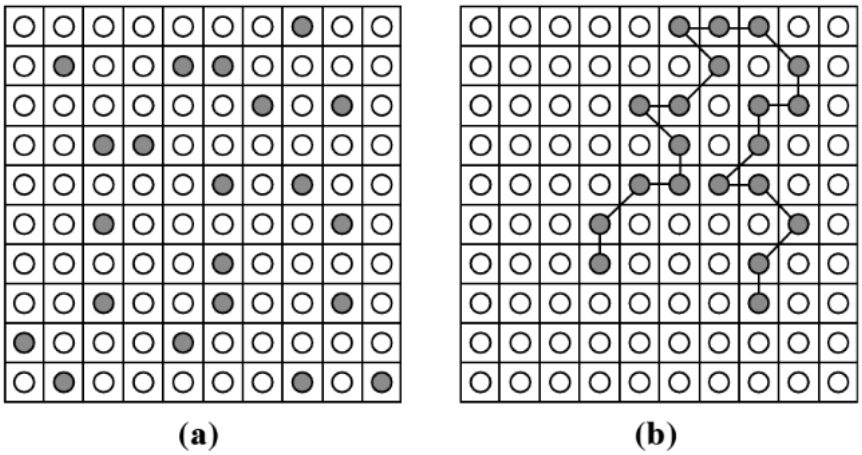

Figure 2.1 Two-dimensional lattice model solubility: (a) low molecular weight solute and (b) polymeric solute. The filled circles represent the solute molecules and the hollow circles represent the solvent molecules. Reproduced from Brazel and Rosen [65] Copyright 2012, Wiley.

Anionic polyelectrolytes bearing carboxylic or sulfonate groups have been evaluated as the draw solutes for FO desalination process. For example, low molecular weight poly (sodium acrylate) (PSA) [36] (Mw ~ 1,800) was used as draw solute which could generate osmotic pressure equal to seawater solution with minimum reverse solute flux. However, the performance of this polyelectrolyte in real application might be hindered by its viscosity [47]. To overcome this, FO unit was coupled with membrane distillation (MD) to recycle this PSA at elevated temperature in order to reduce its viscosity [68]. Another strategy to reduce the viscosity of polyelectrolytes is to use polymers with dendritic structure such as poly (amidoamine) dendrimer [69] as FO draw solute which has lower viscosity than linear polymers due to its unique structure [70]. In contrast to PSA, high molecular weight (Mw ~ 70,000) poly (sodium 4-styrenesulfonate) (PSSS) [67] could generate similar water flux and had relatively lower viscosity than PSA at ambient

temperature. However, the reverse solute flux of PSSS was higher than that of PSA. Additionally, poly (aspartic acid sodium salt) (PAspNa) [71] was evaluated as the draw solute material. This polyelectrolyte showed much larger osmotic pressure than PSA due to the presence of more freely mobile counterions. More importantly, PAspNa has an anti-scalant property which decreased the formation of inorganic scaling on the surface of membranes while the use of thermolytic solutes caused membrane scaling due to reverse diffusion of carbonate ions into feed solution [72].

On the other hand, a limited number of cationic polyelectrolytes have been applied as draw solute material for FO desalination. Poly (2-(dimethylamino) ethyl methacrylate) (PDMAEMA) containing tertiary amine moieties has been evaluated as draw materials for FO process [73]. The tertiary amine was firstly protonated by bubbling carbon dioxide which resulted in the increase of osmotic pressure of the solution before being circulated in the FO cell. The diluted polymer solution was then recovered by bubbling nitrogen gas and mild heating combined with ultrafiltration process to produce clean water. The schematic diagram of this system is shown in Figure 2.2.

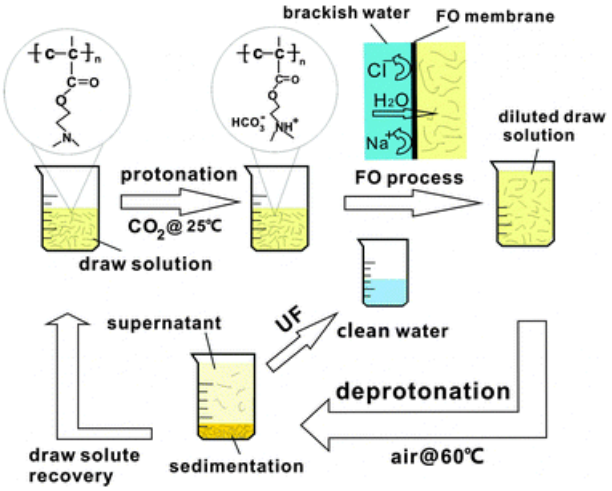

Figure 2.2 CO_2 responsive polymer-driven forward osmosis desalination system. Reproduced with permission from Cai et al. [73] Copyright 2013, Royal Society of Chemistry

Other cationic polyelectrolytes such as branched polyethyleneimine (*b*PEI) with different molecular weights have also been evaluated as the potential draw solutes for FO process [74]. The water flux generated against DI water was comparable with the PDMAEMA at the same concentration. Although adjusting the pH of the *b*PEI solution increased the water flux due to the protonation of amino groups, the reverse solute flux also increased due to structural shrinkage of the polymers.

Finally, non-ionic linear polymers based on N-isopropylacrylamide (NIPAM) having thermoresponsive properties have also been proposed as draw solute for FO process. PNIPAM was copolymerized with various ionic co-monomers such as sodium acrylate (SA) [37] and sodium-4-styrenesulfonate (SSS) [75] to further increase the osmotic pressure of the polymer solution [76]. The copolymer of NIPAM and SSS (PNIPAM-*co*-PSSS) showed higher flux than the copolymer of NIPAM and SA (PNIPAM-*co*-PSA) due to strong ionization of the PNIPAM-*co*-PSSS caused by sulfonate functional groups. Furthermore, a recent study using

copolymer of N-isopropylacrylamide and acrylic acid (PNIPAM-*co*-AA) used pH adjustment and heating to aid in water recovery [77]. Although high water recovery could be achieved using this method, the pH-responsiveness of acrylic acid might be reduced due to salt accumulation in the solution from multiple pH adjustment [78].

At the same time, poly (ethylene glycol) (PEG) has also been proposed as draw material for FO process [79]. Increasing molecular weight of PEG reduced the FO water flux due to severe concentration polarization. However, another study showed that increasing molecular weight of PEG to 20 kDa improved the water flux due to the increase of hydrophilicity [80]. In addition, short PEG-based vinyl monomer showing thermoresponsive properties, *2*-(*2*-methoxyethoxy) ethyl methacrylate (MEO_2MA), has also been evaluated as draw solute for FO desalination [81]. Based on its LCST at ~ 26 ºC [82], ME_2OMA is relatively hydrophobic and the ionic comonomer of 2-(methacryloyloxy) ethyl trimethylammonium chloride (MTAC) was copolymerized with ME_2OMA to increase the osmotic pressure of the resulting polymer solution. The study showed that relatively low theoretical energy consumption, around 0.03 kWh/m^3 water recovered, can be achieved using microfiltration process in water recovery stage. Table 2.2 summarizes the FO performance of recent linear polymers as draw solutes using commercial CTA FO membranes.

Table 2.2 Summary of FO performance for different polymers

Polymer Draw Solutes	DS concentration	FO Performance	Water Recovery	Ref.
Anionic Polyelectrolytes				
Poly(sodium acrylate)	0.72 g/mL	Water flux:~ 18 LMH Reverse flux: 0.08 g/m^{2}h Feed: DI water	Ultrafiltration	[36]
Poly(sodium *4*-styrenesulfonate)	0.24 g/mL	Water flux:~ 18 LMH Reverse flux: 20 – 60 g/m^{2}h Feed: DI water	Ultrafiltration	[67]
Poly(aspartic acid sodium salt)	0.3 g/mL	Water flux:~7.5 – 16 LMH Reverse flux: up to 2.4 g/m^{2}h Feed: DI water	Nanofiltration Membrane Distillation	[71]
Poly(amidoamine) dendrimer	33.3 wt%	Water flux: 19.8 – 31.8 LMH Reverse flux: 4.5 – 11 g/m^{2}h Feed: DI water	Membrane Distillation	[69]
Cationic Polyelectrolytes				
Poly(*2*-(dimethylamino) ethyl methacrylate)	0.2 g/g	Water flux:~ 3.5 – 5 LMH Reverse flux: ~0.11 – 0.16 g/m^{2}h Feed: DI water	Microfiltration	[73]
Polyethyleneimine	5 wt%	Water flux:~5 LMH Reverse flux: ~0.012 g/m^{2}h Feed: DI water	Nanofiltration	[83]
Thermoresponsive Polyelectrolytes				
PNIPAM-*co*-PSA	14.3 wt%	Water flux: ~0.1 – 0.75 LMH Feed: DI water	Hot Ultrafiltration	[37]
PNIPAM-*co*-PSSS	33.3 wt%	Water flux: up to 4 LMH Reverse flux: 2 g/m^{2}h Feed: 0.6 M NaCl	Membrane Distillation	[75]
PNIPAM-*co*-PAA	0.38 g/mL	Water flux: 2.95 LMH Feed: DI Water	Heating, pH adjustment and centrifugation	[77]
PME$_2$OMA-*co*-	0.1 g/mL	Water flux:~ 1 – 11 LMH	Hot microfiltration	[81]

PMTAC		Feed: DI water		
		Non-ionic Polymers		
Poly(ethylene glycol)	600 g/L	Water flux: 6.3 LMH Reverse flux: 2 g/m^{2}h Feed: DI water	Nanofiltration	[80]

2.4.2 Polymer hydrogels

Hydrogels which are partially cross linked water-soluble polymers have been previously used in adsorption desalination process by immersing the dried hydrogels directly in the saline solution [84, 85]. However, this approach has relatively low efficiency in removing salt from saline feed solution and requires considerable amount of energy in water recovery stage through evaporation process or applied pressure. Furthermore, salt accumulation in the hydrogels might decrease the effectiveness of the process in subsequent cycles [78].

Thermoresponsive hydrogels were recently introduced as semi-solid draw agents for FO desalination [39, 86]. The deswollen hydrogels absorb water from the feed solution when they are brought into contact with FO membrane due to the difference in the chemical potential between the feed solution and the hydrogels. The hydrogels can be heated to release the absorbed water and the deswollen hydrogels are reused to absorb water from the feed solution. The schematic diagram showing the working principle of thermoresponsive hydrogel-driven FO desalination and its water flux and water recovery performance are shown in Figure 2.3. The hydrogels were composed primarily of NIPAM to provide thermoresponsive properties. Non-ionic and ionic comonomers were used to increase the osmotic pressure of the hydrogels. Pure water could be recovered when the hydrogels were heated above their volume phase

transition temperature (VPTT). The homopolymer hydrogel of sodium acrylate was able to generate the highest water flux due to abundant ionic carboxylic moieties in the hydrogel while the copolymer hydrogel of NIPAM and SA (PNIPAM-PSA) absorb water at moderate flux as shown in Figure 2.3b. In terms of water recovery, the homopolymer hydrogel of sodium acrylate released the smallest amount of water at elevated temperature due to strong ionic interaction between water and carboxylic group while PNIPAM-PSA hydrogel released slightly higher water due to the change of PNIPAM moieties into hydrophobic above the VPTT of the hydrogel as shown in Figure 2.3c.

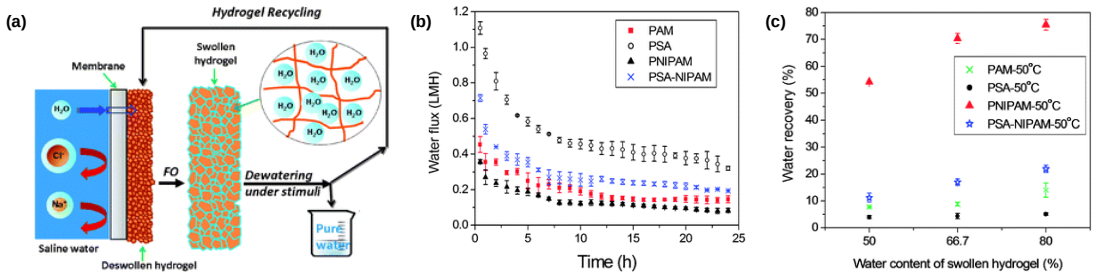

Figure 2.3 (a) Thermoresponsive hydrogel-driven FO desalination process; (b) water flux profile of different hydrogels over 24 h water adsorption period; (c) Water recovery from different hydrogels at different water content and temperatures. Adapted with permission from Li et al. [39] Copyright 2011, Royal Society of Chemistry

Semi interpenetrating network of thermoresponsive hydrogels of NIPAM and SA (SI-PSA) and NIPAM and poly (vinyl alcohol) (SI-PVA) were then introduced to overcome the poor water recovery in PNIPAM-PSA [40]. These hydrogels were able to release more water above the VPTT due to the mobility of linear hydrophilic polymer inside NIPAM network which mitigated the influence of ionic contribution on hydrophobic formation. Other interpenetrating network composed of hyaluronic

acid and poly (vinyl alcohol) have also been synthesized via freeze-thawing method and was evaluated as draw materials for FO process [87]. This hydrogel showed electro-responsive properties under applied electric field due to the migration of ions toward the cathode which increased the osmotic pressure of the hydrogel. As a result, enhanced water flux was observed when electric field was applied to the hydrogel.

Composite thermoresponsive hydrogels incorporating carbon particles [88, 89], reduced graphene oxide (*r*GO) [90] and magnetic nanoparticles [91] were also proposed to further improve the performance of hydrogel-driven FO desalination process. The water flux was improved when carbon and *r*GO particles were incorporated into hydrogels due to improved swelling ratios of the composite hydrogels. The water recovery, especially in the liquid form, was improved when magnetic hydrogels were used as draw agent due to uniform heating generated by the dispersed magnetic nanoparticles when alternating magnetic field was applied to the hydrogel.

Although FO performance can be improved by using composite hydrogels, it was still far away from the conventional FO desalination using thermolytic solutes or synthetic organic solutes [45, 47, 52, 92]. A series of thermoresponsive microgels of NIPAM with different contents of acrylic acid (AA) were recently synthesized and evaluated as the draw solutes to overcome the disadvantages of thermoresponsive hydrogels [93]. The study used different approach to measure water flux by monitoring the change of conductivity of feed solution with time, which was able to minimize the error arise from interval gravimetric method when calculating the water flux from hydrogel-driven FO desalination. Interestingly, reducing the size of hydrogels into sub-micron scale significantly improved the water drawing ability of

the hydrogels due to high surface area of these microgels [94]. Relatively higher water recovered than bulk hydrogels in liquid form was achieved when the microgels were heated above their VPTTs. This is due to the absence of skin formation during the deswelling process in the microgels [91, 95]. Table 2.3 summarizes the FO performance of thermoresponsive hydrogels and microgels using commercial CTA FO membrane and 2000 ppm NaCl as the feed solution.

Table 2.3 FO performance of various thermoresponsive hydrogels and microgels

Polymer Hydrogels	Mass of Hydrogels	FO Water Flux	Water Recovery	Ref.
PNIPAM-PSA hydrogels	1 g	Particle size: 50 – 150 µm 0.55 LMH	17%	[39, 96]
		Particle size: 2 – 25 µm 1.3 LMH	-	
Semi-IPN hydrogels	0.4 g	SI-PSA hydrogels Particle size: 200 µm ~0.21 LMH	~91%	[40]
		SI-PVA hydrogels Particle size: 200 µm ~0.16 LMH	~99%	
Composite hydrogels of PNIPAM-PSA	1 g	Carbon sphere 0.77 LMH	12%	[88, 90, 91]
		Reduced graphene oxide (1.2 wt%) 1.7 LMH	45%	
		Magnetic nanoparticles (16 wt%) ~ 1.3 LMH	~60%	
Functionalized microgels (PNIPAM-AA)	0.1 g	PNIPAM 8.9 LMH	72%	[93]
		PNIPAM-AA (8% AA) 23.8 LMH	52%	

2.4.3 Polymer – magnetic nanoparticles hybrid

Hydrophilic superparamagnetic nanoparticles (MNPs) have been proposed as the FO draw solutes due to its ease of recovery using external magnetic field. The main drawback of using MNPs as draw solute is particle aggregation after water recovery process in the presence of high magnetic field [97-99]. Thermoresponsive polymer, PNIPAM, was then coated on the surface of MNPs to induce reversible particle clustering which allowed the separation conducted at lower magnetic field, and thus mitigating the irreversible MNPs aggregation [100]. Coating these magnetic nanoparticles with polyelectrolytes such as acrylic acid [38, 101], sodium *2*-acrylamido-*2*-methylpropane sulfonate [102] and sodium styrene-*4*-sulfonate [103] or hydrophilic polymers such as poly (ethylene glycol) diacid [99] and dextran [104] also improved the performance of these MNPs in FO process. However, complete separation of these MNPs usually requires a combination of magnetic separator and ultrafiltration process which will increases the capital and operating cost [102, 103]. Furthermore, coating with organic compounds might promote growth of bacteria in these MNPs which would reduce the performance of these materials in the long term [104]. Table 2.4 summarizes the FO performance of polymer – magnetic nanoparticle hybrid as FO draw solutes using commercial CTA FO membrane and DI water as the feed solution.

Table 2.4 FO performance of various polymer – magnetic nanoparticles hybrid

Coating Materials for MNPs	DS Concentration	FO Water Flux	Water Recovery	Ref.
PNIPAM	-	~ 1.8 LMH	Heating and magnetic field	[100]
PNIPAM-*co*-AA	0.02 g/mL	0.11 LMH	Heating and	[102]

PNIPAM-*co*-AMPS		0.26 LMH	magnetic field	
PNIPAM-*co*-PSSS	33 wt%	14.9 LMH	Magnetic field and ultrafiltration	[103]
Poly(ethylene glycol) diacid	0.065 M	13 LMH	Magnetic field	[99]
Dextran	0.5 M	~ 4 LMH	Magnetic field	[104]

2.5 Switchable polarity solvents

Switchable polarity solvent (SPS) is the solvent that can be reversibly switched from ionic form to non-ionic form by the addition or removal carbon dioxide (CO_2) [105]. The SPS has tertiary amine functional group similar to the cationic polyelectrolyte of PDMAEMA, which can be switched to protonated state by bubbling the solution with CO_2. The addition of CO_2 in SPS will protonate the tertiary amine groups of solvents and form ionic carbamates in the solution. This causes the solvent to have high polarity and be water-miscible while removing CO_2 by bubbling nitrogen gas will deprotonate the tertiary amine moieties as illustrated in Figure 2.4a [106].

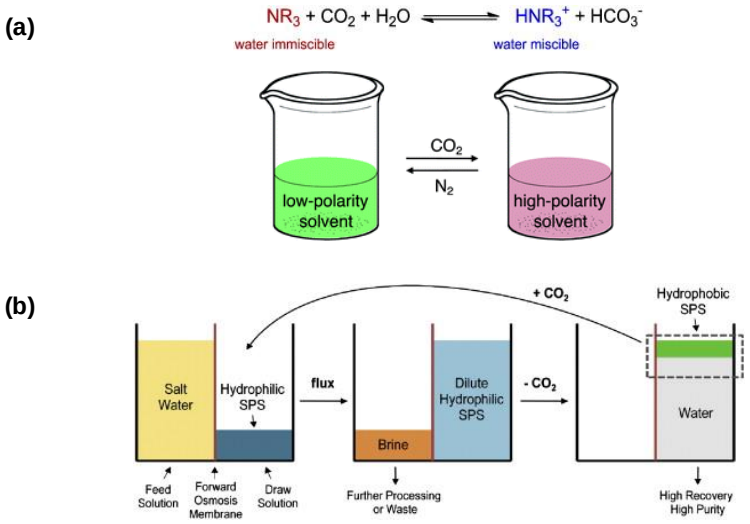

Figure 2.4 (a) Reversible ionic to non-ionic transition in switchable polarity solvents and (b) Schematic diagram of SPS-driven FO desalination system. Adapted with the permission from Stone et al. [41] Copyright 2013, Elsevier and Jessop et al. [106] Copyright 2012, Royal Society of Chemistry

N,*N*-dimethylcyclohexylamine (DMCHA) was evaluated as draw solvent to treat saline water equivalent to seawater solution and could generate relatively high water flux (11 LMH) [41]. The protonated solvent will absorb water from the feed solution due to the difference in osmotic pressure. After the solvent is saturated with water, the carbon dioxide (CO_2) is removed by bubbling nitrogen which will cause the solvent to phase separate from water due to its non-polar form. The hydrophobic solvent can be recycled back to perform water absorption. This working principle is illustrated in Figure 2.4b.

Although relatively high water flux and high water recovery could be achieved using DMCHA as switchable polarity solvent, the membrane degradation and incomplete separation were the main drawbacks using this draw solvent [107]. *1*-Cyclohexylpiperidine (CHP) was then proposed to overcome aforementioned

problems of DMCHA [107]. The water flux generated by CHP was slightly lower than (8.5 LMH) the water flux of DMHCA which is probably due to more hydrophobic nature of this material. However, the study showed that CHP had better membrane stability than DMCHA. In addition, theoretical energy analysis of SPS-driven FO desalination showed that the process has energy consumption ranged from 2.4 to 4 kWh/m^3 recovered water which is lower than RO desalination process [108]. The high water drawing capability due to high polarity property of SPS in their protonated state might also find niche application in treating challenging feed solution such as high salinity produced water from oil and gas field [4, 30, 51].

2.6 Thermoresponsive ionic liquids

Thermo-responsive ionic liquids are liquid-like salt comprising organic cations and anions that undergo phase separation if heated or cooled past their critical phase transition temperatures. The thermo-responsive properties of ionic liquids can be divided into two types as the lower critical solution temperature (LCST) and the upper critical solution temperature (UCST) behaviors [109]. An example of ionic liquid showing LCST behavior used as FO draw solute is tetrabutylphosphonium *2,4*-dimethylbenzenesulfonate while ionic liquid showing UCST behavior is betaine *bis*(trifluoromethylsulfonyl)imide. Due to their strong ionic property and relatively large molecular size, these materials have recently been introduced as a new class of draw solute for FO desalination process. The schematic diagram of ionic liquid-driven FO desalination is shown in Figure 2.5a. The water transport through semipermeable membrane will occur automatically due to the difference in osmotic pressure between salty water and ionic liquid. The diluted ionic liquid was then heated or cooled past their critical temperature to induce phase separation between

ionic liquid and absorbed water. The concentrated ionic liquid can be recycled back to FO unit to absorb more water.

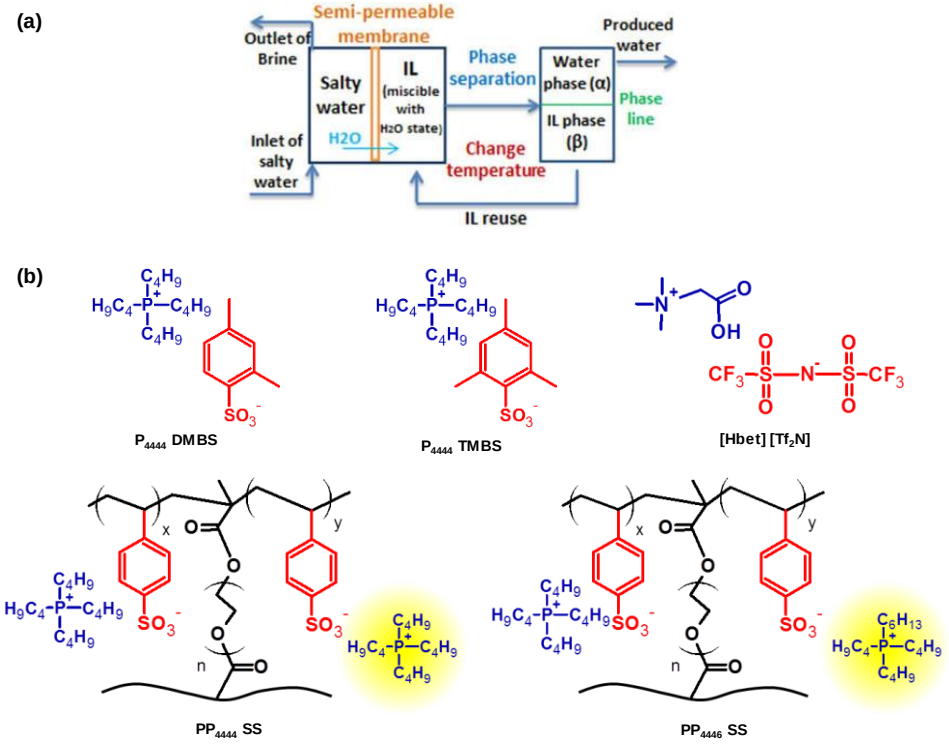

Figure 2.5 (a) Schematic diagram of ionic-liquid driven FO desalination system and (b) chemical structures of different thermoresponsive ionic liquid used as draw solute materials. Adapted with the permission from Zhong et al. [43] Copyright 2015, American Chemical Society

Thermoresponsive ionic liquids showing the LCST behavior such as tetrabutylphosphonium *2,4*-dimethylbenzenesulfonate (P_{4444}DMBS) and tetrabutylphosphonium mesitylenesulfonate (P_{4444} TMBS), were recently evaluated as draw solutes for FO desalination to treat high salinity solution [44]. Both of ionic liquids could generate osmotic pressure higher than seawater solution and had LCST less than 50 ^{o}C. P_{4444}DMBS had higher water flux (~ 3 – 11 LMH) than P_{4444} TMBS (~ 0.1 – 8 LMH) when tested against saline solution at different concentration. This

is due to the anion structure of P_{4444} TMBS having an additional methyl group as shown in Figure 2.5b which made P_{4444} TMBS more hydrophobic than P_{4444}DMBS [110]. Theoretical energy consumption of this system was estimated to be around 1.80 kWh/m^3.

Recently, ionic liquid based on protonated betaine *bis*(trifluoromethylsulfonyl) imide ([Hbet][Tf_2N]) was also evaluated as draw solute material for FO desalination [43]. This ionic liquid had to be operated at elevated temperature above its critical temperature which may increase the FO performance due to mass transfer enhancement [111, 112]. It was reported that ([Hbet][Tf_2N] was able to draw water at high salinity level up to 3 M which was higher than the drawing ability previously reported LCST-type ionic liquids. Although operated at elevated temperature, this draw solute had lower water fluxes (~ 0.3 – 2.2 LMH) than LCST-type ionic liquids described previously. The chemical structure of its anion shown in Figure 2.5b might also play a role due to the presence of fluorine moieties which imparts strong hydrophobic character to this material [113].

Despite the superior water drawing performance of thermoresponsive ionic liquid in treating high salinity solution, pressure-driven membrane process such as nanofiltration or reverse osmosis is still required to remove the trace residual of ionic liquids from the water product which might increase the total operating cost. Thermoresponsive poly (ionic liquid) hydrogels was then proposed to overcome the aforementioned issue. The application of poly (ionic liquid) hydrogels as draw material might prevent the loss of solute via reverse solute flux [86]. This is especially important because the relatively expensive some types of ionic liquids materials [114]. Thermoresponsive poly (ionic liquid) hydrogels based on

tetrabutylphosphonium *p*-styrenesulfonate (PP_{4444} SS) and tributyl-hexyl phosphonium p-styrenesulfonate (PP_{4446} SS) were synthesized and evaluated as draw materials in FO process [115]. These hydrogels could generate higher water flux than PNIPAM hydrogels due to the hydrophilic character caused by the presence of organic cations and anions in the hydrogels as shown in Figure 2.6a. In another study, some ionic liquids also showed antibacterial property which could prevent biofilm formation that impacts membrane performance [42]. However, the water recovery performance of these materials suffered due to the presence of strong ionic interaction in the hydrogels as can be seen from slower deswelling kinetics curves of PP_{4444} SS and PP_{4446} SS than PNIPAM hydrogels as shown in Figure 2.6b.

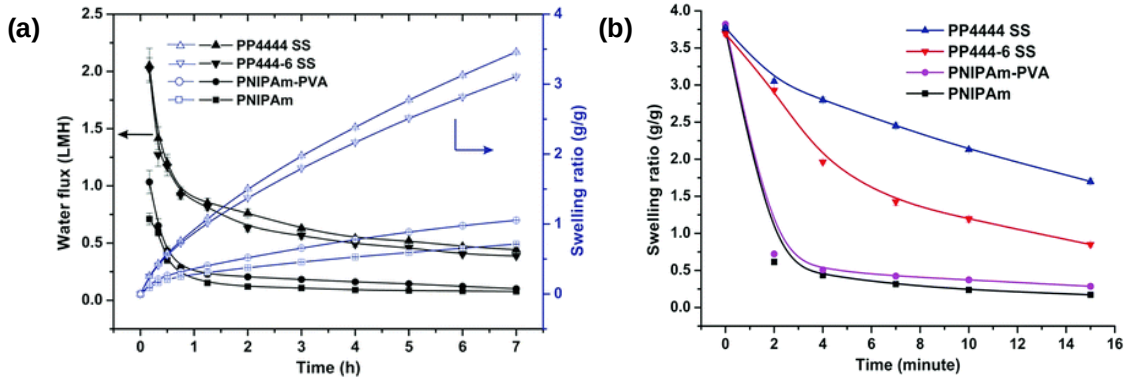

Figure 2.6 (a) Water flux and swelling ratio of different thermoresponsive poly (ionic liquid) hydrogels and (b) Deswelling kinetics of different thermoresponsive poly (ionic liquid) hydrogels compared to NIPAM-based hydrogels. Adapted with the permission from Cai et al. [115] Copyright 2015, Royal Society of Chemistry.

2.7 Conclusion and future perspectives

Research on draw solute materials for FO desalination has gained a lot of interest over the past decades due to its potential to lower energy consumption in membrane-

based desalination process. The main advantage using synthetic materials as draw solute is the ability to tune the generated osmotic pressure without necessarily increasing the draw solute concentration. This would extend the application of FO to treat challenging feed water with high salinity level. There is a trend that molecular size of draw solute materials is increasing from simple organic solutes to polymer hydrogels to minimize the reverse solute flux. However, the FO performance might be compromised due to concentration polarization phenomena in large draw solute materials. Furthermore, the process design of these draw solute materials such as polymer hydrogels should be further considered to achieve practical FO desalination process in industrial setting. Generally, more draw solute materials being developed to date have stimuli-responsive properties such as temperature, pH and CO_2. This allows FO desalination process to tap into low grade heat as energy source or abundant CO_2 availability for water recovery process. These sources are generally cheaper than electrical energy used to power high pressure pump in RO process. Therefore, we expect that synthetic materials with stimuli-responsive properties might continue to dominate this area in the future.

2.8 References

[1] McCutcheon JR, McGinnis RL, Elimelech M. A novel ammonia-carbon dioxide forward (direct) osmosis desalination process. Desalination. 2005;174:1-11.

[2] Phuntsho S, Shon HK, Hong S, Lee S, Vigneswaran S. A novel low energy fertilizer driven forward osmosis desalination for direct fertigation: Evaluating the performance of fertilizer draw solutions. Journal of Membrane Science. 2011;375:172-81.

[3] Zhao S, Zou L, Mulcahy D. Brackish water desalination by a hybrid forward osmosis–nanofiltration system using divalent draw solute. Desalination. 2012;284:175-81.

[4] Shaffer DL, Arias Chavez LH, Ben-Sasson M, Romero-Vargas Castrillón S, Yip NY, Elimelech M. Desalination and Reuse of High-Salinity Shale Gas Produced Water: Drivers, Technologies, and Future Directions. Environmental Science & Technology. 2013;47:9569-83.

[5] Achilli A, Cath TY, Marchand EA, Childress AE. The forward osmosis membrane bioreactor: A low fouling alternative to MBR processes. Desalination. 2009;239:10-21.

[6] Coday BD, Yaffe BGM, Xu P, Cath TY. Rejection of Trace Organic Compounds by Forward Osmosis Membranes: A Literature Review. Environmental Science & Technology. 2014;48:3612-24.

[7] Xie M, Nghiem LD, Price WE, Elimelech M. Toward Resource Recovery from Wastewater: Extraction of Phosphorus from Digested Sludge Using a Hybrid Forward Osmosis–Membrane Distillation Process. Environmental Science & Technology Letters. 2014;1:191-5.

[8] Jiao B, Cassano A, Drioli E. Recent advances on membrane processes for the concentration of fruit juices: a review. Journal of Food Engineering. 2004;63:303-24.

[9] Long Q, Qi G, Wang Y. Evaluation of Renewable Gluconate Salts as Draw Solutes in Forward Osmosis Process. ACS Sustainable Chemistry & Engineering. 2015.

[10] Ge Q, Chung T-S. Oxalic acid complexes: promising draw solutes for forward osmosis (FO) in protein enrichment. Chemical Communications. 2015;51:4854-7.

[11] Mondal D, Mahto A, Veerababu P, Bhatt J, Prasad K, Nataraj SK. Deep eutectic solvents as a new class of draw agent to enrich low abundance DNA and proteins using forward osmosis. RSC Advances. 2015;5:89539-44.

[12] Gawande N, Mungray AA. Superabsorbent polymer (SAP) hydrogels for protein enrichment. Separation and Purification Technology. 2015;150:86-94.

[13] Zhang F, Brastad KS, He Z. Integrating Forward Osmosis into Microbial Fuel Cells for Wastewater Treatment, Water Extraction and Bioelectricity Generation. Environmental Science & Technology. 2011;45:6690-6.

[14] Werner CM, Logan BE, Saikaly PE, Amy GL. Wastewater treatment, energy recovery and desalination using a forward osmosis membrane in an air-cathode microbial osmotic fuel cell. Journal of Membrane Science. 2013;428:116-22.

[15] Cath TY, Childress AE, Elimelech M. Forward osmosis: Principles, applications, and recent developments. Journal of Membrane Science. 2006;281:70-87.

[16] Mi B, Elimelech M. Organic fouling of forward osmosis membranes: Fouling reversibility and cleaning without chemical reagents. Journal of Membrane Science. 2010;348:337-45.

[17] Kim Y, Elimelech M, Shon HK, Hong S. Combined organic and colloidal fouling in forward osmosis: Fouling reversibility and the role of applied pressure. Journal of Membrane Science. 2014;460:206-12.

[18] McGinnis RL, Elimelech M. Energy requirements of ammonia-carbon dioxide forward osmosis desalination. Desalination. 2007;207:370-82.

[19] Gray GT, McCutcheon JR, Elimelech M. Internal concentration polarization in forward osmosis: role of membrane orientation. Desalination. 2006;197:1-8.

[20] Hancock NT, Cath TY. Solute Coupled Diffusion in Osmotically Driven Membrane Processes. Environmental Science & Technology. 2009;43:6769-75.

[21] McCutcheon JR, Elimelech M. Influence of membrane support layer hydrophobicity on water flux in osmotically driven membrane processes. Journal of Membrane Science. 2008;318:458-66.

[22] Bui NN, Lind ML, Hoek EMV, McCutcheon JR. Electrospun nanofiber supported thin film composite membranes for engineered osmosis. Journal of Membrane Science. 2011;385:10-9.

[23] Han G, Chung T-S, Toriida M, Tamai S. Thin-film composite forward osmosis membranes with novel hydrophilic supports for desalination. Journal of Membrane Science. 2012;423–424:543-55.

[24] Huang LW, Bui NN, Meyering MT, Hamlin TJ, McCutcheon JR. Novel hydrophilic nylon 6,6 microfiltration membrane supported thin film composite membranes for engineered osmosis. Journal of Membrane Science. 2013;437:141-9.

[25] Ma N, Wei J, Qi S, Zhao Y, Gao Y, Tang CY. Nanocomposite substrates for controlling internal concentration polarization in forward osmosis membranes. Journal of Membrane Science. 2013;441:54-62.

[26] Widjojo N, Chung TS, Weber M, Maletzko C, Warzelhan V. A sulfonated polyphenylenesulfone (sPPSU) as the supporting substrate in thin film composite (TFC) membranes with enhanced performance for forward osmosis (FO). Chemical Engineering Journal. 2013;220:15-23.

[27] Park MJ, Phuntsho S, He T, Nisola GM, Tijing LD, Li X-M, et al. Graphene oxide incorporated polysulfone substrate for the fabrication of flat-sheet thin-film composite forward osmosis membranes. Journal of Membrane Science. 2015;493:496-507.

[28] Emadzadeh D, Lau WJ, Matsuura T, Rahbari-Sisakht M, Ismail AF. A novel thin film composite forward osmosis membrane prepared from PSf–TiO2 nanocomposite substrate for water desalination. Chemical Engineering Journal. 2014;237:70-80.

[29] Lee J-Y, She Q, Huo F, Tang CY. Metal–organic framework-based porous matrix membranes for improving mass transfer in forward osmosis membranes. Journal of Membrane Science. 2015;492:392-9.

[30] Shaffer DL, Werber JR, Jaramillo H, Lin S, Elimelech M. Forward osmosis: Where are we now? Desalination. 2015;356:271-84.

[31] McGovern RK, Lienhard V JH. On the potential of forward osmosis to energetically outperform reverse osmosis desalination. Journal of Membrane Science. 2014;469:245-50.

[32] Semiat R. Energy Issues in Desalination Processes. Environmental Science & Technology. 2008;42:8193-201.

[33] Swee Kuan Y, Mehnas FNH, Minglue S, Kai Yu W, Tai-Shung C. Study of draw solutes using 2-methylimidazole-based compounds in forward osmosis. Journal of Membrane Science. 2010;364:242-52.

[34] Noh M, Mok Y, Lee S, Kim H, Lee SH, Jin G-w, et al. Novel lower critical solution temperature phase transition materials effectively control osmosis by mild temperature changes. Chemical Communications. 2012;48:3845-7.

[35] Ge QC, Chung TS. Hydroacid complexes: a new class of draw solutes to promote forward osmosis (FO) processes. Chemical Communications. 2013;49:8471-3.

[36] Ge Q, Su J, Amy GL, Chung T-S. Exploration of polyelectrolytes as draw solutes in forward osmosis processes. Water Research. 2012;46:1318-26.

[37] Ou R, Wang Y, Wang H, Xu T. Thermo-sensitive polyelectrolytes as draw solutions in forward osmosis process. Desalination. 2013;318:48-55.

[38] Ling MM, Chung T-S. Desalination process using super hydrophilic nanoparticles via forward osmosis integrated with ultrafiltration regeneration. Desalination. 2011;278:194-202.

[39] Li D, Zhang X, Yao J, Simon GP, Wang H. Stimuli-responsive polymer hydrogels as a new class of draw agent for forward osmosis desalination. Chemical Communications. 2011;47:1710-2.

[40] Cai Y, Shen W, Loo SL, Krantz WB, Wang R, Fane AG, et al. Towards temperature driven forward osmosis desalination using Semi-IPN hydrogels as reversible draw agents. Water Research. 2013;47:3773-81.

[41] Stone ML, Rae C, Stewart FF, Wilson AD. Switchable polarity solvents as draw solutes for forward osmosis. Desalination. 2013;312:124-9.

[42] Kim J-j, Kang H, Choi Y-S, Yu YA, Lee J-C. Thermo-responsive oligomeric poly(tetrabutylphosphonium styrenesulfonate)s as draw solutes for forward osmosis (FO) applications. Desalination. 2016;381:84-94.

[43] Zhong Y, Feng X, Chen W, Wang X, Huang KW, Gnanou Y, et al. Using UCST Ionic Liquid as a Draw Solute in Forward Osmosis to Treat High-Salinity Water. Environ Sci Technol. 2015.

[44] Cai Y, Shen W, Wei J, Chong TH, Wang R, Krantz WB, et al. Energy-efficient desalination by forward osmosis using responsive ionic liquid draw solutes. Environmental Science: Water Research & Technology. 2015;1:341-7.

[45] Ge QC, Ling MM, Chung TS. Draw solutions for forward osmosis processes: Developments, challenges, and prospects for the future. Journal of Membrane Science. 2013;442:225-37.

[46] Luo H, Wang Q, Zhang TC, Tao T, Zhou A, Chen L, et al. A review on the recovery methods of draw solutes in forward osmosis. Journal of Water Process Engineering. 2014;4:212-23.

[47] Chekli L, Phuntsho S, Kim JE, Kim J, Choi JY, Choi J-S, et al. A comprehensive review of hybrid forward osmosis systems: Performance, applications and future prospects. Journal of Membrane Science. 2016;497:430-49.

[48] Qasim M, Darwish NA, Sarp S, Hilal N. Water desalination by forward (direct) osmosis phenomenon: A comprehensive review. Desalination. 2015;374:47-69.

[49] Boo C, Khalil YF, Elimelech M. Performance evaluation of trimethylamine–carbon dioxide thermolytic draw solution for engineered osmosis. Journal of Membrane Science. 2015;473:302-309.

[50] Achilli A, Cath TY, Childress AE. Selection of inorganic-based draw solutions for forward osmosis applications. Journal of Membrane Science. 2010;364:233-41.

[51] Coday BD, Xu P, Beaudry EG, Herron J, Lampi K, Hancock NT, et al. The sweet spot of forward osmosis: Treatment of produced water, drilling wastewater, and other complex and difficult liquid streams. Desalination. 2014;333:23-35.

[52] Klaysom C, Cath TY, Depuydt T, Vankelecom IF. Forward and pressure retarded osmosis: potential solutions for global challenges in energy and water supply. Chem Soc Rev. 2013;42:6959-89.

[53] Nakayama D, Mok Y, Noh M, Park J, Kang S, Lee Y. Lower critical solution temperature (LCST) phase separation of glycol ethers for forward osmotic control. Physical Chemistry Chemical Physics. 2014;16:5319-25.

[54] Stone ML, Wilson AD, Harrup MK, Stewart FF. An initial study of hexavalent phosphazene salts as draw solutes in forward osmosis. Desalination. 2013;312:130-6.

[55] Long Q, Qi G, Wang Y. Synthesis and application of ethylenediamine tetrapropionic salt as a novel draw solute for forward osmosis application. AIChE Journal. 2015;61:1309-21.

[56] Zhao Y, Ren Y, Wang X, Xiao P, Tian E, Wang X, et al. An initial study of EDTA complex based draw solutes in forward osmosis process. Desalination. 2016;378:28-36.

[57] Gadelha G, Nawaz MS, Hankins NP, Khan SJ, Wang R, Tang CY. Assessment of micellar solutions as draw solutions for forward osmosis. Desalination. 2014;354:97-106.

[58] Nguyen HT, Nguyen NC, Chen S-S, Li C-W, Hsu H-T, Wu S-Y. Innovation in Draw Solute for Practical Zero Salt Reverse in Forward Osmosis Desalination. Industrial & Engineering Chemistry Research. 2015;54:6067-74.

[59] Arena JT, Chwatko M, Robillard HA, McCutcheon JR. pH Sensitivity of Ion Exchange through a Thin Film Composite Membrane in Forward Osmosis. Environmental Science & Technology Letters. 2015;2:177-82.

[60] Ge Q, Fu F, Chung T-S. Ferric and cobaltous hydroacid complexes for forward osmosis (FO) processes. Water Research. 2014;58:230-8.

[61] Guo CX, Zhao D, Zhao Q, Wang P, Lu X. Na(+)-functionalized carbon quantum dots: a new draw solute in forward osmosis for seawater desalination. Chem Commun (Camb). 2014;50:7318-21.

[62] Mazlan NM, Peshev D, Livingston AG. Energy consumption for desalination — A comparison of forward osmosis with reverse osmosis, and the potential for perfect membranes. Desalination. 2016;377:138-51.

[63] Nguyen HT, Chen S-S, Nguyen NC, Ngo HH, Guo W, Li C-W. Exploring an innovative surfactant and phosphate-based draw solution for forward osmosis desalination. Journal of Membrane Science. 2015;489:212-9.

[64] Nguyen HT, Nguyen NC, Chen S-S, Ngo HH, Guo W, Li C-W. A new class of draw solutions for minimizing reverse salt flux to improve forward osmosis desalination. Science of The Total Environment. 2015;538:129-36.

[65] Brazel CS, Rosen SL. Fundamental Principles of Polymeric Materials: Wiley; 2012.

[66] Hansen CM. Hansen Solubility Parameters: A User's Handbook, Second Edition: CRC Press; 2007.

[67] Tian E, Hu C, Qin Y, Ren Y, Wang X, Wang X, et al. A study of poly (sodium 4-styrenesulfonate) as draw solute in forward osmosis. Desalination. 2015;360:130-7.

[68] Ge Q, Wang P, Wan C, Chung T-S. Polyelectrolyte-Promoted Forward Osmosis–Membrane Distillation (FO–MD) Hybrid Process for Dye Wastewater Treatment. Environmental Science & Technology. 2012;46:6236-43.

[69] Zhao D, Chen S, Wang P, Zhao Q, Lu X. A Dendrimer-Based Forward Osmosis Draw Solute for Seawater Desalination. Industrial & Engineering Chemistry Research. 2014;53:16170-5.

[70] Nicholson JW. The Chemistry of Polymers: Royal Society of Chemistry; 2012.

[71] Gwak G, Jung B, Han S, Hong S. Evaluation of poly (aspartic acid sodium salt) as a draw solute for forward osmosis. Water Research. 2015;80:294-305.

[72] Li Z, Valladares Linares R, Bucs S, Aubry C, Ghaffour N, Vrouwenvelder JS, et al. Calcium carbonate scaling in seawater desalination by ammonia–carbon dioxide forward osmosis: Mechanism and implications. Journal of Membrane Science. 2015;481:36-43.

[73] Cai YF, Shen WM, Wang R, Krantz WB, Faneb AG, Hu X. CO2 switchable dual responsive polymers as draw solutes for forward osmosis desalination. Chemical Communications. 2013;49:8377-9.

[74] Jun B-M, Nguyen TPN, Ahn S-H, Kim I-C, Kwon Y-N. The application of polyethyleneimine draw solution in a combined forward osmosis/nanofiltration system. Journal of Applied Polymer Science. 2015;132.

[75] Zhao D, Wang P, Zhao Q, Chen N, Lu X. Thermoresponsive copolymer-based draw solution for seawater desalination in a combined process of forward osmosis and membrane distillation. Desalination. 2014;348:26-32.

[76] Zhao D, Chen S, Guo CX, Zhao Q, Lu X. Multi-functional forward osmosis draw solutes for seawater desalination. Chinese Journal of Chemical Engineering.

[77] Wang Y, Yu H, Xie R, Zhao K, Ju X, Wang W, et al. An easily recoverable thermo-sensitive polyelectrolyte as draw agent for forward osmosis process. Chinese Journal of Chemical Engineering.

[78] Zhang Q, Zhu S. Oxygen–Nitrogen Switchable Copolymers of 2,2,2-Trifluoroethyl Methacrylate and N,N-Dimethylaminoethyl Methacrylate. Macromolecular Rapid Communications. 2014;35:1692-6.

[79] Yasukawa M, Tanaka Y, Takahashi T, Shibuya M, Mishima S, Matsuyama H. Effect of Molecular Weight of Draw Solute on Water Permeation in Forward Osmosis Process. Industrial & Engineering Chemistry Research. 2015;54:8239-46.

[80] Sarp S, Lee S, Park K, Park M, Kim JH, Cho J. Using macromolecules as osmotically active compounds in osmosis followed by filtration (OF) system. Desalination and Water Treatment. 2012;43:131-7.

[81] Kim J-j, Chung J-S, Kang H, Yu Y, Choi W, Kim H, et al. Thermo-responsive copolymers with ionic group as novel draw solutes for forward osmosis processes. Macromol Res. 2014;22:963-70.

[82] Lutz J-F, Hoth A. Preparation of Ideal PEG Analogues with a Tunable Thermosensitivity by Controlled Radical Copolymerization of 2-(2-

Methoxyethoxy)ethyl Methacrylate and Oligo(ethylene glycol) Methacrylate. Macromolecules. 2006;39:893-6.

[83] Jun BM, Nguyen TPN, Ahn SH, Kim IC, Kwon YN. The application of polyethyleneimine draw solution in a combined forward osmosis/nanofiltration system. Journal of Applied Polymer Science. 2015;132:n/a-n/a.

[84] Höpfner J, Klein C, Wilhelm M. A Novel Approach for the Desalination of Seawater by Means of Reusable Poly(acrylic acid) Hydrogels and Mechanical Force. Macromolecular Rapid Communications. 2010;31:1337-42.

[85] Ali W, Gebert B, Hennecke T, Graf K, Ulbricht M, Gutmann JS. Design of Thermally Responsive Polymeric Hydrogels for Brackish Water Desalination: Effect of Architecture on Swelling, Deswelling, and Salt Rejection. ACS Applied Materials & Interfaces. 2015;7:15696-706.

[86] Razmjou A, Liu Q, Simon GP, Wang H. Bifunctional Polymer Hydrogel Layers As Forward Osmosis Draw Agents for Continuous Production of Fresh Water Using Solar Energy. Environmental Science & Technology. 2013;47:13160-6.

[87] Zhang H, Li J, Cui H, Li H, Yang F. Forward osmosis using electric-responsive polymer hydrogels as draw agents: Influence of freezing–thawing cycles, voltage, feed solutions on process performance. Chemical Engineering Journal. 2015;259:814-9.

[88] Li D, Zhang X, Yao J, Zeng Y, Simon GP, Wang H. Composite polymer hydrogels as draw agents in forward osmosis and solar dewatering. Soft Matter. 2011;7:10048-56.

[89] Li D, Zhang X, Simon GP, Wang H. Forward osmosis desalination using polymer hydrogels as a draw agent: Influence of draw agent, feed solution and membrane on process performance. Water Research. 2013;47:209-15.

[90] Zeng Y, Qiu L, Wang K, Yao J, Li D, Simon GP, et al. Significantly enhanced water flux in forward osmosis desalination with polymer-graphene composite hydrogels as a draw agent. Rsc Advances. 2013;3:887-94.

[91] Razmjou A, Barati MR, Simon GP, Suzuki K, Wang H. Fast Deswelling of Nanocomposite Polymer Hydrogels via Magnetic Field-Induced Heating for

Emerging FO Desalination. Environmental Science & Technology. 2013;47:6297-305.

[92] Zhao S, Zou L, Tang CY, Mulcahy D. Recent developments in forward osmosis: Opportunities and challenges. Journal of Membrane Science. 2012;396:1-21.

[93] Hartanto Y, Yun S, Jin B, Dai S. Functionalized thermo-responsive microgels for high performance forward osmosis desalination. Water Research. 2015;70:385-93.

[94] Galaev I, Mattiasson B. Smart Polymers: Applications in Biotechnology and Biomedicine, Second Edition: CRC Press; 2007.

[95] Lyon LA, Serpe MJ. Hydrogel Micro and Nanoparticles: Wiley; 2012.

[96] Razmjou A, Simon GP, Wang HT. Effect of particle size on the performance of forward osmosis desalination by stimuli-responsive polymer hydrogels as a draw agent. Chemical Engineering Journal. 2013;215:913-20.

[97] Ling MM, Wang KY, Chung T-S. Highly Water-Soluble Magnetic Nanoparticles as Novel Draw Solutes in Forward Osmosis for Water Reuse. Industrial & Engineering Chemistry Research. 2010;49:5869-76.

[98] Na Y, Yang S, Lee S. Evaluation of citrate-coated magnetic nanoparticles as draw solute for forward osmosis. Desalination. 2014;347:34-42.

[99] Ge QC, Su JC, Chung TS, Amy G. Hydrophilic Superparamagnetic Nanoparticles: Synthesis, Characterization, and Performance in Forward Osmosis Processes. Industrial & Engineering Chemistry Research. 2011;50:382-8.

[100] Ling MM, Chung T-S, Lu X. Facile synthesis of thermosensitive magnetic nanoparticles as "smart" draw solutes in forward osmosis. Chemical Communications. 2011;47:10788-90.

[101] Dey P, Izake EL. Magnetic nanoparticles boosting the osmotic efficiency of a polymeric FO draw agent: Effect of polymer conformation. Desalination. 2015;373:79-85.

[102] Zhou A, Luo H, Wang Q, Chen L, Zhang TC, Tao T. Magnetic thermoresponsive ionic nanogels as novel draw agents in forward osmosis. RSC Advances. 2015;5:15359-65.

[103] Zhao Q, Chen N, Zhao D, Lu X. Thermoresponsive Magnetic Nanoparticles for Seawater Desalination. ACS Applied Materials & Interfaces. 2013;5:11453-61.

[104] Bai H, Liu Z, Sun DD. Highly water soluble and recovered dextran coated Fe3O4 magnetic nanoparticles for brackish water desalination. Separation and Purification Technology. 2011;81:392-9.

[105] Jessop PG, Heldebrant DJ, Li X, Eckert CA, Liotta CL. Green chemistry: Reversible nonpolar-to-polar solvent. Nature. 2005;436:1102-.

[106] Jessop PG, Mercer SM, Heldebrant DJ. CO2-triggered switchable solvents, surfactants, and other materials. Energy & Environmental Science. 2012;5:7240-53.

[107] Orme CJ, Wilson AD. 1-Cyclohexylpiperidine as a thermolytic draw solute for osmotically driven membrane processes. Desalination. 2015;371:126-33.

[108] Wendt DS, Orme CJ, Mines GL, Wilson AD. Energy requirements of the switchable polarity solvent forward osmosis (SPS-FO) water purification process. Desalination. 2015;374:81-91.

[109] Kohno Y, Saita S, Men Y, Yuan J, Ohno H. Thermoresponsive polyelectrolytes derived from ionic liquids. Polymer Chemistry. 2015;6:2163-78.

[110] Kohno Y, Ohno H. Key Factors to Prepare Polyelectrolytes Showing Temperature-Sensitive Lower Critical Solution Temperature-type Phase Transitions in Water. Australian Journal of Chemistry. 2012;65:91-4.

[111] McCutcheon JR, Elimelech M. Influence of concentrative and dilutive internal concentration polarization on flux behavior in forward osmosis. Journal of Membrane Science. 2006;284:237-47.

[112] You SJ, Wang XH, Zhong M, Zhong YJ, Yu C, Ren NQ. Temperature as a factor affecting transmembrane water flux in forward osmosis: Steady-state modeling and experimental validation. Chemical Engineering Journal. 2012;198:52-60.

[113] Fukumoto K, Ohno H. LCST-Type Phase Changes of a Mixture of Water and Ionic Liquids Derived from Amino Acids. Angewandte Chemie International Edition. 2007;46:1852-5.

[114] Plechkova NV, Seddon KR. Applications of ionic liquids in the chemical industry. Chemical Society Reviews. 2008;37:123-50.

[115] Cai Y, Wang R, Krantz WB, Fane AG, Hu XM. Exploration of using thermally responsive polyionic liquid hydrogels as draw agents in forward osmosis. RSC Advances. 2015;5:97143-50.

Chapter 3. Functionalized Thermoresponsive Microgels for High Performance Forward Osmosis Desalination

Yusak Hartanto, Seonho Yun, Bo Jin, Sheng Dai

School of Chemical Engineering, The University of Adelaide, SA 5005, Australia

Graphical Abstract:

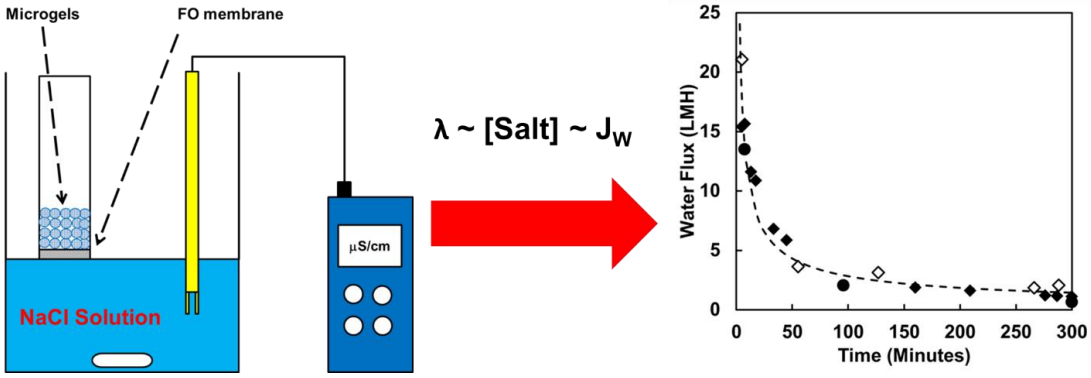

Statement of Authorship

Title of Paper	Functionalized Thermoresponsive Microgels for High Performance Forward Osmosis Desalination
Publication Status	☑ Published ☐ Accepted for Publication ☐ Submitted for Publication ☐ Unpublished and Unsubmitted w ork w ritten in manuscript style
Publication Details	Water Research, 70, 2015, 385 – 393. doi:10.1016/j.watres.2014.12.023

Principal Author

Name of Principal Author (Candidate)	Yusak Hartanto		
Contribution to the Paper	Design the major experiments, data analysis and manuscript writing.		
Overall percentage (%)	60 %		
Certification:	This paper reports on original research I conducted during the period of my Higher Degree by Research candidature and is not subject to any obligations or contractual agreements with a third party that would constrain its inclusion in this thesis. I am the primary author of this paper.		
Signature		Date	

Co-Author Contributions

By signing the Statement of Authorship, each author certifies that:

iv. the candidate's stated contribution to the publication is accurate (as detailed above);

v. permission is granted for the candidate in include the publication in the thesis; and

vi. the sum of all co-author contributions is equal to 100% less the candidate's stated contribution.

Name of Co-Author	Seonho Yun		
Contribution to the Paper	Helped to perform the experiment		
Signature		Date	

Name of Co-Author	Bo Jin		
Contribution to the Paper	Designed the experiment and manuscript correction		
Signature		Date	

Name of Co-Author	Sheng Dai		
Contribution to the Paper	Designed the experiment and manuscript correction		
Signature		Date	27/01/2016

3.1 Abstract

Stimuli-responsive hydrogels were recently proposed for energy-saving forward osmosis (FO) process. However, their low water flux and poor dewatering ability for reuse make them unsuitable for desalination process. In this work, the co-polymer microgels of N-isopropylacrylamide and acrylic acid with different mixing ratios were synthesized using surfactant-free emulsion polymerization to produce submicron-size hydrogels with high surface area and fast swelling-deswelling response. The microgels were employed as draw agents in a laboratory scale FO desalination system to treat synthetic brackish water. The microgel-based FO process displayed a high water flux up to 23.8 LMH and high water recovery ability up to 72.4%. In addition, we explored a new approach to measure water flux via the on-line conductivity measurement of feed solution. This on-line conductivity analysis approach appeared to be an accurate and efficient method for evaluating microgel-based FO desalination performance. Our experimental data revealed that the stimuli-responsive microgel was an efficient draw agent for FO desalination.

Keywords: microgels; forward osmosis; desalination; water flux; dewatering ability; N-isopropylacrylamide; on-line conductivity; thermoresponsive

3.2 Introduction

Water scarcity is one of the top global challenges that currently affects over one-third of world population in water-stressed countries and this situation is worsen due to increasing population, water pollution, industrialization, and climate change (McCutcheon et al., 2006; Elimelech and Phillip, 2011). Over 96 % of water resources worldwide are in the ocean, which have high salinity and cannot be directly used without desalination process (Smalley, 2005). To date, reverse osmosis (RO) process via a polymeric membrane is the most widely used technology for seawater desalination. However, the high energy and capital costs together with the low water permeability and poor fouling resistance associated with RO membrane have been an on-going challenge for its industrial applications. There is a pressing need for the development of a cost-effective desalination process.

In the recent years, forward osmosis (FO) membrane process has gained a lot of attention due to its potential as low energy membrane separation process. The FO desalination is a two-stage desalination process where the water is drawn from a saline solution as a result of osmotic gradient and then the water can be recovered from draw solute by means of membrane separation, distillation, external magnetic field, extraction, precipitation and combination of these separation processes (Luo et al., 2014). Inorganic salts, such as $MgCl_2$, $MgSO_4$, NaCl, KCl, $KHCO_3$, $Ca(NO_3)_2$, NH_4HCO_3 have been employed as the draw solutes for FO processes (Achilli et al., 2010). Although these inorganic reagents have excellent capability to create significant osmotic pressure gradient, pressure-driven membrane processes such as nanofiltration and reverse osmosis are still required to recover water from these salts (Zhao et al., 2012). That leads to an increase in the energy consumption for the

overall FO process. Furthermore, reverse salt flux and internal concentration polarization are present when these salts are employed as draw solutes, which subsequently reduce the performance of separation process. Scientists found that the use of ammonium bicarbonate (NH_4HCO_3) as the draw agents could lead to a low energy FO process, as water can be recovered via low temperature distillation process using low grade heat (McCutcheon et al., 2006; McGinnis and Elimelech, 2007). The draw solute can decompose into ammonia and carbon dioxide upon heating and leave water phase. Unfortunately, the purity of water resulted from such process was not able to meet standard drinking water regulation due to very high ammonium bicarbonate leaked to the water product (Ge et al., 2013).

Subsequent research proposed that poly (ethylene glycol) diacid-coated superparamagnetic nanoparticles could be used as draw solutes and the absorbed water can be recovered using external magnetic field to produce fresh water (Ge et al., 2010). However, water flux performance was far below the water flux generated by inorganic salts. Furthermore, these magnetic nanoparticles formed aggregates during the recovery stage which decreased their effectiveness to be reused (Ling and Chung, 2011; Ling et al, 2011). Other materials have also been explored for FO processes, including the sodium salt of polyacrylic acid (Ge et al., 2012), 2-methylimidazole-based organic compounds (Swee Kuan et al., 2010), switchable polarity solvent (Stone et al., 2013), hydroacid complexes (Ge and Chung, 2013), Na^+ functionalized carbon quantum dots (Guo et al., 2014) and N,N',N"-triacylated tris(2-aminoethyl)amine (acyl-TAEA) derivatives (Noh et al., 2012). Although these materials displayed reasonable water flux, their low water recovery ability is a drawback for their applications in industrial desalination processes.

Stimuli-responsive hydrogels are three dimensional polymer networks that swell and deswell in respond to the applied stimuli, such as temperature, pH, external magnetic field, ionic strength, and light. Due to their ability to reversibly swell and deswell, they have been recently introduced as a new class of draw agent for FO desalination. In the early study, the hydrogel was synthesized using N-isopropylacrylamide and hydrophilic monomers of sodium acrylate or acrylamide (Li et al., 2011). The water contained in the hydrogels was recovered by heating the hydrogels and applying pressure. Unfortunately, the water flux of this hydrogels (0.30-0.96 LMH) with salt rejection of 95.4% was relatively lower than other types of synthetic draw agents. In order to improve the performance of hydrogels-based FO process, composite hydrogels were recently prepared by incorporating inorganic nanoparticles such as carbon particles, magnetic nanoparticles and reduced graphene oxide (*r*GO) (Razmjou et al., 2013a; Zeng et al., 2013). These composite hydrogels showed an enhanced water flux and the water recovery ability. However, the recovered water from hydrogels was mostly in the form of water vapour. Additional condensation unit is then needed to recover water in the form of liquid and will increase the overall costs of FO process.

Currently, the high energy costs for water recovery is still an issue for FO desalination technologies (Altaee et al., 2014). This leads to higher operational cost of FO desalination compared to RO process due to inappropriate selection of water recovery process and materials employed as draw solutes (McGovern and Lienhard V, 2014). Other major limitations are incomplete separation of draw agents and lower water flux compared to the RO process (Cai et al., 2013). In this study, we applied N-isopropylacrylamide (NIPAM) and acrylic acid (AA) as co-monomers to

synthesize functional co-polymer microgels P(NIPAM-AA) as the draw agents for FO process. The microgels with different ratios of AA and NIPAM were prepared using surfactant-free emulsion polymerization (SFEP) approach to eliminate the contamination of small surfactants. Moreover, a laboratory FO system was established to evaluate the desalination performance of the P(NIPAM-AA) microgel-based FO process. Our results show that the employed P(NIPAM-AA) microgels can significantly improve water flux and water recovery ability of the FO desalination process. For the first time, we use microgels in FO desalination process. The microgels are also functionalized with acrylic acid rather than sodium acrylate to improve the water flux. Besides, we explored and employed new on-line conductivity monitoring method to analyze water flux of the FO system.

3.3 Materials and methods

3.3.1 Materials

N-isopropylacrylamide (NIPAM, > 98%), purchased from Tokyo Chemical Industry, was purified by recrystallization in n-hexane and dried at room temperature. N-N'-methylenebisacrylamide (MBA, >98%), acrylic acid (AA, >99.5%) and ammonium persulfate (APS) were purchased from Sigma-Aldrich. Sodium chloride was purchased from VWR. Cellulose triacetate forward osmosis (CTA-FO) membranes were purchased from Hydration Technologies Inc. (HTI, USA).

3.3.2 Synthesis of co-polymer microgels

The P(NIPAM-AA) microgels were synthesized using surfactant-free semi-batch emulsion polymerization. In a typical experiment, 0.5 g of NIPAM/AA mixtures at different mass ratios and 0.005 g of MBA were dissolved in 47 mL of Millipore

water. The solution was transferred to a 250 mL three-necked flask fitted with a condenser, a mechanical stirrer and gas inlet/outlet. The semi-batch feeding solution was prepared by dissolving 2.5 g of NIPAM/AA mixtures at different mass ratios, 0.025 g of MBA and 0.025 g of APS in 30 mL of Millipore water.

After degassing both batch and semi-batch feeding solutions for one hour, the batch solution was heated to 75 °C under nitrogen atmosphere. 3.0 mL of APS solution (0.005 g) was injected to initiate the polymerization. Semi-batch feeding solution was injected slowly at a rate of 6.25 mL/hour using a syringe pump after the batch solution turned into cloudy. The polymerization was carried out overnight under continuous stirring. After cooling, the microgels were purified using membrane dialysis (MWCO 12–14 kDa) against Millipore (or DI) water for three days. During three days purification, the water was changed every two hours. The purification was confirmed by comparing the conductivity of dialysis water and the conductivity of Millipore (or DI) water. The purified microgels were dried at 70 ^{o}C and grounded into fine powders.

3.3.3 Conductometric and potentiometric titration

The amount of acrylic acid in the microgels was quantified using conductometric and potentiometric titration. Typically, the pH of the dispersion of P(NIPAM-AA) microgel (100 mL, ~ 1 mg/mL) was adjusted to pH 3 using hydrochloric acid. The solution was then back titrated using 0.1 M NaOH. After each addition of NaOH, the solution conductivity and pH were measured using a pre-calibrated Aqua-CP/A pH and conductivity meter.

3.3.4 Dynamic light scattering

The hydrodynamic diameters (d_h) of the synthesized P(NIPAM-AA) microgels were measured by dynamic light scattering (DLS) at different temperatures using a Zetasizer (Malvern, Nano-ZS). The DLS data were collected on an autocorrelator and the CONTIN software package was used to analyze the intensity autocorrelation functions. The swelling ratio (SR) of microgels can be calculated using the following equation:

$$SR = \left(\frac{d_{h,25}}{d_{h,40}}\right)^3 \qquad \text{Eq. 3.1}$$

where SR is the swelling ratio of the microgels, $d_{h,25}$ (nm) is the hydrodynamic diameter of the microgels at 25 ^oC and $d_{h,40}$ (nm) is the hydrodynamic diameter of the microgels at 40 ^oC.

3.3.5 Water flux evaluation

100 mg of grounded microgel powders were placed in our customized membrane setup equipped with on-line conductivity monitoring system as shown in Figure 3.1. The photo of this laboratory on-line conductivity monitoring system for FO process can be found in Figure 3.8 (Supporting Information). Calibrated conductivity probe (with probe cell constant, k = 1.0) was immersed in the feed solution of 2000 ppm NaCl to continuously monitor the conductivity against time for five hours. The conductivity data can be converted into the concentration of sodium chloride after fitting with the following equation:

$$\lambda = 1.7821 C_t \qquad \text{Eq. 3.2}$$

where λ is the conductivity of feed solution (μS/cm) and C_t is the feed concentration at time t (ppm).

The water flux was calculated using the conductivity data based on the mass balance equation which is described by the following equations:

$$V_t = \frac{C_i V_i}{C_t} \quad \text{Eq. 3.3}$$

$$J_w = \frac{V_i - V_t}{A\,t} \quad \text{Eq. 3.4}$$

where V_t (mL) is the volume of feed at time t, V_i (mL) is the initial volume of feed, C_i (ppm) is the initial feed concentration, C_t (ppm) is the feed concentration at time t, J_w (LMH) is the water flux, A (m^2) is the effective membrane surface area and t (h) is the time interval where the volume of the feed solution changes.

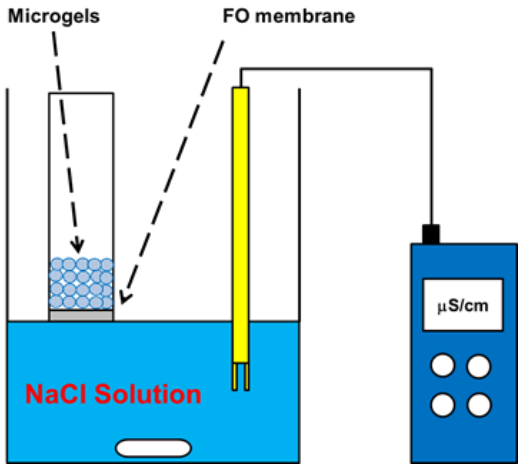

Figure 3.1 Forward osmosis setup using a conductivity probe to monitor water flux.

3.3.6 Water recovery

After five hours, the swelled microgels were transferred to centrifuge tubes and weighed. The swelled microgels were then centrifuged at 40 ^oC and 12,000 rpm for 10 minutes to separate absorbed water from polymer microgels. The recovered water

was determined using gravimetric analysis. The water recovered from microgel deswelling was calculated using the following equations:

$$C_p = \frac{W_d}{W_d + W_w} \quad \text{Eq. 3.5}$$

$$W_g = W_m(1 - C_p) \quad \text{Eq. 3.6}$$

$$R = \frac{W_R}{W_g}\ x\ 100\% \quad \text{Eq. 3.7}$$

where C_P (g microgels/g H_2O) is the concentration of microgels in the centrifuge tube, W_d (g) is the weight of dry microgel powders, W_W (g) is the weight of water absorbed by the microgels determined from water absorption from water flux measurement, W_g (g) is the weight of water in the microgels, W_m (g) is the weight of microgels in the centrifuge tube, W_R (g) is the weight of absorbed water recovered from the tube and R (%) is the percentage of water recovered from the deswelled microgels.

3.3.7 Microgels recycling in three cycles

The swelled microgels after the 1st cycle were dried in oven until constant weights. The dried microgels were grounded into fine powders and placed in our FO system for the 2nd cycle measurement, where the conductivity readings of sodium chloride solution against time were recorded to calculate water flux. Similar approach was repeated for the 3rd cycle measurement.

3.4 Results and Discussion

3.4.1 Synthesis and characterization of the microgels

Semi-solid forward osmosis draw agent like stimuli-responsive hydrogels requires fast water absorption and releasing capability in order to produce high water flux and water recovery rate. Unfortunately, hydrogels synthesized by bulk polymerization approach has slower water absorption and releasing rate compared to small hydrogels (microgels) synthesized using emulsion polymerization approach. This is due to the formation of dense skin layer in bulk hydrogels which retards water diffusion in and out of hydrogels (Hoare, 2012). For this reason, emulsion polymerization is chosen to overcome this problem to produce faster water absorption and releasing rate.

The conventional approach to synthesize microgels is emulsion polymerization where surfactants, such as sodium dodecyl sulphate (SDS), are added to the mixture of monomers, cross linker and initiator to stabilize the formed microgels. The obtained microgels can be purified by dialysis against deionized water to remove surfactants and unreacted monomers. However, complete removal of all surfactant might be difficult. These unremoved surfactants could affect physico-chemical characteristics and performance of the microgels, depending upon their final applications (Pelton and Hoare, 2011). For example, the water absorption capability of the microgels could be reduced in the presence of charged surfactants. For this reason, surfactant-free emulsion polymerization (SFEP) synthesis route was chosen in this study. Different from traditional emulsion polymerization, SFEP always produces monodisperse microgels. In addition, the synthesis was conducted in a semi-batch mode rather than a batch mode to produce high solids content of microgel suspension which is an effective technique for mass production of microgels to meet

the industrial scale quantity of draw agent for microgels-based FO desalination. The yields of the microgels vary in a range of 70-90%, indicating most of feed monomers have been polymerized.

The amount of AA incorporated into the microgels can be calculated from pH and conductivity titration curves as shown in Figure 3.9 (Supporting Information). The calculated amount of AA incorporated into the microgels is above 75% of the feed for all microgels, indicating high conversions of AA during copolymerization. The high incorporation of AA is crucial when doing copolymerization as some co-monomers are not readily incorporated due to their different reactivity ratios with other monomers (Sheikholeslami et al., 2012). Furthermore, dynamic light scattering was performed at different temperatures to determine the volume phase transition temperature (VPTT) of the microgels. This characterization method serves two main purposes, determination of individual microgel particle size and VPTT. Size larger than FO membrane pore size is needed to prevent leakage of microgels to the feed solution and hence minimizing draw agent replenishment. The VPTTs of microgels can be useful preliminary information on energy requirement of dewatering process of microgels. Microgels with higher VPTTs require more energy in the form of heat to raise their temperature and to recover the absorbed water. Dynamic light scattering was performed at different temperatures to determine the VPTT of the microgels. The profiles of hydrodynamic diameter vs. temperature are shown in Figure 3.2a. Table 3.1 shows that the hydrodynamic particle sizes of the microgels at 25 ^{o}C vary in a range of 200-300 nm. Below the transition temperatures, the microgels show a swelled state where polymers are fully hydrated. As temperature increases to phase transition temperatures, the microgels shrink significantly due to the dehydration of

PNIPAM segments (Shen et al., 2014). As a result, the microgels can release up to 70% of water absorbed into bulk solution. Shen et al. (2012) observed that the VPTTs of these microgels did not change significantly as the AA mass varied between 0 wt% and 50 wt%. This result agrees well with the obtained VPTTs from our P(NIPAM-AA) microgels with AA varied from 0 to 70 wt% (Table 3.1).

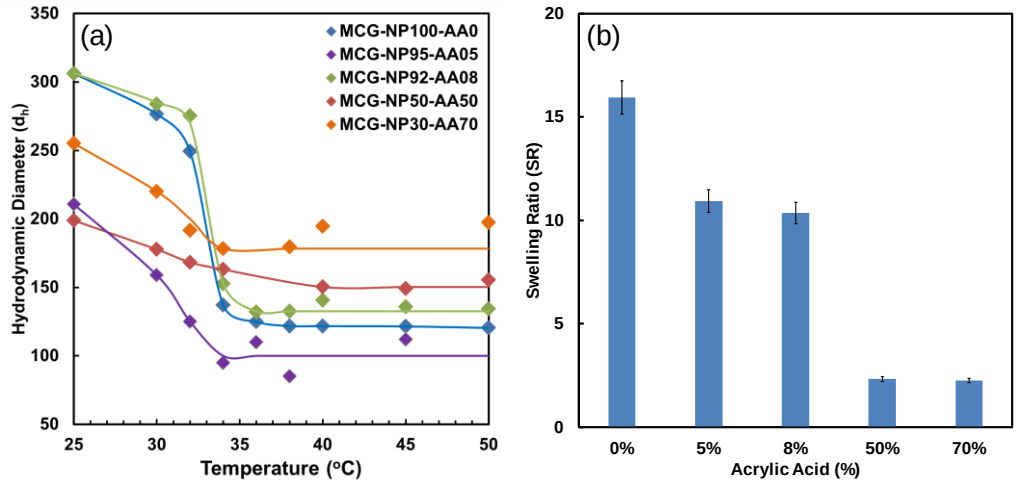

Figure 3.2 (a) Volume phase transition temperatures (VPTT) of P(NIPAM)-AA microgels with different of acrylic acid contents; and (b) Swelling ratios of various P(NIPAM-AA) microgels at 40 ^{o}C.

While the AA content in this study does not affect the VPTTs of the microgels, the swelling ratios do vary with the AA contents in the microgels. The swelling ratios of the microgels with different AA contents at 40 ^{o}C are shown in Figure 3.2b. As the AA content increases in a range of 0 – 70%, the swelling ratio decreases from 15.9 to 2.3. The microgels with a low AA content (5% or 8%) display higher swelling ratio than those with a high content of AA (50% or 70%). That is due to the fact that PNIPAM moieties dominate the hydrophobic interaction in NIPAM-rich microgels. The high AA content microgels shrink slightly due to the strong

electrostatic repulsion among these deprotonated carboxylic groups, preventing polymer network to collapse.

Table 3.1 Synthesis and characterization of P(NIPAM-AA) microgels

Nomenclature	Monomer Content in Feed (g)		MBA	APS (g)	AA content (mmol g^{-1} polymer)		Yield	d_h*	VPTT**
	NIPAM	AA	(g)		Observed	Theoretical	(%)	(nm)	(ºC)
MCG-NP100-AA0	4.00	-	0.04	0.04	0	0	88	306	34
MCG-NP95-AA5	3.80	0.20	0.04	0.04	0.56	0.74	72	211	33
MCG-NP92-AA8	3.68	0.32	0.04	0.04	0.82	1.10	97	306	34
MCG-NP50-AA50	2.00	2.00	0.04	0.04	5.71	6.79	84	200	32
MCG-NP30-AA70	1.20	2.80	0.04	0.04	9.23	9.71	69	255	32

* Hydrodynamic diameters of microgels measured at 25 ºC in water

**Determined from the tangent line of the inflexion point of hydrodynamic diameter *vs.* temperature curves

3.4.2 New method for water flux evaluation via conductivity measurement

The commonly used technique to quantify water flux is to measure the mass increase of hydrogels through gravimetric method, where the mass of swelled hydrogels is weighed at certain time intervals (Li et al., 2011; Razmjou et al., 2013a; Cai et al., 2013; Razmjou et al., 2013b; Razmjou et al., 2013c). However, this approach could lead to large systematic errors when the powder quantity is small. We found that the water flux data fluctuate during the measurement period, as presented in Figure 3.10 (Supporting Information). In this study, we developed a new approach to analyze water flux for batch microgel-based FO process. Due to the difference in the osmotic pressures of feed solution and microgels at both sides of FO membrane, water is transferred to microgels, resulting in changing the feed concentration with time (Wang et al., 2014). These concentration changes can be monitored using a conductivity meter. Our data revealed that conductivity measurement provides much more accurate results of water flux for laboratory based evaluation than the commonly used gravimetric method. Importantly, the conductivity analysis can provide efficient on-line measurements to determine desalination performance of FO process. The conductivity calibration curve in Figure 3.3 shows a linear relationship between sodium chloride concentration and solution conductivities, which was established using statistic regression method. Based on the calibration curve, the concentration of sodium chloride can be calculated from conductivity measurement based on Eq. 3.2. The variation in NaCl concentration can be further used to calculate the amount of water drawn by microgels using Eq. 3.3. Then, the water flux can be estimated from Eq. 3.4 by dividing the water absorption rate with effective membrane area.

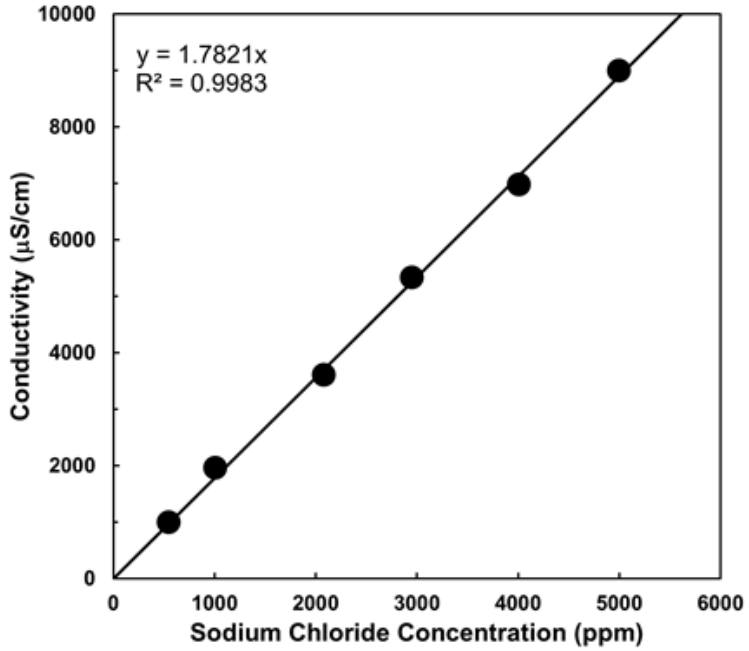

Figure 3.3 Relationship profile between conductivity (k = 1.0) and concentration of sodium chloride.

Before each conductivity measurement, the FO membrane was allowed to soak in 2000 ppm NaCl solution overnight to reach an equilibrium condition (Li et al., 2011). The equilibrium condition is needed to saturate the FO membrane with sodium chloride and to minimize the diffusion of sodium chloride through the membrane. Furthermore, the transport of water molecules is faster than the transfer of sodium chloride through cellulose acetate membrane (Lonsdale et al., 1965). Hence, the assumption of no sodium chloride leakage during the water flux evaluation is valid. In addition, the conductivity probe was conditioned for 30 minutes in 2000 ppm NaCl solution prior to conductivity measurement to ensure that the conductivity changes are not affected due to external factors, such as temperature, possible NaCl adsorption on the membrane and equilibrium readings in conductivity meter. In order to validate the reproducibility of our new method of

using conductivity measurement to calculate water flux, all experiments were conducted three times for each microgel. Figure 3.4 presents these calculated water flux results, indicating that a good repeatability of conductivity method for all microgels. Water flux for each sample follows a similar profile where high fluxes are observed during the first 5 to 10 minutes, resulting in a rapid change in conductivity. After 60 minutes, water flux declines rapidly and reaches equilibrium. In contrast, high water fluxes for bulk P(NIPAM) and bulk co-polymer of NIPAM and sodium acrylate hydrogels, P(NIPAM-SA), were observed during the first two hours and reached equilibrium after 7 hours (Li et al., 2011). The flux for P(NIPAM) hydrogels after 60 minutes was 0.30 LMH, while a water flux of 0.55 LMH was given by P(NIPAM-SA) hydrogels with 50 wt% of SA. Another study conducted by the same group, using the P(NIPAM-SA) hydrogel with 50 wt% of SA as a model draw agent, showed that the dimensions of the hydrogel affect water flux magnitudes. They reported that small hydrogel had a higher water flux than the large one due to greater membrane contact area. The water fluxes for the hydrogels with sizes of 2-25 μm and 500-1000 μm were approximately 1.3 LMH and 0.8 LMH, respectively, in the first hour (Razmjou et al., 2013b). On the other hand, the water flux of our P(NIPAM) and P(NIPAM-AA) microgels with the same monomers were approximately 2 LMH and 4 LMH, respectively. The higher fluxes observed from our study can be the result of the large surface area of the microgels produced from surfactant-free emulsion polymerization. The large surface area of the microgels is beneficial for enhancing interfacial contact between microgels and FO membrane, and therefore results in a shorter time needed to reach the equilibrium condition

compared to bulk hydrogels reported by Li et al. (2011). Table 3.2 summarizes key results from this and previous studies on hydrogel-based FO process.

Table 3.2 Summary of the water flux and swelling equilibrium time of bulk hydrogels and microgels

Draw agents	Composition (wt%)			Synthesis Method	Particle size (μm)	Initial Water Flux (LMH)	Water Recovery (%)	Equilibrium Swelling Time (minutes)	References
	NIPAM	SA	AA						
Homo polymer Hydrogels	100	-	-	Bulk Polymerization	50-150	0.30	75	420	(Li et al., 2011)
Co-polymer Hydrogels	50	50	-			0.55	17		
Co-polymer Hydrogels	50	50	-	Bulk Polymerization	500-1000	0.8	-	600	(Razmjou et al., 2013b)
					2-25	1.3			
Microgels	100	-	-	Surfactant-free Emulsion Polymerization	0.306	2	72	60	This study
	50	-	50		0.200	4	-		

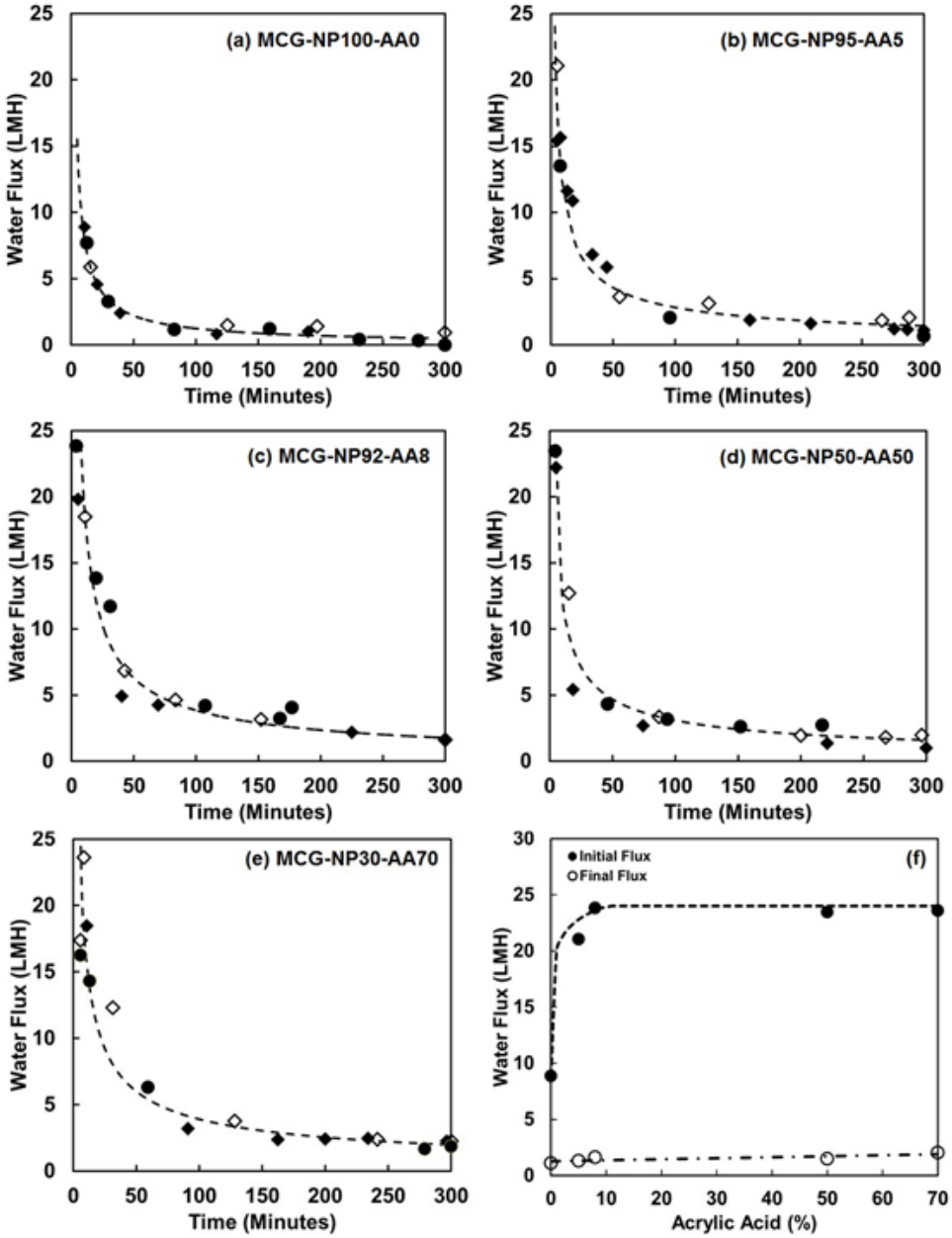

Figure 3.4 (a)-(e) Water flux for the co-polymer microgels with different acrylic acid contents over a five hour test period; and (f) effect of acrylic acid contents on the water flux.

3.4.3 Effect of acrylic acid on water flux

In practice, thermoresponsive microgels are rarely polymerized from a single monomer. Co-monomers are usually employed to synthesize microgels with objectives to provide certain functionalities, such as dual-response microgels

(temperature and pH), growing inorganic nanoparticles inside the microgels (Zhang et al., 2004), and enhanced swelling-deswelling ratios. Our results show that the AA contents in P(NIPAM-AA) can significantly influence the hydrophilic and hydrophobic properties of the microgels. Below the pKa of AA (~ 4.75), the AA moieties are hydrophobic after their protonation. As the pH is above the pKa of AA, the carboxylic groups become deprotonated and thus make the microgels be hydrophilic. The hydrophilic characteristic of the microgels at moderate pH will facilitate water absorption.

Figure 3.4f shows that the P(NIPAM-AA) microgels perform an improved water flux compared to the P(NIPAM) microgels. For example, the addition of 5% acrylic acid resulted in a significantly higher water flux of 21 LMH than the initial water flux of 8.9 LMH for the microgels without AA incorporation. The flux increases slightly to 23.8 LMH when microgels are synthesized with 8% AA. It is interesting to note the addition of excess AA from 50% to 70% appears to have limited impact on the water flux of the co-polymer microgels measured after five hours. The water flux after five hours absorption period for P(NIPAM) microgels is 1.01 LMH, while P(NIPAM-AA) microgels with 5% and 8% AA show a flux of 1.31 LMH and 1.62 LMH, respectively. A further increase in AA moieties to 50% and 70% results in slight improvement of water flux from 1.49 LMH to 2.05 LMH, respectively. In summary, AA does not have important effect on the water flux when its content is beyond 8% in the microgels.

The water fluxes of our microgels are higher than the hydrogels reported in previous study (Li et al., 2011). The major reason might come from the structure-property relationship of materials synthesized. In this work, we used emulsion

polymerization method to synthesize submicron-size gels as the building block for temperature responsive hydrogels compared to those prepared by bulk polymerization in previous studies. This approach allows us to produce submicron-size gels which have large surface area and fast response. As a result, the water fluxes are improved significantly for microgels.

3.4.4 Effect of acrylic acid on dewatering performance of the microgels

As the temperature is above the VPTT, the PNIPAM moieties become hydrophobic, resulting in shrinking the microgels, and consequently releasing the absorbed water. However, AA moieties do not change their chemical properties since the carboxylic groups only response to pH variation. When the swelled microgels are heated to 40 ^{o}C, the co-polymer microgels with up to 8% AA undergo a phase separation while the microgels incorporated with 50% or more AA do not show obvious phase separation. As the AA content increases, the hydrophilicity of the microgels increases because of the increment of carboxylic groups in microgels. This means that microgels with a higher AA content can keep more water than the PNIPAM homopolymer microgels. As a result, an increase in AA has adverse effect on the recovery of absorbed water as increasing temperature over their VPTTs.

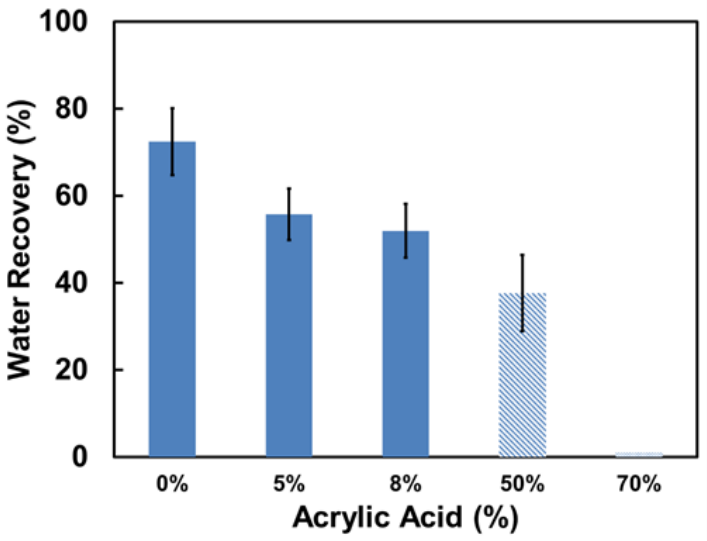

Figure 3.5 Water recovery ability of the co-polymer microgels with different acrylic acid contents (The pH of microgels with 50wt% AA is adjusted using hydrochloric acid).

Figure 3.5 shows that the dewatering ability of the microgels decreases as AA contents increase. Homopolymer PNIPAM microgels demonstrate the highest water recovery (72%), while the co-polymer P(NIPAM-AA) microgels with 5% and 8% AA have 55% and 52% water recovery. It is interesting to note that when the AA content in the microgels is high, such as 50% and 70%, almost no water can be recovered from the microgels at the temperature beyond the VPTT. However, when trace amount of hydrochloric acid is added to adjust the pH to about 5, a temperature of 40 ^{o}C can lead to a phase separation of the microgels with 50%wt of AA. The pH change using hydrochloric acid facilitates the protonation of carboxylate and relevant dewatering performance of microgels. The amount of water recovered from our microgel-based FO process is over 50% for PNIPAM-AA microgels which is higher than the water recovery from previous studies where only over 17% of absorbed water recovered (Li et al., 2011).

Increasing AA moieties has an opposite effect on water flux and water recovery in our microgel-based FO system. A high AA content of the microgels leads to an enhanced water flux, while reducing the water recovery. To determine the best microgels which show a balanced performance in water flux and water recovery, the water flux and water recovery are multiplied to give the overall water production rate from microgel-based FO process. Figure 3.6 presents the overall water production rates of FO process using the co-polymer P(NIPAM-AA) microgels. We note that overall FO performance is the function of the AA contents in microgels, and the microgel with 8% AA gives the best overall water production rate.

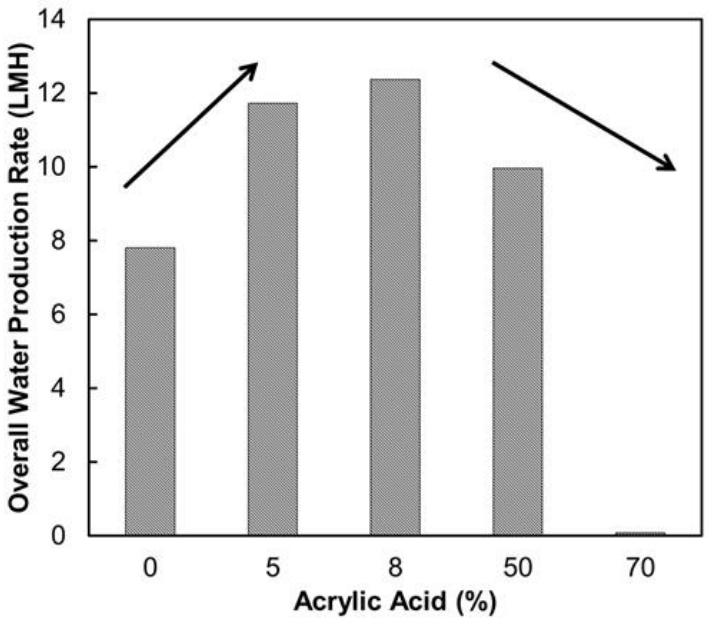

Figure 3.6 Effect of acrylic acid contents on the overall water production rates of the microgel-based FO process (Overall water production rate = water flux (LMH) x water recovery (%))

3.4.5 Recyclability of thermoresponsive microgels in forward osmosis

FO process relies on the reversible abilities of water absorption and releasing of the draw agent. In order to examine the recycling ability of our thermoresponsive microgels for the reuse in the FO desalination, recycling experiments were carried out three times to assess the performance of water flux and water recovery. Homopolymer and co-polymer microgels with 8% AA are compared in this study in terms of their recovery recyclability. Figure 3.7 shows that both thermoresponsive homopolymer and co-polymer microgels demonstrate promising water flux and water recovery performance in the three recycling FO processes. Generally, the initial water flux remains constant throughout the subsequent cycles and the equilibrium swelling time remains the same as the first cycle except for the copolymer microgels with 8% AA where a slight decrease of water flux from 23.8 LMH to 20.6 LMH.

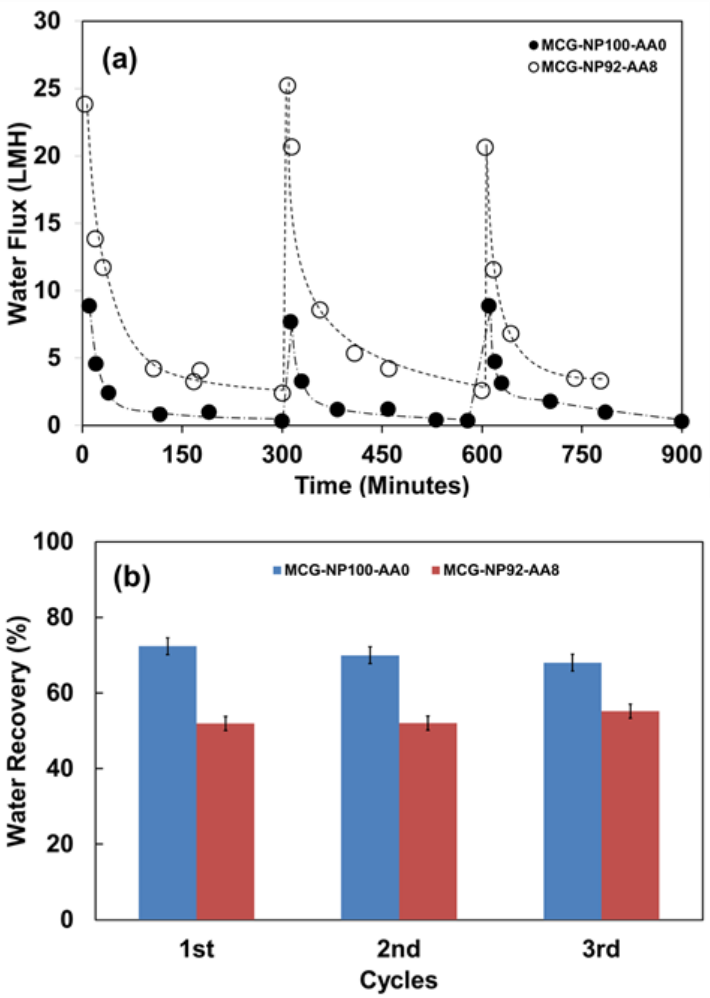

Figure 3.7 (a) Water flux profiles for MCG-NP100-AA0 and MCG-NP92-AA8 microgels for three consecutive cycles; and (b) water recovery for MCG-NP100-AA0 and MCG-NP92-AA8 microgels for three consecutive cycles.

3.5 Conclusion

A series of co-polymer P(NIPAM-AA) microgels was prepared by surfactant-free emulsion polymerization. Their desalination performance in terms of water flux and dewatering ability were evaluated in a laboratory FO system. We for the first time developed an on-line conductivity method to evaluate water flux of microgel-based FO process. This method was confirmed as an accurate and efficient approach to

assess the FO performance. The systematic results showed that the application of microgels can lead to a cost-effective FO desalination process. Co-polymer P(NIPAM-AA) microgels show comparably higher water flux and water recovery ability than those prepared by bulk polymerization, while a shorter equilibrium time for water absorption is required. Thermoresponsive microgels also show promising recyclability of water absorption and water recovery.

3.6 References

Achilli, A., Cath, T.Y. and Childress, A.E., 2010. Selection of inorganic-based draw solutions for forward osmosis applications. Journal of Membrane Science 364(1–2), 233-241.

Altaee, A., Zaragoza, G. and van Tonningen, H.R., 2014. Comparison between Forward Osmosis-Reverse Osmosis and Reverse Osmosis processes for seawater desalination. Desalination 336, 50-57.

Cai, Y., Shen, W., Loo, S.L., Krantz, W.B., Wang, R., Fane, A.G. and Hu, X., 2013. Towards temperature driven forward osmosis desalination using Semi-IPN hydrogels as reversible draw agents. Water Research 47(11), 3773-3781.

Elimelech, M. and Phillip, W.A., 2011. The Future of Seawater Desalination: Energy, Technology, and the Environment. Science 333(6043), 712-717.

Ge, Q., Su, J., Amy, G.L. and Chung, T.S., 2012. Exploration of polyelectrolytes as draw solutes in forward osmosis processes. Water Research 46(4), 1318-1326.

Ge, Q., Su, J., Chung, T.S. and Amy, G., 2010. Hydrophilic Superparamagnetic Nanoparticles: Synthesis, Characterization, and Performance in Forward Osmosis Processes. Industrial & Engineering Chemistry Research 50(1), 382-388.

Ge, Q.C. and Chung, T.S. (2013) Hydroacid complexes: a new class of draw solutes to promote forward osmosis (FO) processes. Chemical Communications 49(76), 8471-8473.

Ge, Q.C., Ling, M.M. and Chung, T.S. (2013) Draw solutions for forward osmosis processes: Developments, challenges, and prospects for the future. Journal of Membrane Science 442, 225-237.

Guo, C.X., Zhao, D., Zhao, Q., Wang, P. and Lu, X., 2014. Na(+)-functionalized carbon quantum dots: a new draw solute in forward osmosis for seawater desalination. Chemical Communications 50(55), 7318-7321.

Hoare, T. (2012) Hydrogel Micro and Nanoparticles, pp. 281-315, Wiley-VCH Verlag GmbH & Co. KGaA.

Li, D., Zhang, X., Yao, J., Simon, G.P. and Wang, H., 2011. Stimuli-responsive polymer hydrogels as a new class of draw agent for forward osmosis desalination. Chemical Communications 47(6), 1710-1712.

Ling, M.M. and Chung, T.S., 2011. Desalination process using super hydrophilic nanoparticles via forward osmosis integrated with ultrafiltration regeneration. Desalination 278(1–3), 194-202.

Ling, M.M., Chung, T.S. and Lu, X.M., 2011. Facile synthesis of thermosensitive magnetic nanoparticles as "smart" draw solutes in forward osmosis. Chemical Communications 47(38), 10788-10790.

Lonsdale, H.K., Merten, U. and Riley, R.L. (1965) Transport properties of cellulose acetate osmotic membranes. Journal of Applied Polymer Science 9(4), 1341-1362.

Luo, H., Wang, Q., Zhang, T.C., Tao, T., Zhou, A., Chen, L. and Bie, X. (2014) A review on the recovery methods of draw solutes in forward osmosis. Journal of Water Process Engineering 4, 212-223.

McCutcheon, J.R., McGinnis, R.L. and Elimelech, M., 2006. Desalination by ammonia–carbon dioxide forward osmosis: Influence of draw and feed solution concentrations on process performance. Journal of Membrane Science 278(1–2), 114-123.

McGinnis, R.L. and Elimelech, M., 2007. Energy requirements of ammonia-carbon dioxide forward osmosis desalination. Desalination 207(1-3), 370-382.

McGovern, R.K. and Lienhard V, J.H. (2014) On the potential of forward osmosis to energetically outperform reverse osmosis desalination. Journal of Membrane Science 469,245-250.

Noh, M., Mok, Y., Lee, S., Kim, H., Lee, S.H., Jin, G. W., Seo, J.H., Koo, H., Park, T.H. and Lee, Y., 2012. Novel lower critical solution temperature phase transition materials effectively control osmosis by mild temperature changes. Chemical Communications 48(32), 3845-3847.

Pelton, R. and Hoare, T., 2011. Microgel Suspensions, pp. 1-32, Wiley-VCH Verlag GmbH & Co. KGaA.

Razmjou, A., Barati, M.R., Simon, G.P., Suzuki, K. and Wang, H., 2013a, Fast Deswelling of Nanocomposite Polymer Hydrogels via Magnetic Field-Induced Heating for Emerging FO Desalination. Environmental Science & Technology 47(12), 6297-6305.

Razmjou, A., Liu, Q., Simon, G.P. and Wang, H., 2013c. Bifunctional Polymer Hydrogel Layers As Forward Osmosis Draw Agents for Continuous Production of Fresh Water Using Solar Energy. Environmental Science & Technology 47(22), 13160-13166.

Razmjou, A., Simon, G.P. and Wang, H., 2013b. Effect of particle size on the performance of forward osmosis desalination by stimuli-responsive polymer hydrogels as a draw agent. Chemical Engineering Journal 215–216, 913-920.

Sheikholeslami, P., Ewaschuk, C., Ahmed, S., Greenlay, B. and Hoare, T. (2012) Semi-batch control over functional group distributions in thermoresponsive microgels. Colloid and Polymer Science 290(12), 1181-1192.

Shen, Z., Bi, J., Shi, B., Nguyen, D., Xian, C.J., Zhang, H. and Dai, S., 2012. Exploring thermal reversible hydrogels for stem cell expansion in three-dimensions. Soft Matter 8(27), 7250-7257.

Shen, Z., Mellati, A., Bi, J., Zhang, H. and Dai, S., 2014. A thermally responsive cationic nanogel-based platform for three-dimensional cell culture and recovery. RSC Advances 4(55), 29146-29156.

Smalley, R.E., 2005. Future global energy prosperity: The terawatt challenge. MRS Bulletin 30(6), 412-417.

Stone, M.L., Rae, C., Stewart, F.F. and Wilson, A.D., 2013. Switchable polarity solvents as draw solutes for forward osmosis. Desalination 312, 124-129.

Swee Kuan, Y., Mehnas, F.N.H., Minglue, S., Kai Yu, W. and Tai-Shung, C., 2010. Study of draw solutes using 2-methylimidazole-based compounds in forward osmosis. Journal of Membrane Science 364(1-2), 242-252.

Wang, H., Wei, J. and Simon, G.P., 2014. Response to Osmotic Pressure versus Swelling Pressure: Comment on "Bifunctional Polymer Hydrogel Layers As Forward Osmosis Draw Agents for Continuous Production of Fresh Water Using Solar Energy". Environmental Science & Technology 48(7), 4214-4215.

Zeng, Y., Qiu, L., Wang, K., Yao, J., Li, D., Simon, G.P., Wang, R. and Wang, H., 2013. Significantly enhanced water flux in forward osmosis desalination with polymer-graphene composite hydrogels as a draw agent. RSC Advances 3(3), 887-894.

Zhang, J., Xu, S. and Kumacheva, E., 2004. Polymer Microgels: Reactors for Semiconductor, Metal, and Magnetic Nanoparticles. Journal of the American Chemical Society 126(25), 7908-7914.

Zhao, S., Zou, L. and Mulcahy, D., 2012. Brackish water desalination by a hybrid forward osmosis–nanofiltration system using divalent draw solute. Desalination 284, 175-18.

3.7 Supporting Information

3.7.1 Homemade FO setup for microgel-driven FO desalination

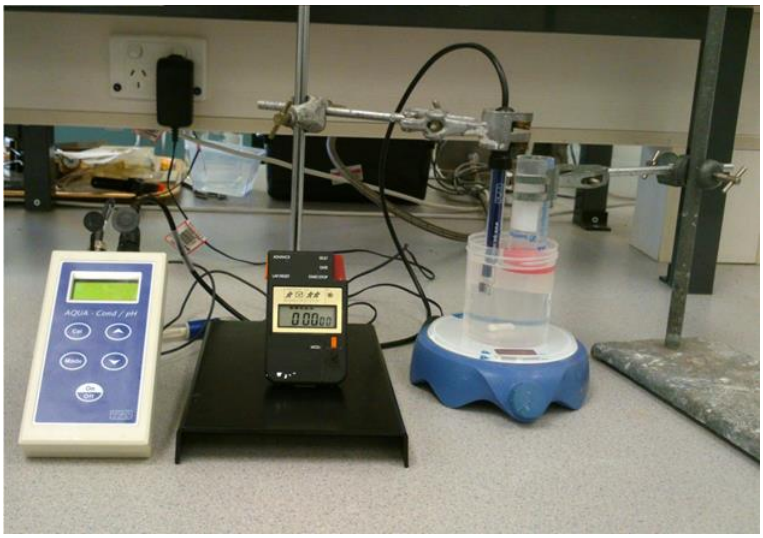

Figure 3.8 A New Setup of On-line Conductivity Measurement Approach for Microgel-based FO Water Flux Analysis.

3.7.2 pH and conductivity titration curves for various N-isopropylacrylamide-co-acrylic acid microgels

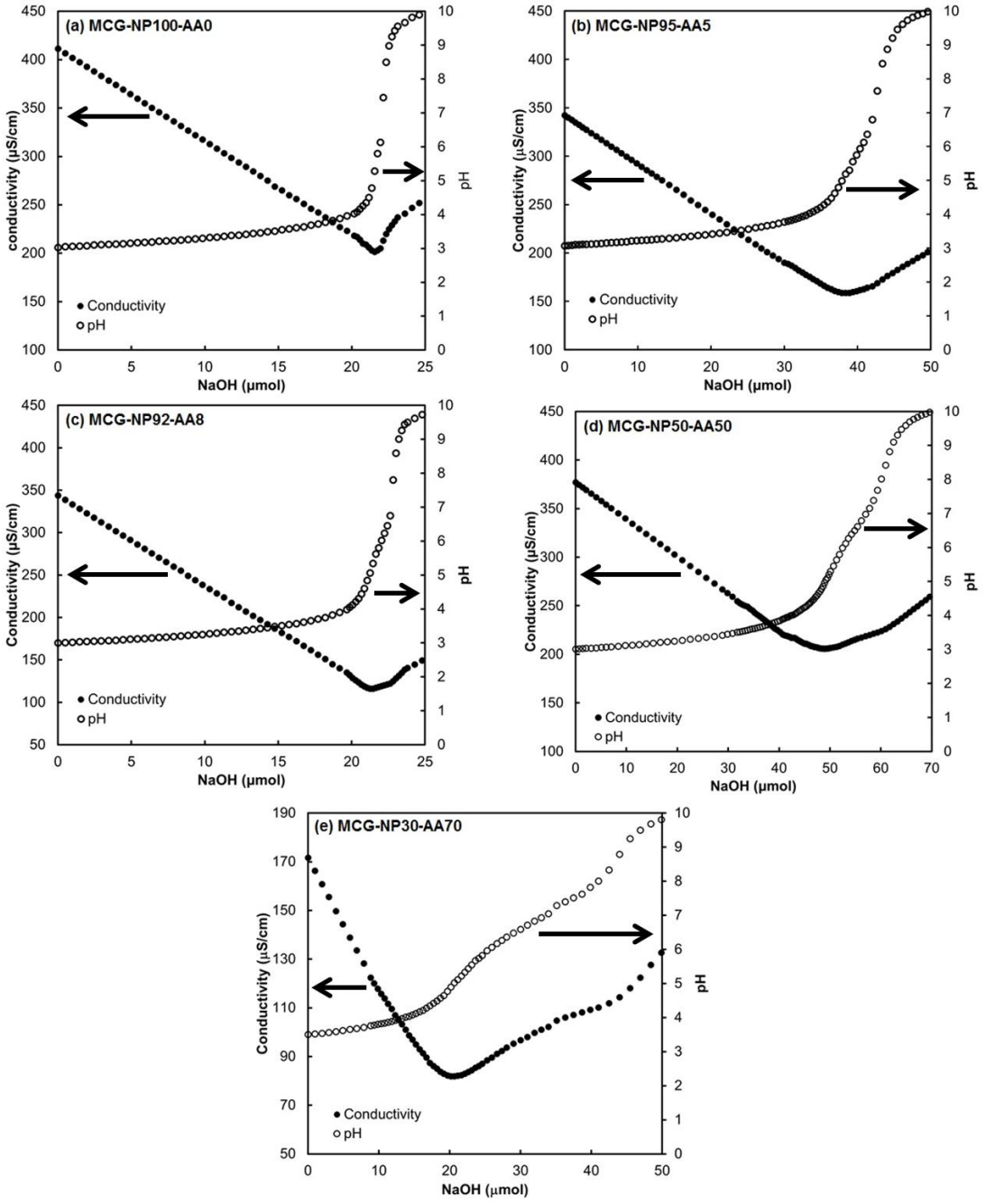

Figure 3.9 pH and conductivity titrations for various microgels to determine the averaged incorporated AA in these microgels.

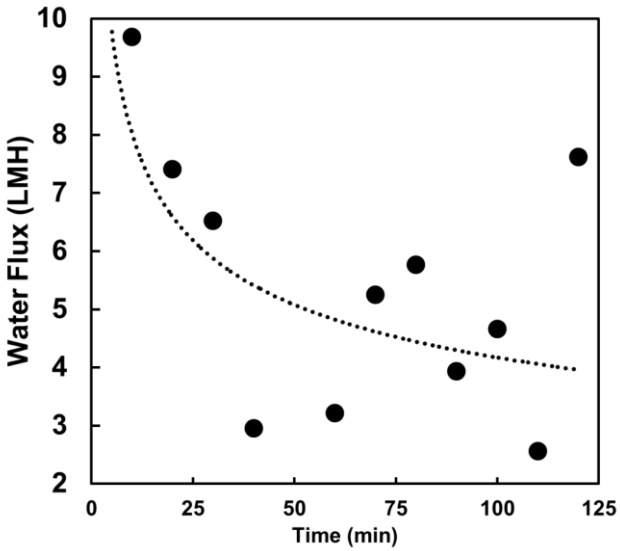

Figure 3.10 Water flux profile for MCG-NP92-AA8 over a two-hour test period as measured by gravimetric approach.

Chapter 4. Thermoresponsive Acidic Microgels as Functional Draw Agents for Forward Osmosis Desalination

Yusak Hartanto[1], Masoumeh Zargar[1], Haihui Wang[2], Bo Jin[1], Sheng Dai[1]

School of Chemical Engineering, The University of Adelaide, SA 5005, Australia

School of Chemistry & Chemical Engineering, South China University of Technology, Guangzhou 510640, People's Republic of China

Graphical Abstract:

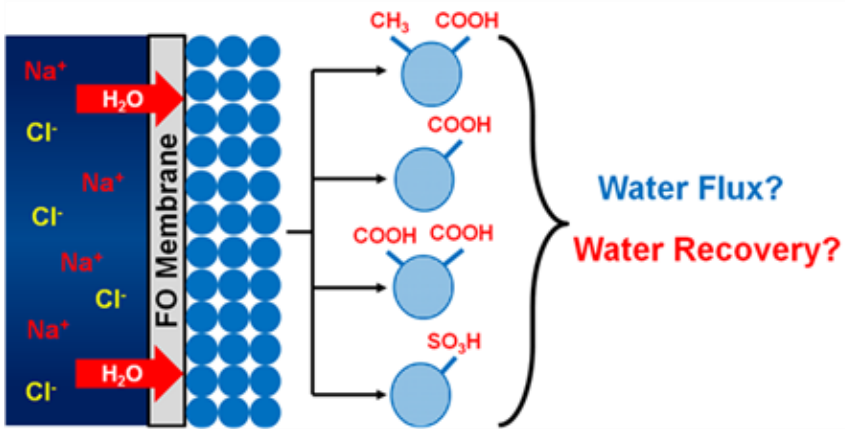

Statement of Authorship

Title of Paper	Thermoresponsive Acidic Microgels as Functional Draw Agents for Forward Osmosis Desalination
Publication Status	☑ Published ☐ Accepted for Publication ☐ Submitted for Publication ☐ Unpublished and Unsubmitted w ork w ritten in manuscript style
Publication Details	*Environ. Sci. Technol.*, **2016**, *50* (8), pp 4221–4228 **DOI:** 10.1021/acs.est.5b04123

Principal Author

Name of Principal Author (Candidate)	Yusak Hartanto		
Contribution to the Paper	Design the major experiments, data analysis and manuscript writing.		
Overall percentage (%)	60 %		
Certification:	This paper reports on original research I conducted during the period of my Higher Degree by Research candidature and is not subject to any obligations or contractual agreements with a third party that would constrain its inclusion in this thesis. I am the primary author of this paper.		
Signature		Date	

Co-Author Contributions

By signing the Statement of Authorship, each author certifies that:

i. the candidate's stated contribution to the publication is accurate (as detailed above);

ii. permission is granted for the candidate in include the publication in the thesis; and

iii. the sum of all co-author contributions is equal to 100% less the candidate's stated contribution.

Name of Co-Author	Masoumeh Zargar
Contribution to the Paper	Helped to perform the experiment

Signature		Date	12/01/2016

Name of Co-Author	Haihui Wang		
Contribution to the Paper	Designed the experiment and manuscript correction		
Signature		Date	

Name of Co-Author	Bo Jin		
Contribution to the Paper	Designed the experiment and manuscript correction		
Signature		Date	

Name of Co-Author	Sheng Dai		
Contribution to the Paper	Designed the experiment and manuscript correction		
Signature		Date	27/01/2016

Hartanto, Y., Zargar, M., Wang, H., Jin, B. and Dai, S. (2016). Thermoresponsive Acidic Microgels as Functional Draw Agents for Forward Osmosis Desalination. *Environmental Science and Technology*, 50 (8), pp 4221–4228.

Chapter 5. Thermoresponsive Cationic Copolymer Microgels as High Performance Draw Agents in Forward Osmosis Desalination

Yusak Hartanto, Masoumeh Zargar, Xiaolin Cui, Bo Jin, Sheng Dai

School of Chemical Engineering, The University of Adelaide, SA 5005, Australia

Graphical Abstract:

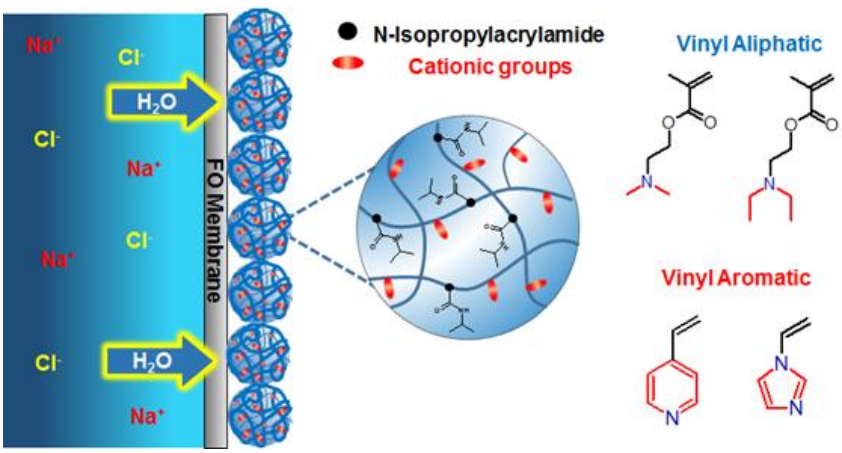

Statement of Authorship

Title of Paper	Thermoresponsive Cationic Copolymer Microgels as High Performance Draw Agents in Forward Osmosis Desalination
Publication Status	☐ Published ☐ Accepted for Publication ☑ Submitted for Publication ☐ Unpublished and Unsubmitted work written in manuscript style
Publication Details	In Revision for Journal of Membrane Science

Principal Author

Name of Principal Author (Candidate)	Yusak Hartanto		
Contribution to the Paper	Design the major experiments, data analysis and manuscript writing.		
Overall percentage (%)	60 %		
Certification:	This paper reports on original research I conducted during the period of my Higher Degree by Research candidature and is not subject to any obligations or contractual agreements with a third party that would constrain its inclusion in this thesis. I am the primary author of this paper.		
Signature		Date	

Co-Author Contributions

By signing the Statement of Authorship, each author certifies that:

i. the candidate's stated contribution to the publication is accurate (as detailed above);

ii. permission is granted for the candidate in include the publication in the thesis; and

iii. the sum of all co-author contributions is equal to 100% less the candidate's stated contribution.

Name of Co-Author	Masoumeh Zargar
Contribution to the Paper	Helped to perform the experiment

Signature		Date	12/01/2016

Name of Co-Author	Xiaolin Cui		
Contribution to the Paper	Designed the experiment and manuscript correction		
Signature		Date	

Name of Co-Author	Bo Jin		
Contribution to the Paper	Designed the experiment and manuscript correction		
Signature		Date	

Name of Co-Author	Sheng Dai		
Contribution to the Paper	Designed the experiment and manuscript correction		
Signature		Date	27/01/2016

5.1 Abstract

Thermoresponsive cationic copolymer microgels with aliphatic and aromatic cationic comonomers were synthesized and applied as forward osmosis (FO) draw agents for the first time. The results show that the FO desalination performance depends on the chemical structures and the dissociation constants (pK_a) of the cationic comonomers. Cationic copolymer microgel with *2*-(diethylamino) ethyl methacrylate as a comonomer has the best FO overall performance with the initial water flux of 45.6 LMH and water recovery of 44.8%. Furthermore, this microgel has the shortest equilibrium swelling time which in turn shows a significant improvement in apparent flux of 5.5 LMH compared to other cationic copolymer microgels. Furthermore, Hansen solubility parameters are used to correlate the solvation behavior of these cationic microgels and their performance in forward osmosis desalination for the first time. Our results show that Hansen solubility parameters and the dissociation constants of cationic comonomers play critical roles in determining the performance of cationic copolymer microgels in FO desalination.

Keywords: N-Isopropylacrylamide; cationic; microgels; forward osmosis; Hansen solubility parameters; desalination.

5.2 Introduction

Forward osmosis (FO) is an emerging membrane-based separation process that has a potential to lower the energy consumption in desalination process compared to reverse osmosis (RO) process due to the absence of high applied hydraulic pressure [1]. However, current FO desalination technology still consumes more energy than RO desalination process due to the thermodynamic constrain in water recovery process [2]. In order to solve this issue, thermolytic solutes were proposed as FO draw agents [3, 4] due to their phase separation ability at mild temperature where low grade heat can be used to reduce the energy cost of water recovery. Although this strategy can reduce the energy cost of FO desalination, several drawbacks such as membrane stability [5], membrane scaling [6] , final water quality [7] and reverse solute flux [8] still exist which hinder the practical application of these materials.

In order to overcome the drawbacks of thermolytic solutes, various class of materials such as linear polymers [9-11], magnetic nanoparticles [12-14], synthetic organic solutes [5, 15, 16], ionic liquids [17, 18] and switchable polarity solvents [19] were proposed as FO draw agents. Although reduced reverse solute flux can be achieved due to the large molecular size of these materials, these large molecules led to severe concentration polarization which decreases the performance of these materials in water-drawing process. Furthermore, pressure-driven membrane processes such as ultrafiltration, nanofiltration and reverse osmosis are still used as water recovery process which might increase the total energy cost of this process [2].

Thermoresponsive polymer hydrogels which are able to reversibly swell and deswell in respond to temperature change were recently proposed as FO draw agents [20-22]. The absence of reverse solute flux is one of the advantages of using hydrogels

as FO draw agents [23]. However, the water flux generated from these hydrogels is much lower than other materials mentioned previously which could be caused by the poor contact between the hydrogel particles and the membrane surface [24]. Furthermore, poor liquid water recovery is also another problem using hydrogels as FO draw agents due to the formation of dense skin when the hydrogels deswelled above their phase transition temperature [25]. Although some strategies have been done to improve the performance of these hydrogels in absorbing water such as composite hydrogels [26-28], semi-interpenetrating network [21] and bifunctional layers formation [29], the water flux generated is still low compared to small molecules as draw materials.

Thermoresponsive copolymer microgels of N-isopropylacrylamide and acrylic acid were then proposed as FO draw agents to overcome the problems in thermoresponsive bulk hydrogels [30]. Due to their large surface areas, these microgels promote better contact on the membrane surface which results in significant improvement in water flux performance. Furthermore, the amount of acrylic acid also plays an important role on water flux and water recovery performance. Subsequent study investigated the effect of different acidic comonomers on the performance of microgel-driven FO desalination. The study shows that acidic copolymer microgels with dicarboxylic acid comonomers were able to generate high water flux while maintaining moderate water recovery. Apparent water flux was also used in the study to assess the overall performance of these acidic copolymer microgels. Although there was an improvement in water flux performance, the apparent water flux was still low due to long equilibrium swelling times of these acidic copolymer microgels. Therefore, improving the swelling kinetics of microgels is needed to achieve high apparent water flux.

Previously, a study investigating the FO performance of cationic polyelectrolytes of poly *2*-(dimethylamino) ethyl methacrylate demonstrated that these polyelectrolytes were able to generate very high osmolality in their protonated state [31] compared to weak acidic polyelectrolytes such as polyacrylic acid [9]. In this paper, we prepared different thermoresponsive cationic copolymer microgels and applied them as FO draw agents for the first time. Our results show the FO performance of these cationic microgels depends on the chemical structures of cationic comonomers and their dissociation constants (pK_a). Microgels with aliphatic cationic comonomers show higher water flux than those with aromatic cationic comonomers and the opposite behavior is observed in water recovery. Copolymer microgel with *2*-(diethylamino) ethyl methacrylate as a cationic comonomer shows the highest water flux and the shortest equilibrium swelling time among other cationic copolymer microgels. This results in the highest apparent water flux observed in this cationic microgel.

5.3 Materials and Methods

5.3.1 Materials

N-Isopropylacrylamide (NP, > 98%), purchased from Tokyo Chemical Industry, was purified by recrystallization from n-hexane and dried overnight. N-N'-methylenebisacrylamide (BIS, >98%), *2*-(dimethylamino) ethyl methacrylate (DMAEMA, 98%), *2*-(diethylamino) ethyl methacrylate (DEAEMA, 99%) and *4*-vinylpyridine (VP, 95%) were purchased from Sigma-Aldrich. *1*-vinylimidazole (VI, 99%) was purchased from VWR International. *2,2*'-Azobis(2-methylpropionamidine dihydrochloride (V-50) was purchased from Novachem. Sodium chloride was

purchased from VWR. Cellulose triacetate forward osmosis (CTA-FO) membranes were purchased from Hydration Technologies Inc. (HTI, USA).

5.3.2 Synthesis of cationic thermoresponsive copolymer microgels

Different thermoresponsive cationic copolymer microgels were synthesized using surfactant-free semi-batch emulsion polymerization. In a typical experiment, 0.735 g of NP, 0.015 g of cationic comonomer, 0.0075 g of BIS and 75 mL of DI water were mixed in a 250 mL three-necked flask fitted with a condenser, a mechanical stirrer and gas inlet and outlet. The semi-batch feeding solution was prepared by dissolving 2.205 g of NP, 0.045 g of cationic comonomer and 0.0225 g of BIS in 45 mL of DI water. After degassing the solution for 45 minutes with nitrogen, the three-necked flask was immersed into a preheated oil bath at 70 °C under nitrogen protection. A 3 mL of V-50 aqueous solution (0.03 g) was then injected to the flask to start the polymerization. The feeding solution was injected at a rate of 3 mL/h using a syringe pump one hour after the batch solution turned cloudy. The polymerization was carried out overnight under continuous stirring and nitrogen protection. After cooling, the microgels were purified using membrane dialysis (MWCO 12–14 kDa) against DI water for several days to remove any unreacted compounds. Finally, the purified microgels were dried at 65 ^{o}C and grounded into fine powders.

5.3.3 Characterization of cationic thermoresponsive microgels

5.3.3.1 Dynamic light scattering and zeta potential measurements

The hydrodynamic diameters (d_h) of the cationic microgels at different temperatures (20 ^{o}C – 50 ^{o}C) and their zeta potentials at pH ~6.8 and 20 ^{o}C were measured using a Zetasizer (Malvern, Nano-ZS). The swelling ratios (SR) of cationic copolymer microgels are calculated using the following equation:

$$SR = \left(\frac{d_{h,To}}{d_{h,Ti}}\right)^3 \quad \text{Eq. 5.1}$$

where SR is the swelling ratio of the microgel, $d_{h,To}$ (nm) is the hydrodynamic diameter of the microgel at To ^oC (20 ^oC) and $d_{h,Ti}$ (nm) is the hydrodynamic diameter of the microgels at Ti ^oC.

5.3.3.2 Conductometric and potentiometric titration

The amounts of incorporated cationic comonomers in the microgels were determined using conductometric and potentiometric titrations. Typically, the pH of a 100 mL MCG-NP-DMAEMA microgel dispersion (~ 1 mg/mL) was adjusted to 3 using concentrated hydrochloric acid. The solution was then titrated using a 0.1 M NaOH solution. After each addition of NaOH, the conductivity and pH of the solution were measured using a pre-calibrated Aqua-CP/A pH and conductivity meter.

5.3.4 Forward Osmosis Desalination Evaluation

5.3.4.1 Water flux evaluation

A 100 mg of dried microgel was loaded in our homemade FO membrane setup equipped with an on-line conductivity monitoring system [30]. The membrane configuration adopted in this experiment was the active layer facing draw solute (AL-DS). A conductivity probe (probe cell constant, k = 1.0) was immersed in the feed solution of 2000 ppm NaCl to continuously monitor the change in conductivity of the feed solution against time for two hours. The system was conditioned by immersing the membrane in the feed solution for 30 minutes before loading the microgels on the membrane. The conductivity data was converted into the concentration of sodium chloride in the feed solution through a calibration curve.

The water flux is calculated using the conductivity data using the following equations:

$$V_t = \frac{C_i V_i}{C_t} \quad \text{Eq. 5.2}$$

$$J_w = \frac{V_i - V_t}{A\ t} \quad \text{Eq. 5.3}$$

where V_t (mL) is the volume of feed at time t, V_i (mL) is the initial volume of feed, C_i (ppm) is the initial feed concentration, C_t (ppm) is the feed concentration at time t, J_w (LMH) is the water flux, A (m^2) is the effective membrane surface area and t (h) is the time where the conductivity of the feed solution changes.

5.3.4.2 Water recovery

The water-saturated microgels were transferred to centrifuge tubes and weighed after two-hour water absorption period. The microgels were then centrifuged at 40 ^oC and 10,000 rpm for 10 minutes to separate absorbed water from the microgels. The recovered water was measured using gravimetric method. The water recovered from the deswelled microgels was calculated using the following equations:

$$C_p = \frac{W_d}{W_d + W_w} \quad \text{Eq. 5.4}$$

$$W_g = W_m(1 - C_p) \quad \text{Eq. 5.5}$$

$$R = \frac{W_R}{W_g}\ x\ 100\% \quad \text{Eq. 5.6}$$

where C_p (g microgels/g water) is the concentration of microgels in the centrifuge tube, W_p (g) is the weight of dry microgel, W_w (g) is the weight of water absorbed by the microgels calculated from water flux data, W_g (g) is the weight of water in the microgels, W_m (g) is the weight of microgels in the centrifuge tube, W_R (g) is the

weight of absorbed water recovered from the tube and R (%) is the percentage of water recovered from the microgels.

5.3.4.3 Apparent water flux

Apparent water flux is defined as the amount of water that can be released from the microgels per unit area per unit cycling time and written as follows [23]:

$$J_{app} = \frac{m_W}{(T_{eq} + T_R)A} \quad \text{Eq. 5.7}$$

where J_{app} (LMH) is the apparent water flux, m_W (L) is the volume of water that can be released during dewatering process, T_{eq} (h) is the time needed to reach equilibrium condition, T_R (h) is the time needed to dewater the microgels and A (m^2) is the effective membrane area.

5.3.4.4 Microgel recycling evaluation

The microgels were removed from the membrane setup and dried in oven until constant weight after the first evaluation. The dried microgels were grounded into fine powders and placed again on the membrane for the second cycle measurement, where the conductivities of feed solution against time were recorded to calculate water flux. The same approach was repeated for the subsequent cycles. The water recovery cycle measurement was conducted using similar fashion using gravimetric method.

5.3.5 Hansen solubility parameter (HSP) analysis

The solubility parameter components predicted using group contributions can be calculated using the following equations:

$$\delta_d = \frac{\sum F_{di}}{V} \quad \text{Eq. 5.8}$$

$$\delta_p = \frac{\sqrt{\sum F_{pi}^2}}{V} \quad \text{Eq. 5.9}$$

$$\delta_h = \sqrt{\frac{\sum E_{hi}}{V}} \quad \text{Eq. 5.10}$$

$$\delta_{total} = \sqrt{\delta_d^2 + \delta_p^2 + \delta_h^2} \quad \text{Eq. 5.11}$$

Where δ_d ($MPa^{1/2}$) is the dispersion interaction parameter, F_{di} ($[MJ/m^3]^{1/2}.mol^{-1}$) is molar attraction constant for the dispersion component, δ_p ($MPa^{1/2}$) is the polar interaction parameter, F_{pi} ($[MJ/m^3]^{1/2}.mol^{-1}$) is the group contribution constant for the polar component, δ_h ($MPa^{1/2}$) is the hydrogen bonding interaction parameter, E_{hi} ($J.mol^{-1}$) is the hydrogen bonding energy, V (cm^3/mol) is the molar volume and δ_{total} ($MPa^{1/2}$) is the overall solubility parameter.

The distance of solubility parameter, relative energy difference (RED) and ratio of cohesion energy densities (H), can be calculated using the following equations [32]:

$$(R_a)^2 = 4(\delta_{d2} - \delta_{d1})^2 + \left(\delta_{p2} - \delta_{p1}\right)^2 + (\delta_{h2} - \delta_{h1})^2 \quad \text{Eq. 5.12}$$

$$RED = \frac{R_a}{R_o} \quad \text{Eq. 5.13}$$

$$RA = \frac{R_a}{2};\ R_M = \frac{R_o}{2} \quad \text{Eq. 5.14}$$

$$H = \left(\frac{RA}{R_M}\right)^2 \quad \text{Eq. 5.15}$$

where R_a ($MPa^{1/2}$) is a modified difference between HSP for water (1) and monomer (2). R_o ($MPa^{1/2}$) is the radius of interaction of an HSP solubility sphere.

5.4 Results and Discussions

5.4.1 Synthesis and characterization of thermoresponsive cationic copolymer microgels

Thermoresponsive cationic copolymer microgels were prepared via semi-batch surfactant-free emulsion polymerization to eliminate the influence of surfactant on final physicochemical properties of these microgels. The comonomer feed ratio used in this study was 2 wt% because the large amount of ionic comonomer will eliminate the thermoresponsive properties of the microgels [30]. The initial pH of the reaction mixture was adjusted to ~ 4 to protonate the cationic comonomer, which assists particle stabilization [33]. After the synthesis, the microgels were transferred to dialysis bags for purification before characterization and evaluation studies. The purification was confirmed by comparing the conductivity of dialysis water and the conductivity of DI water. We choose two different groups of cationic comonomers shown in Figure 5.1, aliphatic and aromatic comonomers, in this study to examine the effect of different chemical structures of cationic comonomers on the FO performance.

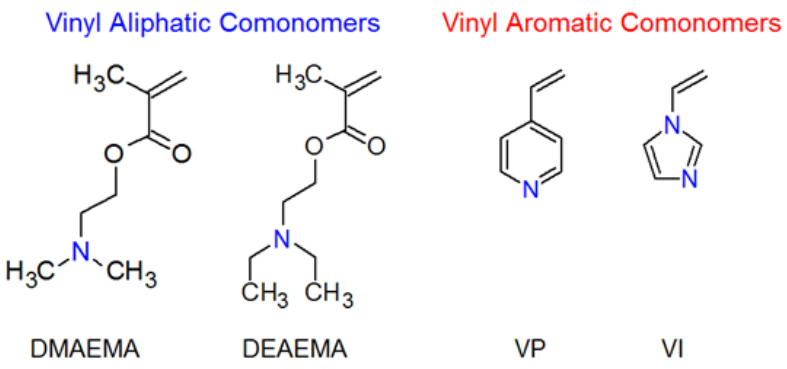

Figure 5.1 Chemical structures of different cationic comonomers used in synthesized cationic copolymer microgels.

Dynamic light scattering measurements were performed to determine the apparent diameters of the microgels at different temperatures and their volume phase transition temperatures (VPTTs). Cationic N-isopropylacrylamide microgel was synthesized as a control to compare its swelling/deswelling behavior with other cationic copolymer microgels. Figure 5.2a shows the hydrodynamic diameters of cationic copolymer microgels as a function of temperature. The incorporation of different cationic comonomers shifts the VPTTs of resulting cationic microgels due to the different degrees of ionization of cationic comonomers indicated by their different pK_a values [34]. Copolymerization with aliphatic comonomers leads to the less shift of VPTTs to lower temperature than those with aromatic comonomers due to the stronger solvation behavior of these aliphatic comonomers [35] than their aromatic counterparts [36, 37]. The pK_a of different cationic comonomers used in this study is shown in Table 5.1.

Table 5.1 Dissociation constants (pKa) of different cationic comonomers

Cationic Comonomers	pK_a	Ref.
DMAEMA	8.40	38
DEAEMA	9.50	39
VP	5.39	36
VI	6.95	40

Swelling ratios of the cationic microgels at specific temperatures near their VPTTs are shown in Figure 5.2b. MCG-NP-DMAEMA has the lowest swelling ratio among other cationic microgels at 30 ^{o}C. However, the swelling ratio of this

microgel is slightly higher than the swelling ratio of MCG-NP at 35 ºC and 40 ºC. Furthermore, the swelling ratio of MCG-NP-DEAEMA is higher at all temperature than MCG-NP and MCG-NP-DMAEMA due to hydrophobic characteristic of this comonomer [39]. On the other hand, the cationic copolymer microgels with aromatic comonomers show higher swelling ratios than cationic microgels with aliphatic comonomers at all temperatures due to the presence of hydrophobic aromatic ring. MCG-NP-VP shows remarkable swelling ratio at 40 ºC due to hydrophobic characteristic of this comonomer at its deprotonated state [41] while MCG-NP-VI microgels have slightly lower swelling ratio than MCG-NP-VP at 40 ºC due to slight protonation of the tertiary amines in this comonomer.

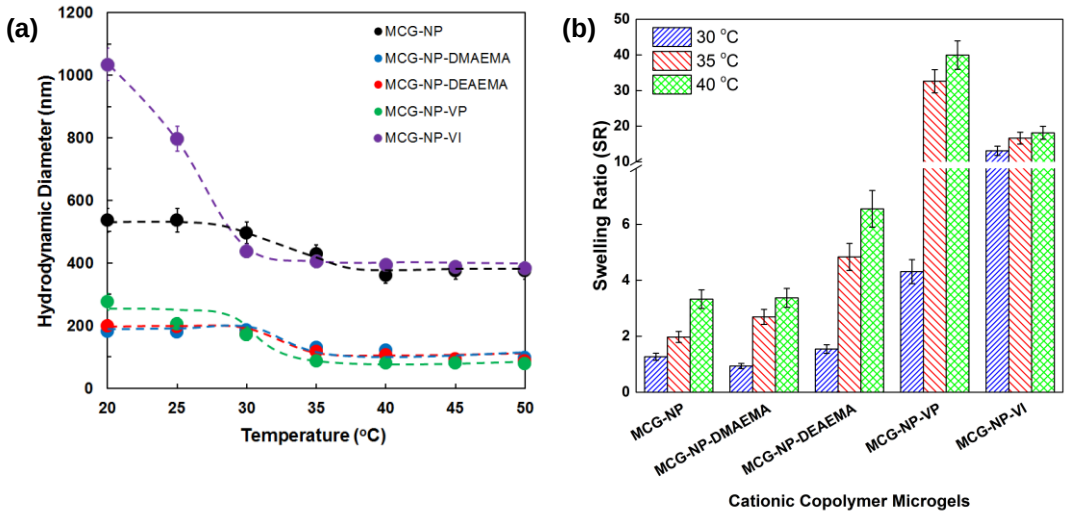

Figure 5.2 (a) Hydrodynamic diameters of thermoresponsive microgels at different temperatures and pH 6.8; (b) Swelling ratios of cationic thermoresponsive microgels at 30 ºC, 35 ºC and 40 ºC at pH 6.8.

The incorporation of cationic comonomers into copolymer microgels can be characterized qualitatively and quantitatively using pH and conductivity titration curves. The highlighted areas in Figure 5.9 showing the presence of tertiary amines

confirm the successful incorporation of cationic comonomers in the microgels. The calculated amounts of tertiary amines in the microgels determined from pH and conductivity titration curves shown in Table 5.5 are close to the feeding amounts indicating high conversion of these comonomers (80 – 90%). In addition, zeta potential measurements at 20 ^{o}C and pH ~6.8 were carried out to elucidate the surface charge of cationic microgels and to further confirm the presence of cationic comonomers in the microgels. The values of zeta potential measurements for each cationic microgel in Figure 5.10 show all cationic copolymer microgels have higher zeta potential than cationic N-isopropylacrylamide microgel except for MCG-NP-VP due to the deprotonated state of tertiary amines in this microgel at pH ~6.8.

5.4.2 Water flux and water content profiles for thermoresponsive cationic copolymer microgels

Water flux and water content profiles for each thermoresponsive cationic microgel are shown in Figure 5.3. Incorporation of different cationic comonomers leads to varied water absorption rates, water contents and equilibrium swelling time. MCG-NP-DMAEMA shows faster equilibrium swelling time and higher water flux than MCG-NP due to improved solvation behavior of this microgel caused by the protonated tertiary amines. The equilibrium swelling times for MCG-NP-DMAEMA and MCG-NP are 40 min and 100 min, respectively. Furthermore, the shortest equilibrium swelling time (30 min) and highest water flux are observed in MCG-NP-DEAEMA due to high protonation of DEAEMA indicated by its highest pK_a in Table 5.1 which results in strong solvation behavior of this copolymer microgel.

On the other hand, cationic microgels with aromatic comonomers have lower water flux than those with aliphatic comonomers due to the presence of hydrophobic

aromatic ring which contributes to the solvation interaction of the microgels [42]. In addition, the hydrophobicity also results in longer equilibrium swelling time in these microgels than the microgels with aliphatic comonomers. The equilibrium swelling time for MCG-NP-VP (80 min) is longer than MCG-NP-VI (70 min) due to hydrophobic characteristic of *4*-vinylpyridine in its deprotonated state [43]. The shorter equilibrium swelling time in MCG-NP-VI is caused by the stronger solvation of this microgel than MCG-NP-VP as indicated by its higher pK_a value in Table 5.1.

The final water content of MCG-NP-DEAEMA is higher than the final water contents of MCG-NP-DEAEMA and MCG-NP. Similar result is also observed in microgels with aromatic comonomers where MCG-NP-VP had slightly higher final water content than MCG-NP-VI despite the hydrophobic characteristic of VP in its deprotonated state. This phenomenon can be explained by the micro phase separation during the polymerization when slightly hydrophobic comonomers such as DEAEMA and VP are introduced during polymerization process. This results in MCG-NP-DEAEMA and MCG-NP-VP have more porous structures which cause these copolymer microgels could retain more water than MCG-NP-DMAEMA and MCG-NP-VI [44, 45].

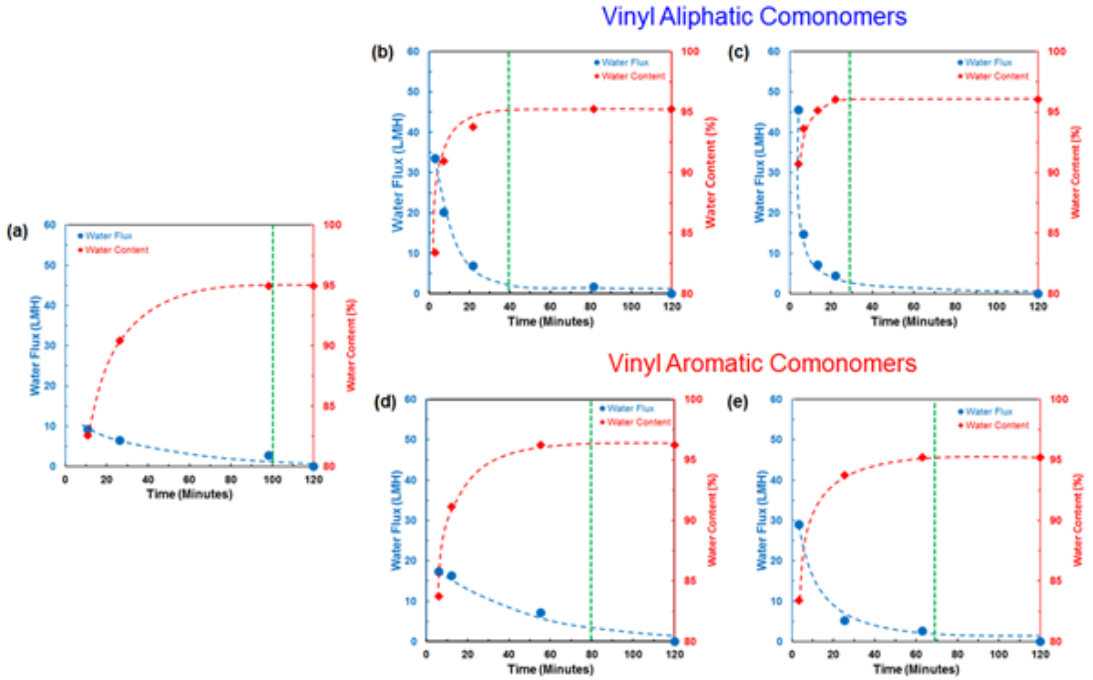

Figure 5.3 Water flux and water content profiles of different cationic co-polymer thermoresponsive microgels: (a) MCG-NP, (b) MCG-NP-DMAEMA, (c) MCG-NP-DEAEMA, (d) MCG-NP-VP and (e) MCG-NP-VI, during two-hour water absorption period. Feed solution is 2000 ppm NaCl and the room temperature was maintained at 20 ± 1 ^{o}C. The green vertical lines show the equilibrium condition.

5.4.3 Initial water flux and water recovery of thermoresponsive cationic copolymer microgels

The initial water flux and water recovery for various cationic thermoresponsive microgels are shown in Figure 5.4. MCG-NP has the lowest water flux (8.5 LMH) among other cationic copolymer microgels while its water recovery is 40.2%. This water recovery is lower than the previously synthesized anionic N-isopropylacrylamide microgel [30] which can be caused by the strong hydrogen bonding between water and the primary and secondary amines from 2,2'-azobis (2-methylpropioaminidine dihydrochloride) [46]. MCG-NP-DMAEMA and MCG-NP-DEAEMA show higher water fluxes than MCG-NP due to the contribution of

protonated tertiary amines from the cationic comonomers. However, the water flux for MCG-NP-DEAEMA is higher than MCG-NP-DMAEMA due to the presence of more protonated tertiary amines in MCG-NP-DEAEMA than MCG-NP-DMAEMA as indicated by their pK_a values in Table 5.1 which results in higher osmotic pressure in MCG-NP-DEAEMA than MCG-NP-DMAEMA. The water fluxes of MCG-NP-DMAEMA and MCG-NP-DEAEMA are 33.5 LMH and 45.6 LMH, respectively while their water recovery are 34.1% and 44.8%, respectively. The higher water recovery in MCG-NP-DEAEMA could be from the hydrophobic character of DEAEMA. In addition, high swelling ratio of MCG-NP-DEAEMA above the VPTT shown in Figure 5.2 confirms the higher water recovery in MCG-NP-DEAEMA than MCG-NP-DMAEMA [39].

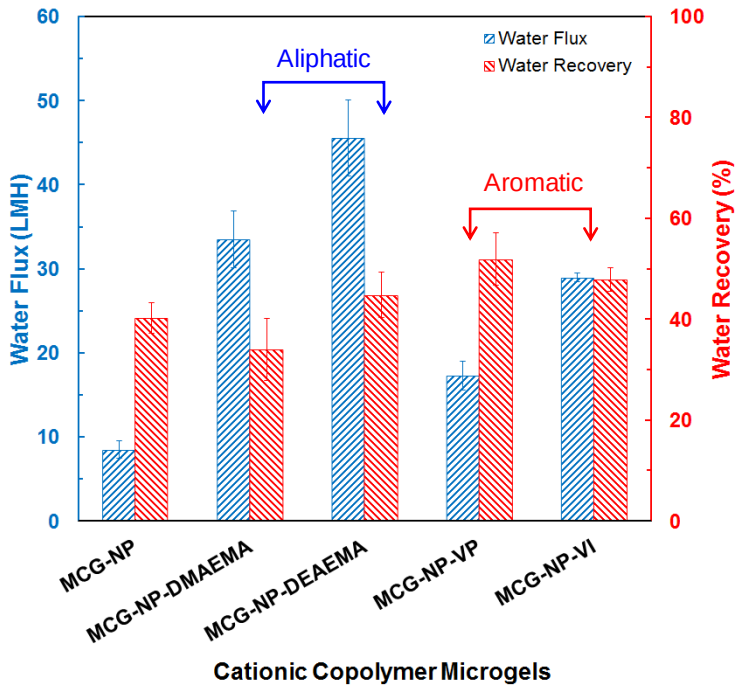

Figure 5.4 Initial water flux and water recovery for different cationic thermoresponsive co-polymer microgels. Feed solution concentration is 2000 ppm, pH of the feed solution is 6.8 and the feed temperature is 20 ± 1 °C.

On the other hand, MCG-NP-VP microgel shows reduced water flux (17.3 LMH) but improved water recovery due to its deprotonated tertiary amines which results in strong hydrophobic properties from the aromatic ring dominates the physicochemical properties of the microgel. The water recovery of MCG-NP-VP microgels is 51.9%. Interestingly, MCG-NP-VI microgel shows higher water flux (28.9 LMH) than MCG-NP-VP despite the presence of aromatic ring structure in this comonomer. However, its water flux is less than MCG-NP-DMAEMA and MCG-NP-DEAEMA due to the lower pK_a value of this comonomer which results in low amount of protonated tertiary amines in this microgels [40]. The water recovery of MCG-NP-VI (47.9%) is comparable with that observed in MCG-NP-VP implying this microgel has balanced water flux and water recovery performance.

5.4.4 Apparent water flux of thermoresponsive cationic copolymer microgels

Apparent water flux shown in Figure 5.5 measures the amount of water per unit time that can be recovered from the microgel in one cycle [23]. The apparent water flux of MCG-NP is 1.5 LMH which is the lowest among other cationic copolymer microgels due to its low water absorption, water recovery and slow equilibrium swelling time. Incorporating DMAEMA and DEAEMA as comonomers into the microgels improves their apparent fluxes due to improved water flux and recovery performance. The apparent water flux of MCG-NP-DMAEMA and MCG-NP-DEAEMA are 1.7 LMH and 5.5 LMH, respectively. The apparent flux of MCG-NP-DEAEMA is significantly higher than MCG-NP-DMAEMA due to its faster equilibrium swelling time and higher water recovery than MCG-NP-DMAEMA.

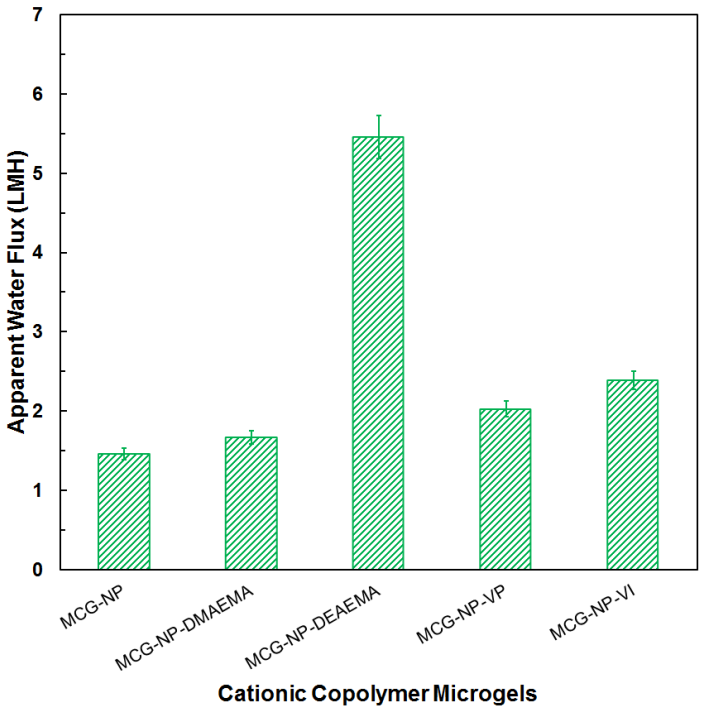

Figure 5.5 Apparent water fluxes of different thermoresponsive cationic copolymer microgels.

Although MCG-NP-VP and MCG-NP-VI have higher water recovery than MCG-NP-DEAEMA, their apparent fluxes are lower than MCG-NP-DEAEMA due to their long equilibrium swelling time. The apparent water fluxes of MCG-NP-VP and MCG-NP-VI are 2 LMH and 2.4 LMH, respectively. Therefore, MCG-NP-DEAEMA has the best overall performance among other cationic copolymer microgels due to its fast equilibrium swelling times and relatively high water recovery. Furthermore, the apparent water flux of this microgel is significantly higher than bulk thermoresponsive hydrogels published in the literature [23]. Table 5.2 provides a summary of initial water flux, water recovery and apparent water flux.

Table 5.2 Summary of initial water flux, water recovery and apparent water flux for different thermoresponsive cationic copolymer microgels

Microgels	Initial Water Flux (LMH)	Water Recovery (%)	Apparent Water Flux (LMH)
MCG-NP	8.5	40.2	1.5
MCG-NP-DMAEMA	33.5	34.1	1.7
MCG-NP-DEAEMA	45.6	44.8	5.5
MCG-NP-VP	17.3	51.9	2.0
MCG-NP-VI	28.9	47.9	2.4

5.4.5 Swelling – deswelling cycles and recyclability of thermoresponsive cationic copolymer microgels

The microgel recycling test was conducted to assess the recyclability performance of our thermoresponsive cationic copolymer microgels. We choose to study the recyclability of MCG-NP-DEAEMA as this microgel has the best apparent water flux. Swelling – deswelling cycles conducted using dynamic light scattering by cycling the temperatures of the microgel solution shows that this microgel is fully swellable and deswellable as shown in Figure 5.6a. The water flux and water recovery evaluation were also carried out to confirm the reusability of this microgel following the dynamic light scattering study. The cycles of water flux and water recovery shown in Figure 5.6b confirm that this microgel is able to maintain its water flux and water recovery performance in five cycles.

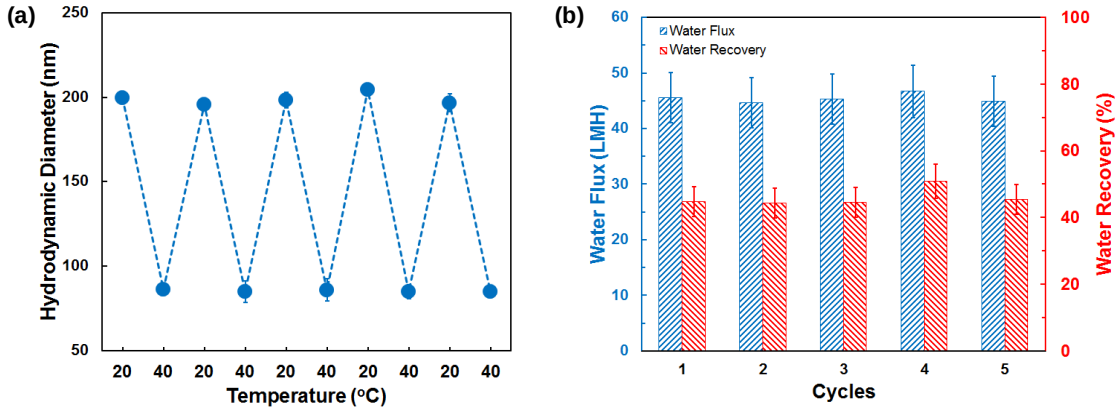

Figure 5.6 (a) Swelling – deswelling cycles for MCG-NP-DEAEMA and (b) Water flux and water recovery cycles for MCG-NP-DEAEMA.

5.4.6 Relationship between the performance of cationic copolymer microgels in FO desalination and their Hansen solubility parameters

To gain insight on microgel – water interaction, we calculated the Hansen solubility parameters for the monomer and comonomers used in this study. This will assist in designing which monomer/co-monomer pair that will lead to optimized FO performance in the future.

Hansen solubility parameters consist of three terms, the dispersion, δ_d, polar, δ_p, and hydrogen bonding, δ_h, interaction parameters [32]. The values of individual parameter can be determined directly from experimental data or numerical estimation. Estimation using group contribution method such as the Hoftyzer – Van Kreleven method has reasonable accuracy for most polymer – solvent systems [47]. The calculated values of Hansen solubility parameters using the Hoftyzer – Van Krevelen method are presented in Table 5.3.

Table 5.3 Hansen solubility parameters of water and various monomer and comonomer used in this study predicted using Hoftyzer – Van Krevelen method

Chemical Species	δ_d (MPa)$^{1/2}$	δ_p (MPa)$^{1/2}$	δ_h (MPa)$^{1/2}$	δ_{total} (MPa)$^{1/2}$
Water*	18.1	12.9	15.5	27.1
NP	16.7	7.8	7.0	19.7
DMAEMA	14.3	7.0	7.7	18.4
DEAEMA	14.7	5.9	7.1	17.9
VP	13.3	7.4	6.8	17.6
VI	13.0	12.5	10.5	21.7

*The values were obtained from ref. 32

The simple way to determine whether a molecule can dissolve in a given solvent is by looking at the difference between total solubility parameter, δ_{total}. This difference must be small enough for the molecule to dissolve in a given solvent. From Table 5.3, the differences between δ_{total} for water and δ_{total} for all monomers are quite large. For example, the difference between δ_{total} for water and δ_{total} for NP is 7.4 while it is known that water is a good solvent for poly(N-isopropylacrylamide) at the temperature below the lower critical solution temperature (LCST) of this homopolymer [48]. As a result, this approach cannot be used to determine the solubility behavior of the monomers in water.

To determine the monomer – water interaction, plotting the dispersion solubility parameter, δ_d, vs. the sum of polar and hydrogen bonding component, $(\delta_p^2 + \delta_h^2)^{1/2}$ allows us to further examine the water affinity towards the individual monomers [49]. As can be seen from Figure 5.7, VI has the closest distance to water among other comonomers which means that this monomer can be solvated easily while DMAEMA has further distance from NP and water. Furthermore, DEAEMA and VP

have less interaction with water as evidenced by their further distance from water than DMAEMA and VI.

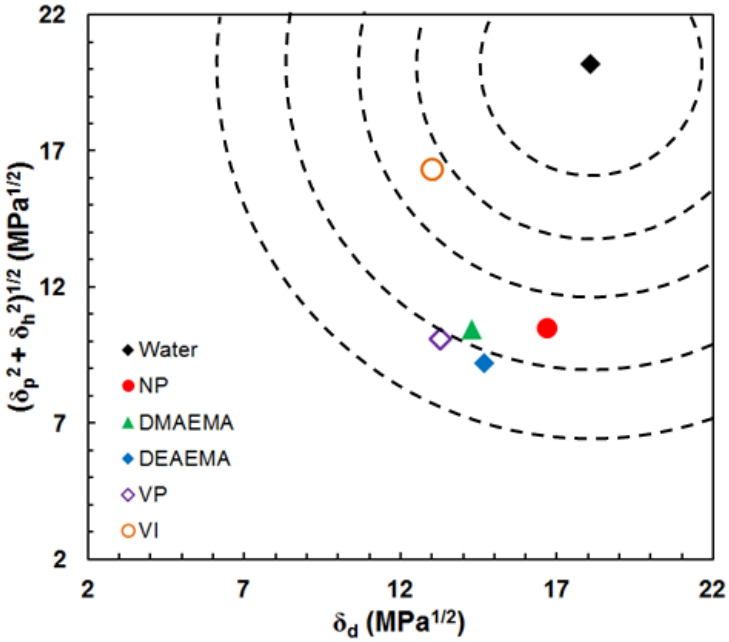

Figure 5.7 Hansen solubility plot for determining water affinity toward N-Isopropylacrylamide and cationic comonomers. The dotted lines are the guided lines as a measure of the radial distance of the monomers from water.

The distance in Figure 5.7 can be measured quantitatively using relative energy difference (RED) and cohesion energy density (H) parameters calculated using Equation 12 – 15. The values of RED and H of N-isopropylacrylamide and various cationic comonomers are summarized in Table 5.4. It can be seen that all the values of RED and H for the monomers used in this study are less than 1 except for VP which implies that all the microgels are water swellable. VP has the largest values of RED and H which means that this comonomer is close to the boundary of Hansen solubility space and has more hydrophobic character than other monomers.

Table 5.4 The solubility distance parameter (Ra), relative energy difference (RED) parameter and the cohesion energy densities (H) parameter of monomer/co-monomer with water

Monomer/Comonomer – Water	Ra	RED	H
NP – Water	10.3	0.74	0.55
DMAEMA – Water	12.4	0.89	0.79
DEAEMA – Water	12.9	0.93	0.87
VP – Water	14.1	1.01	1.03
VI – Water	11.3	0.81	0.66

The analysis of Hansen solubility parameter is generally aligned with the observed FO performance of thermoresponsive cationic copolymer microgels in this work. For example, MCG-NP-VP shows improved water recovery but less water flux compared to other cationic copolymer microgels due to the high values of RED and H for VP which indicates very weak interaction between water and this microgel. Furthermore, the smallest value of hydrogen bonding interaction parameter (δ_h) of VP in Table 5.3 further confirms the weak interaction of this comonomer with water. In contrast, VI has smaller values of RED and H than VP which means that MCG-NP-VI has better water interaction than MCG-NP-VP. This analysis is in agreement with the higher water flux generated by MCG-NP-VI than MCG-NP-VP.

On the other hand, microgels with aliphatic comonomers, MCG-NP-DEAEMA and MCG-NP-DMAEMA, generated higher water flux than MCG-NP despite their relatively high RED and H values. This means the protonation of tertiary amines also plays a key role in determining water flux performance of cationic microgels as discussed in previous section. However, the contribution of RED and H values for these microgels is more significant during the deswelling process where the higher

amount of water can be recovered in MCG-NP-DEAEMA than MCG-NP-DMAEMA. This means the interaction of water with DEAEMA is weaker than the water interaction with DMAEMA above the VPTTs of these cationic copolymer microgels. These results also confirm the swelling ratio of MCG-NP-DEAEMA is higher than the swelling ratio of MCG-NP-DMAEMA above the phase transition temperature as shown in Figure 5.2.

5.5 Conclusions

Thermoresponsive cationic copolymer microgels with different cationic comonomers have been synthesized and used as draw agents for forward osmosis desalination. The FO performance of these cationic microgels strongly depends on the chemical structures of the cationic comonomers and the dissociation constants (pK_a). Furthermore, short equilibrium time can be achieved by microgel with 2-(diethylamino) ethyl methacrylate due to its balanced performance in water flux and water recovery which makes this microgel has the highest overall performance among other cationic copolymer microgels. We also carry out in-depth analysis of the relationship between Hansen solubility parameters for each monomer and the FO performance of these microgels. Our results show Hansen solubility parameters and the dissociation constants (pK_a) of cationic comonomers have contribution to the FO performance of the cationic copolymer microgels in water flux and water recovery. This study might assist in designing optimized microgel materials that will lead to optimized microgel-driven FO desalination performance.

5.6 Acknowledgement

The authors would like to thank the financial support from the Australian Research Council (DP110102877). YH would like to appreciate the support of Adelaide Graduate Research Scholarships (AGRS).

5.7 References

1. Coday, B. D.; Xu, P.; Beaudry, E. G.; Herron, J.; Lampi, K.; Hancock, N. T.; Cath, T. Y., The sweet spot of forward osmosis: Treatment of produced water, drilling wastewater, and other complex and difficult liquid streams. *Desalination* **2014,** *333*, (1), 23-35.

2. Shaffer, D. L.; Werber, J. R.; Jaramillo, H.; Lin, S.; Elimelech, M., Forward osmosis: Where are we now? *Desalination* **2015,** *356*, 271-284.

3. McCutcheon, J. R.; McGinnis, R. L.; Elimelech, M., A novel ammonia-carbon dioxide forward (direct) osmosis desalination process. *Desalination* **2005,** *174*, (1), 1-11.

4. Boo, C.; Khalil, Y. F.; Elimelech, M., Performance evaluation of trimethylamine–carbon dioxide thermolytic draw solution for engineered osmosis. *Journal of Membrane Science* **2015,** *473*, 302-309.

5. Noh, M.; Mok, Y.; Lee, S.; Kim, H.; Lee, S. H.; Jin, G.-w.; Seo, J.-H.; Koo, H.; Park, T. H.; Lee, Y., Novel lower critical solution temperature phase transition materials effectively control osmosis by mild temperature changes. *Chemical Communications* **2012,** *48*, (32), 3845-3847.

6. Li, Z.; Valladares Linares, R.; Bucs, S.; Aubry, C.; Ghaffour, N.; Vrouwenvelder, J. S.; Amy, G., Calcium carbonate scaling in seawater desalination by ammonia–carbon dioxide forward osmosis: Mechanism and implications. *Journal of Membrane Science* **2015,** *481*, 36-43.

7. Ge, Q. C.; Ling, M. M.; Chung, T. S., Draw solutions for forward osmosis processes: Developments, challenges, and prospects for the future. *Journal of Membrane Science* **2013,** *442*, 225-237.

8. Chekli, L.; Phuntsho, S.; Kim, J. E.; Kim, J.; Choi, J. Y.; Choi, J.-S.; Kim, S.; Kim, J. H.; Hong, S.; Sohn, J.; Shon, H. K., A comprehensive review of hybrid forward osmosis systems: Performance, applications and future prospects. *Journal of Membrane Science* **2016,** *497*, 430-449.

9. Ge, Q.; Su, J.; Amy, G. L.; Chung, T.-S., Exploration of polyelectrolytes as draw solutes in forward osmosis processes. *Water Research* **2012,** *46*, (4), 1318-1326.

10. Ou, R.; Wang, Y.; Wang, H.; Xu, T., Thermo-sensitive polyelectrolytes as draw solutions in forward osmosis process. *Desalination* **2013,** *318*, 48-55.

11. Tian, E.; Hu, C.; Qin, Y.; Ren, Y.; Wang, X.; Wang, X.; Xiao, P.; Yang, X., A study of poly (sodium 4-styrenesulfonate) as draw solute in forward osmosis. *Desalination* **2015,** *360*, 130-137.

12. Zhao, Q.; Chen, N.; Zhao, D.; Lu, X., Thermoresponsive Magnetic Nanoparticles for Seawater Desalination. *ACS Applied Materials & Interfaces* **2013,** *5*, (21), 11453-11461.

13. Na, Y.; Yang, S.; Lee, S., Evaluation of citrate-coated magnetic nanoparticles as draw solute for forward osmosis. *Desalination* **2014,** *347*, 34-42.

14. Dey, P.; Izake, E. L., Magnetic nanoparticles boosting the osmotic efficiency of a polymeric FO draw agent: Effect of polymer conformation. *Desalination* **2015,** *373*, 79-85.

15. Stone, M. L.; Wilson, A. D.; Harrup, M. K.; Stewart, F. F., An initial study of hexavalent phosphazene salts as draw solutes in forward osmosis. *Desalination* **2013,** *312*, 130-136.

16. Long, Q.; Qi, G.; Wang, Y., Synthesis and application of ethylenediamine tetrapropionic salt as a novel draw solute for forward osmosis application. *AIChE Journal* **2015,** *61*, (4), 1309-1321.

17. Zhong, Y.; Feng, X.; Chen, W.; Wang, X.; Huang, K. W.; Gnanou, Y.; Lai, Z., Using UCST Ionic Liquid as a Draw Solute in Forward Osmosis to Treat High-Salinity Water. *Environ Sci Technol* **2016,** *50* (2), 1039-45.

18. Cai, Y.; Shen, W.; Wei, J.; Chong, T. H.; Wang, R.; Krantz, W. B.; Fane, A. G.; Hu, X., Energy-efficient desalination by forward osmosis using responsive ionic liquid draw solutes. *Environmental Science: Water Research & Technology* **2015,** *1*, (3), 341-347.

19. Stone, M. L.; Rae, C.; Stewart, F. F.; Wilson, A. D., Switchable polarity solvents as draw solutes for forward osmosis. *Desalination* **2013,** *312*, 124-129.

20. Li, D.; Zhang, X.; Yao, J.; Simon, G. P.; Wang, H., Stimuli-responsive polymer hydrogels as a new class of draw agent for forward osmosis desalination. *Chemical Communications* **2011,** *47*, (6), 1710-1712.

21. Cai, Y.; Shen, W.; Loo, S. L.; Krantz, W. B.; Wang, R.; Fane, A. G.; Hu, X., Towards temperature driven forward osmosis desalination using Semi-IPN hydrogels as reversible draw agents. *Water Research* **2013,** *47*, (11), 3773-3781.

22. Li, D.; Zhang, X.; Simon, G. P.; Wang, H., Forward osmosis desalination using polymer hydrogels as a draw agent: Influence of draw agent, feed solution and membrane on process performance. *Water Research* **2013,** *47*, (1), 209-215.

23. Cai, Y.; Wang, R.; Krantz, W. B.; Fane, A. G.; Hu, X. M., Exploration of using thermally responsive polyionic liquid hydrogels as draw agents in forward osmosis. *RSC Advances* **2015,** *5*, (118), 97143-97150.

24. Razmjou, A.; Simon, G. P.; Wang, H. T., Effect of particle size on the performance of forward osmosis desalination by stimuli-responsive polymer hydrogels as a draw agent. *Chemical Engineering Journal* **2013,** *215*, 913-920.

25. Zhang, X.-Z.; Yang, Y.-Y.; Chung, T.-S., The Influence of Cold Treatment on Properties of Temperature-Sensitive Poly(N-isopropylacrylamide) Hydrogels. *Journal of Colloid and Interface Science* **2002,** *246*, (1), 105-111.

26. Li, D.; Zhang, X.; Yao, J.; Zeng, Y.; Simon, G. P.; Wang, H., Composite polymer hydrogels as draw agents in forward osmosis and solar dewatering. *Soft Matter* **2011,** *7*, (21), 10048-10056.

27. Razmjou, A.; Barati, M. R.; Simon, G. P.; Suzuki, K.; Wang, H., Fast Deswelling of Nanocomposite Polymer Hydrogels via Magnetic Field-Induced Heating for Emerging FO Desalination. *Environmental Science & Technology* **2013,** *47*, (12), 6297-6305.

28. Zeng, Y.; Qiu, L.; Wang, K.; Yao, J.; Li, D.; Simon, G. P.; Wang, R.; Wang, H., Significantly enhanced water flux in forward osmosis desalination with polymer-graphene composite hydrogels as a draw agent. *Rsc Advances* **2013,** *3*, (3), 887-894.

29. Razmjou, A.; Liu, Q.; Simon, G. P.; Wang, H., Bifunctional Polymer Hydrogel Layers As Forward Osmosis Draw Agents for Continuous Production of Fresh Water Using Solar Energy. *Environmental Science & Technology* **2013,** *47*, (22), 13160-13166.

30. Hartanto, Y.; Yun, S.; Jin, B.; Dai, S., Functionalized thermo-responsive microgels for high performance forward osmosis desalination. *Water Research* **2015,** *70*, 385-393.

31. Cai, Y. F.; Shen, W. M.; Wang, R.; Krantz, W. B.; Faneb, A. G.; Hu, X., CO2 switchable dual responsive polymers as draw solutes for forward osmosis desalination. *Chemical Communications* **2013,** *49*, (75), 8377-8379.

32. Hansen, C. M., *Hansen Solubility Parameters: A User's Handbook, Second Edition*. CRC Press: 2007.

33. Zha, L.; Hu, J.; Wang, C.; Fu, S.; Elaissari, A.; Zhang, Y., Preparation and characterization of poly (N-isopropylacrylamide-co-dimethylaminoethyl methacrylate) microgel latexes. *Colloid Polym Sci* **2002,** *280*, (1), 1-6.

34. Das, M.; Kumacheva, E., From polyelectrolyte to polyampholyte microgels: comparison of swelling properties. *Colloid Polym Sci* **2006,** *284*, (10), 1073-1084.

35. Hoare, T.; Pelton, R., Highly pH and Temperature Responsive Microgels Functionalized with Vinylacetic Acid. *Macromolecules* **2004,** *37*, (7), 2544-2550.

36. Pinkrah, V. T.; Snowden, M. J.; Mitchell, J. C.; Seidel, J.; Chowdhry, B. Z.; Fern, G. R., Physicochemical Properties of Poly(N-isopropylacrylamide-co-4-vinylpyridine) Cationic Polyelectrolyte Colloidal Microgels. *Langmuir* **2003,** *19*, (3), 585-590.

37. Nichifor, M.; Zhu, X. X., Copolymers of N-alkylacrylamides and styrene as new thermosensitive materials. *Polymer* **2003,** *44*, (10), 3053-3060.

38. van de Wetering, P.; Zuidam, N. J.; van Steenbergen, M. J.; van der Houwen, O. A. G. J.; Underberg, W. J. M.; Hennink, W. E., A Mechanistic Study of the Hydrolytic Stability of Poly(2-(dimethylamino)ethyl methacrylate). *Macromolecules* **1998,** *31*, (23), 8063-8068.

39. Dai, S.; Ravi, P.; Tam, K. C., pH-Responsive polymers: synthesis, properties and applications. *Soft Matter* **2008,** *4*, (3), 435-449.

40. Li, X.; Goh, S. H.; Lai, Y. H.; Wee, A. T. S., Miscibility and interactions in blends of carboxyl-containing polysiloxane with poly(1-vinylimidazole). *Polymer* **2001,** *42*, (12), 5463-5469.

41. Mika, A. M.; Childs, R. F., Acid/base properties of poly(4-vinylpyridine) anchored within microporous membranes. *Journal of Membrane Science* **1999,** *152*, (1), 129-140.

42. Mauser, T.; Déjugnat, C.; Sukhorukov, G. B., Balance of Hydrophobic and Electrostatic Forces in the pH Response of Weak Polyelectrolyte Capsules. *The Journal of Physical Chemistry B* **2006,** *110*, (41), 20246-20253.

43. Nur, H.; Pinkrah, V. T.; Mitchell, J. C.; Benée, L. S.; Snowden, M. J., Synthesis and properties of polyelectrolyte microgel particles. *Advances in Colloid and Interface Science* **2010,** *158*, (1–2), 15-20.

44. Kabiri, K.; Omidian, H.; Hashemi, S. A.; Zohuriaan-Mehr, M. J., Synthesis of fast-swelling superabsorbent hydrogels: effect of crosslinker type and

concentration on porosity and absorption rate. *European Polymer Journal* **2003,** *39*, (7), 1341-1348.

45. Zhao, Q.; Sun, J.; Zhou, Q., Synthesis of macroporous poly(N-isopropylacrylamide) hydrogel with ultrarapid swelling–deswelling properties. *Journal of Applied Polymer Science* **2007,** *104*, (6), 4080-4087.

46. Carey, F. A., *Organic chemistry*. McGraw-Hill: 2000.

47. Van Krevelen, D. W.; Te Nijenhuis, K., Chapter 7 - Cohesive Properties and Solubility. In *Properties of Polymers (Fourth Edition)*, by, D. W. V. K.; Nijenhuis, K. T., Eds. Elsevier: Amsterdam, 2009; pp 189-227.

48. Brandrup, J.; Immergut, E. H.; Grulke, E. A., *Polymer Handbook*. Wiley: 1999.

49. Gu, M.; Kilduff, J. E.; Belfort, G., High throughput atmospheric pressure plasma-induced graft polymerization for identifying protein-resistant surfaces. *Biomaterials* **2012,** *33*, (5), 1261-1270.

5.8 Supporting information

5.8.1 Digital photos of thermoresponsive cationic copolymer microgels before and after FO process

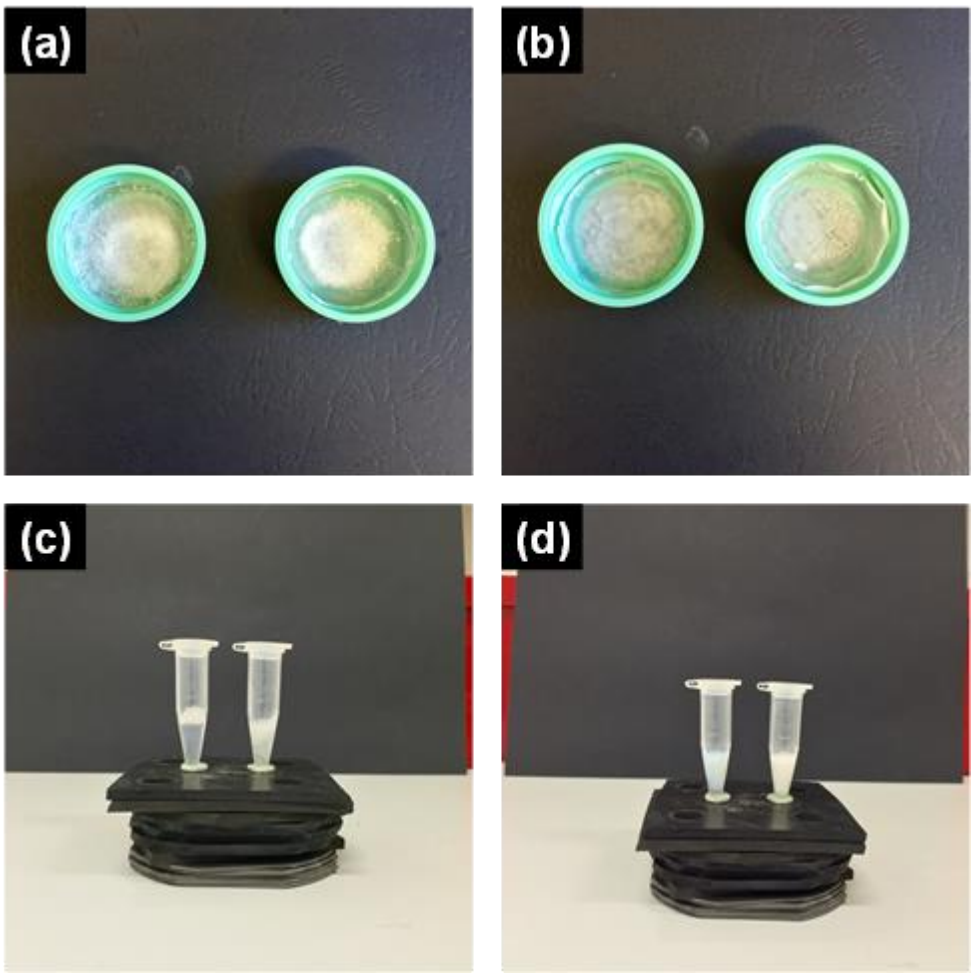

Figure 5.8 Digital image of MCG-NP-DEAEMA (left) and MCG-NP-VI (right) thermoresponsive cationic microgels (a) before FO process; (b) after FO process; (c) at room temperature and (d) at 40 ^{o}C.

5.8.2 pH and conductivity titration curves of thermoresponsive cationic copolymer microgels

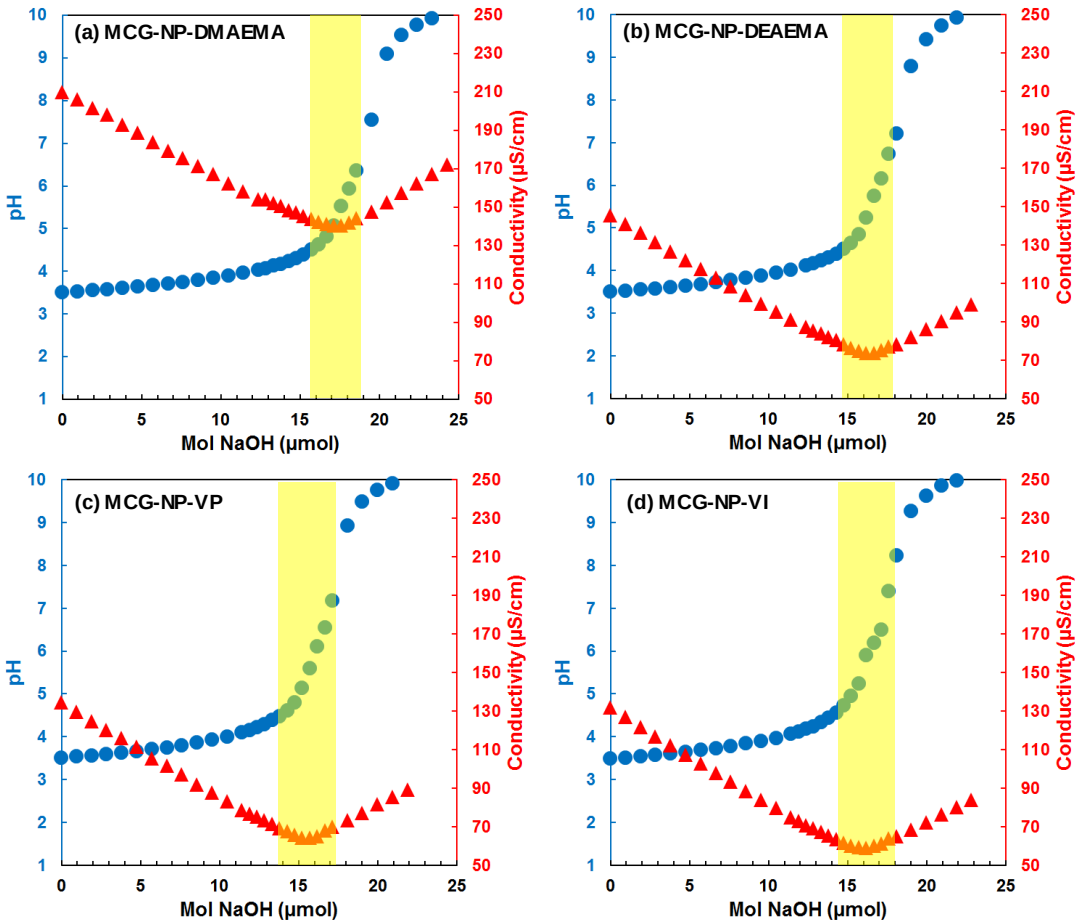

Figure 5.9 pH and conductivity titration curves of cationic thermoresponsive copolymer microgels. The concentration of microgel sample is ~ 1 mg/mL. Diluted hydrochloric acid was used to adjust the pH of the solution to ~ 3.5 prior titration. Sodium hydroxide was used as a titrant.

5.8.3 Zeta potential measurements of thermoresponsive cationic copolymer microgels

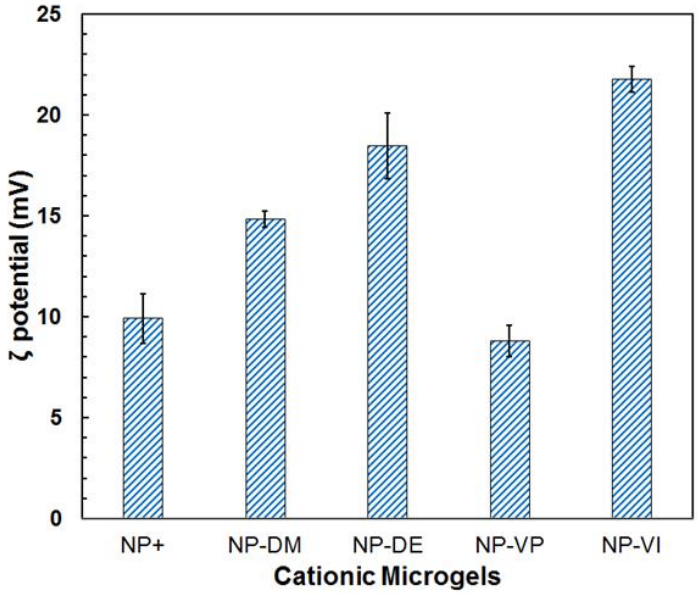

Figure 5.10 Zeta potential measurement for each cationic copolymer microgels in water with at 20 ºC and pH 6.8

Table 5.5 Synthesis and characterization of thermoresponsive cationic copolymer microgels

Nomenclature	Monomer Content in Feed (g)		BIS (g)	V-50 (g)	Comonomers content (mmol g^{-1} polymer)	
	NP	Co-monomers			Measured**	Theoretical*
MCG-NP	3.00	-	0.03	0.03	-	-
MCG-NP-DMAEMA	2.94	0.06	0.03	0.03	0.12	0.13
MCG-NP-DEAEMA	2.94	0.06	0.03	0.03	0.10	0.11
NP-VP	2.94	0.06	0.03	0.03	0.18	0.19
NP-VI	2.94	0.06	0.03	0.03	0.18	0.21

*Calculated from the feed

*Measured from pH and conductivity titrations

5.8.4 Solubility parameter component group contributions (Hoftyzer – Van Krevelen)

5.8.4.1 N-Isopropylacrylamide

Density: 1.1 g/cm^3

Molecular weight: 113.16

Table 5.6 Solubility parameter component group contributions for N-isopropylacrylamide

Group	Amount	F_{di} $(MJ/m^3)^{1/2}.mol^{-1}$	F_{pi}^2 $(MJ/m^3).mol^{-2}$	E_{hi} $J.mol^{-1}$
-CH_3	2	840	0	0
-CH_2-	1	270	0	0
>CH-	2	160	0	0
-CO-	1	290	592,900	2,000
-NH-	1	160	44,100	3,100
Σ		1,720	637,000	5,100

5.8.4.2 2-(Dimethylamino) ethyl methacrylate

Density: 0.933 g/cm^3

Molecular weight: 157.21

Table 5.7 Solubility parameter component group contributions for 2-(dimethylamino) ethyl methacrylate

Group	Amount	F_{di} $(MJ/m^3)^{1/2}.mol^{-1}$	F_{pi}^2 $(MJ/m^3).mol^{-2}$	E_{hi} $J.mol^{-1}$
-CH_3	3	1,260	0	0
-CH_2-	3	810	0	0
-CO-	1	290	592,900	2,000
-O-	1	100	160,000	3,000
>C<	1	-70	0	0
>N-	1	20	640,000	5,000
Σ		2,410	1,392,900	10,000

5.8.4.3 2-(Diethylamino) ethyl methacrylate

Density: 0.922 g/cm^3

Molecular weight: 185.26

Table 5.8 Solubility parameter component group contributions for 2-(diethylamino) ethyl methacrylate

Group	Amount	F_{di} $(MJ/m^3)^{1/2}.mol^{-1}$	F_{pi}^2 $(MJ/m^3).mol^{-2}$	E_{hi} $J.mol^{-1}$
$-CH_3$	3	1,260	0	0
$-CH_2-$	5	1,350	0	0
>C<	1	-70	0	0
-CO-	1	290	592,900	2,000
-O-	1	100	160,000	3,000
>N-	1	20	640,000	5,000
Σ		2,950	1,392,900	10,000

5.8.4.4 4-Vinylpyridine

Density: 0.975 g/cm^3

Molecular weight: 105.14

Table 5.9 Solubility parameter component group contributions for 4-vinylpyridine

Group	Amount	F_{di} $(MJ/m^3)^{1/2}.mol^{-1}$	F_{pi}^2 $(MJ/m^3).mol^{-2}$	E_{hi} $J.mol^{-1}$
$-CH_2-$	1	270	0	0
>CH-	1	80	0	0
=CH-	4	800	0	0
Ring	1	190	0	0
>C<	1	70	0	0
>N-	1	20	640,000	5,000
Σ		1,430	640,000	5,000

1-Vinylimidazole

Density: 1.039 g/cm^3

Molecular weight: 94.11

Table 5.10 Solubility parameter component group contributions for 1-vinylimidazole

Group	Amount	F_{di} $(MJ/m^3)^{1/2}.mol^{-1}$	F_{pi}^2 $(MJ/m^3).mol^{-2}$	E_{hi} $J.mol^{-1}$
$-CH_2-$	1	270	0	0
>CH-	1	80	0	0
=CH-	3	600	0	0
Ring	1	190	0	0
>N-	2	40	1,280,000	10,000
Σ		1,180	684,100	10,000

Chapter 6. Thermoresponsive Non-ionic Copolymer Microgels as Forward Osmosis Draw Agents for Enhanced Water Separation Process

Yusak Hartanto, Masoumeh Zargar, Xiaolin Cui, Bo Jin, Sheng Dai

School of Chemical Engineering, The University of Adelaide, SA 5005, Australia

Graphical Abstract:

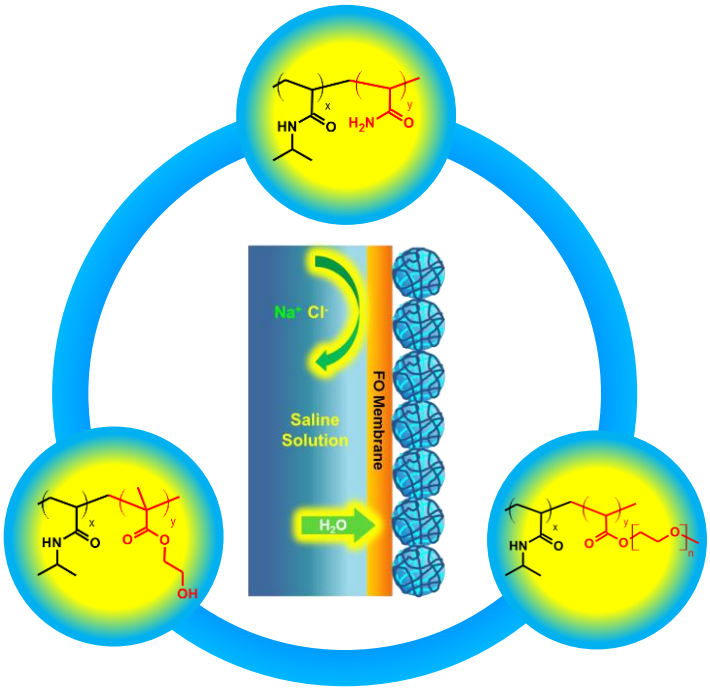

Statement of Authorship

Title of Paper	Non-ionic Thermoresponsive Copolymer Microgels as Draw Agents for Enhanced Water Recovery in Forward Osmosis Desalination
Publication Status	☐ Published ☐ Accepted for Publication ☐ Submitted for Publication ☑ Unpublished and Unsubmitted work written in manuscript style
Publication Details	In preparation

Principal Author

Name of Principal Author (Candidate)	Yusak Hartanto		
Contribution to the Paper	Design the major experiments, data analysis and manuscript writing.		
Overall percentage (%)	60 %		
Certification:	This paper reports on original research I conducted during the period of my Higher Degree by Research candidature and is not subject to any obligations or contractual agreements with a third party that would constrain its inclusion in this thesis. I am the primary author of this paper.		
Signature		Date	

Co-Author Contributions

By signing the Statement of Authorship, each author certifies that:

i. the candidate's stated contribution to the publication is accurate (as detailed above);

ii. permission is granted for the candidate in include the publication in the thesis; and

iii. the sum of all co-author contributions is equal to 100% less the candidate's stated contribution.

Name of Co-Author	Masoumeh Zargar
Contribution to the Paper	Helped to perform the experiment

Signature		Date	12/01/2016

Name of Co-Author	Xiaolin Cui		
Contribution to the Paper	Designed the experiment and manuscript correction		
Signature		Date	

Name of Co-Author	Bo Jin		
Contribution to the Paper	Designed the experiment and manuscript correction		
Signature		Date	

Name of Co-Author	Sheng Dai		
Contribution to the Paper	Designed the experiment and manuscript correction		
Signature		Date	27/01/2016

6.1 Abstract

Thermoresponsive microgels with ionic comonomers have been recently applied as draw agents for FO desalination. These copolymer microgels are able to generate high water flux depending on the degree of dissociation of the ionic moieties. However, the water recovery performance is compromised due to the contribution of strong solvation interaction of these ionic microgels. To overcome this issue, we prepared N-isopropylacrylamide-based microgels with non-ionic comonomers and applied them as FO draw agents. The thermoresponsive microgels containing acrylamide showed higher water recovery than the previously synthesized ionic microgels while still maintaining relatively high water flux due to the weak hydrogen bonding interaction between water and the hydrophilic acrylamide functional group. The initial water flux and water recovery of the microgel with 5 wt% acrylamide feeding ratio can reach 24.7 LMH and 78.7 %, respectively. Furthermore, this microgel has an apparent water flux of 6.1 LMH. We launched theoretical Hansen solubility parameter analysis to further elucidate the working mechanism of these non-ionic microgels in FO operation. The solubility parameter analysis is well aligned with the experimental results on water flux and water recovery behaviours. This work will pave the way for future development of high performance thermoresponsive microgels as functional draw agents for FO desalination.

Keywords: non-ionic; comonomers; thermoresponsive; microgels; Hansen solubility parameters; N-isopropylacrylamide

6.2 Introduction

Forward osmosis (FO) desalination is an emerging membrane desalination technology that has future potential to be a low energy desalination process due to the absence of high applied pressure during the operation. Furthermore, the membrane fouling in FO process is less severe than that of reverse osmosis (RO) process, which also makes the cleaning process less expensive than the RO process [1]. Typical FO desalination consists two major steps, water absorption and water recovery. In the first step, water permeation process occurs spontaneously due to the gradient of osmotic pressure between feed and draw solutions. The second step involves water recovery from the draw agent where the majority of energy requirement is needed. Thus, the development of suitable draw solute materials is an important issue in FO desalination as they do not only enhance the water absorption, but also decrease the operational costs associated with the water recovery.

In the past years, various draw agents such as thermoresponsive organic solutes [2, 3], hydroacid complexes [4], magnetic nanoparticles [5], carbon quantum dots [6], surfactants [7], ionic liquids [8, 9], and switchable polarity solvents [10, 11] have been proposed to overcome the weaknesses of thermolytic solutes. Although some of these small molecules are able to generate high osmotic pressures comparable to thermolytic solutes to enhance water absorption, the energy consumption during their separation process might still be relatively higher than that of reverse osmosis (RO) desalination due to the thermodynamic limitation [12]. Therefore, finding suitable draw materials that can lower the energy requirement in water recovery process is critical.

Some polyelectrolytes materials have been recently introduced as novel FO draw agents as they can generate high water flux associated with their high strength of

ionization [13-15]. On the other hand, water can be easily recovered using the low-pressure ultrafiltration process, which potentially consumes less energy than thermolytic solutes or inorganic salts as draw agents due to the smaller entropy change of the polymer solution [16, 17]. However, reverse solute flux is still one of the major problems in using linear polyelectrolytes as draw solutes.

Thermoresponsive hydrogels were proposed as FO draw agents to overcome the reverse solute issue of linear polyelectrolytes [18-20]. These hydrogels are able to absorb water from saline solution at room temperature and release the absorbed water when the temperature of the hydrogels is brought to above their volume phase transition temperatures (VPTTs). Nevertheless, the water flux is always lower than their linear polyelectrolytes counterpart due to their bulk volume and poor contact with membrane surface. This leads to high concentration polarization and thus decreases water flux performance [21]. Furthermore, most water are recovered in the form of vapor rather than liquid phase [22] due to the skin formation in the surface of the hydrogels during their deswelling process [23, 24] which might result in the increase of operational cost to further treat the water vapor. Various approaches have been carried out to improve the performance of hydrogel-driven FO desalination such as compositing with magnetic nanoparticles [22], carbon particles [19], reduced graphene oxide (*r*GO) [25], bilayer formation, [26] but the performance is still not as competitive as other draw materials.

Thermoresponsive ionic copolymer microgels were recently introduced as functional FO draw agents to overcome the drawbacks of bulk hydrogels [27]. The microgels can generate higher water flux than the previously synthesized bulk hydrogels due to their smaller sizes, creating high surface areas and improving the

contact with the membrane surface. These microgels have moderate liquid water recovery due to charge repulsion caused by ionized water-soluble moieties from the comonomers.

In this study, we synthesized a series of thermoresponsive microgels with non-ionic water-soluble comonomers and applied them as FO draw agents for the first time. The non-ionic comonomers chosen in this study were acrylamide, 2-hydroxyethyl methacrylate and poly (ethylene glycol) methyl ether acrylate. The FO desalination performance in terms of water flux, water recovery, equilibrium swelling times and water contents of these non-ionic copolymer microgels was evaluated in details. Our results show that the microgels with small amount of acrylamide (~ 5 wt%) have the best overall performance among all the other non-ionic copolymer microgels. Furthermore, Hansen solubility parameter analysis was carried out to correlate the water affinity towards the monomers and FO performance. This approach provides an insight on how to design optimized microgel materials for FO draw agent in the future.

6.3 Materials and methods

6.3.1 Materials

N-Isopropylacrylamide (NP, > 98%), purchased from Tokyo Chemical Industry, was purified by recrystallization from n-hexane and dried overnight at room temperature. N-N'-methylenebisacrylamide (BIS, >98%), acrylamide (AAm, >99%), 2-hydroxyethyl methacrylate (HEMA, > 98%) and poly (ethylene glycol) methyl ether acrylate (PEGA, Mn 480) were purchased from Sigma-Aldrich. Potassium persulfate (KPS) was purchased from Chem-Supply. Sodium chloride was purchased from

VWR. Cellulose triacetate forward osmosis (CTA-FO) membranes were purchased from the Hydration Technologies Inc. (HTI, USA).

6.3.2 Synthesis of non-ionic thermoresponsive microgels

The non-ionic thermoresponsive copolymer microgels of NP and different non-ionic co-monomers were synthesized using semi-batch surfactant-free emulsion polymerization process. In a typical experiment, 0.735 g of NP, 0.015 g of non-ionic co-monomers and 0.0075 g of BIS were dissolved in 75 mL of DI water in a 250 mL three-necked flask fitted with a condenser, a mechanical stirrer and gas inlet/outlet. The semi-batch feeding solution was prepared by mixing 2.205 g of NP, 0.045 g of non-ionic co-monomers and 0.0225 g of BIS in 50 mL of Millipore water. The batch and feeding solutions were bubbled with nitrogen to remove the dissolved oxygen for 1 hour. The batch solution was heated to 70 ^{o}C under nitrogen protection. A KPS solution was then injected to the flask to initiate the polymerization. After the batch solution turned cloudy, the feeding solution was injected at a rate of 3 mL/hour using a syringe pump one hour later. The polymerization was carried out overnight under continuous stirring and nitrogen blanket. After that, the microgel solution were cooled and purified using membrane dialysis (MWCO 12–14 kDa) against DI water for five days with daily change of water to remove any unreacted monomer and comonomer. The purified microgels were then dried at 70 ^{o}C and grounded into powder.

Table **6.1** shows the composition of synthesized thermoresponsive non-ionic copolymer microgels used in this study as FO draw materials.

Table 6.1 Synthesis and characterization of non-ionic thermoresponsive copolymer microgels

Nomenclature	Monomer Content in Feed (g)		MBA (g)	KPS (g)	VPTT* (ºC)
	NIPAM	Co-monomers			
NP	3.0	-	0.03	0.03	32.5
NP99-AM1	2.97	0.03	0.03	0.03	33
NP98-AM2	2.94	0.06	0.03	0.03	34
NP95-AM5	2.85	0.15	0.03	0.03	34
NP90-AM10	2.7	0.3	0.03	0.03	36
NP95-HM5	2.85	0.15	0.03	0.03	30
NP95-PEGA5	2.85	0.15	0.03	0.03	28

6.3.3 Characterization of non-ionic thermoresponsive copolymer microgels

6.3.3.1 Dynamic light scattering measurements

Dynamic light scattering was used to measure the hydrodynamic diameters (d_h) of the non-ionic copolymer microgels between 20 ºC – 50 ºC using a Zetasizer (Malvern, Nano-ZS). The swelling ratio (SR) of the microgels was calculated using the following equation:

$$SR = \left(\frac{d_{h,To}}{d_{h,Ti}}\right)^3 \qquad \text{Eq. 6.1}$$

where SR is the swelling ratio of the microgels, $d_{h,To}$ (nm) is the hydrodynamic diameter of the microgels at To ºC (20 ºC) and $d_{h,Ti}$ (nm) is the hydrodynamic diameter of the microgels at Ti ºC.

6.3.3.2 Fourier Transform Infrared Spectroscopy (FTIR)

Attenuated total reflectance Fourier transform infrared spectroscopy (ATR-FTIR) was used to verify the incorporation of non-ionic comonomers into the copolymer microgels. FTIR bands were recorded using a Thermos Scientific NICOLET 6700 spectrometer equipped with a diamond ATR with wavenumber resolution of 4 cm^{-1} in the range of 400 – 4000 cm^{-1}.

6.3.4 Forward osmosis desalination evaluation

6.3.4.1 Water flux evaluation

A 100 mg of the dried microgels was placed on the surface of FO membrane in our homemade FO membrane setup equipped with an on-line conductivity monitoring system [27]. PRO mode was selected as the membrane configuration in this study. The system was also conditioned for 30 min. prior to loading the microgels to the membrane. The conductivity of the feed solution was converted into the concentrations of sodium chloride using a calibration curve and the water flux was calculated using the following equations:

$$V_t = \frac{C_i V_i}{C_t} \quad \text{Eq. 6.2}$$

$$J_w = \frac{V_i - V_t}{A\ t} \quad \text{Eq. 6.3}$$

where V_t (mL) is the volume of feed at time t, V_i (mL) is the initial volume of feed, C_i (ppm) is the initial feed concentration, C_t (ppm) is the feed concentration at time t, J_w (LMH) is the water flux, A (m^2) is the effective membrane surface area and t (h) is the time where the conductivity of the feed solution changes.

6.3.4.2 Water recovery

The swelled microgels were transferred to centrifuge tubes and weighed after the two-hour water absorption period. The microgels were then centrifuged at 40 ^{o}C and 10,000 rpm for 10 minutes to separate absorbed water from the microgels. The recovered water was determined using gravimetric method. The water recovered from de-swelled microgels was calculated using the following equations:

$$C_p = \frac{W_d}{W_d + W_w} \quad \text{Eq. 6.4}$$

$$W_g = W_m(1 - C_p) \quad \text{Eq. 6.5}$$

$$R = \frac{W_R}{W_g}\, x\, 100\% \quad \text{Eq. 6.6}$$

where C_p (g microgels/g water) is the concentration of microgels in the centrifuge tube, W_p (g) is the weight of dry microgel, W_w (g) is the weight of water absorbed by the microgels calculated from water flux data, W_g (g) is the weight of water in the microgels, W_m (g) is the weight of microgels in the centrifuge tube, W_R (g) is the weight of absorbed water recovered from the tube and R (%) is the percentage of water recovered from the microgels.

6.3.4.3 Apparent water flux

Apparent water flux is expressed as the amount of water that can be released from the microgels per unit area per unit cycling time and written as follows [36]:

$$J_{app} = \frac{m_W}{(T_{eq} + T_R)A} \quad \text{Eq. 6.7}$$

where J_{app} (LMH) is the apparent water flux, m_W (L) is the volume of water that can be released during dewatering process, T_{eq} (h) is the time needed to reach

equilibrium condition, T_R (h) is the time needed to dewater the microgels and A (m^2) is the effective membrane area.

6.3.5 Analysis of Hansen solubility parameter (HSP)

The individual solubility parameter using group contribution approach can be calculated using the following equations:

$$\delta_d = \frac{\sum F_{di}}{V} \quad \text{Eq. 6.8}$$

$$\delta_p = \frac{\sqrt{\sum F_{pi}^2}}{V} \quad \text{Eq. 6.9}$$

$$\delta_h = \sqrt{\frac{\sum E_{hi}}{V}} \quad \text{Eq. 6.10}$$

$$\delta_{total} = \sqrt{\delta_d^2 + \delta_p^2 + \delta_h^2} \quad \text{Eq. 6.11}$$

Where δ_d ($MPa^{1/2}$) is the dispersion interaction parameter, F_{di} ($[MJ/m^3]^{1/2}.mol^{-1}$) is molar attraction constant for the dispersion component, δ_p ($MPa^{1/2}$) is the polar interaction parameter, F_{pi} ($[MJ/m^3]^{1/2}.mol^{-1}$) is the group contribution constant for the polar component, δ_h ($MPa^{1/2}$) is the hydrogen bonding interaction parameter, E_{hi} ($J.mol^{-1}$) is the hydrogen bonding energy, V (cm^3/mol) is the molar volume and δ_{total} ($MPa^{1/2}$) is the total of the solubility parameter.

6.4 Results and Discussion

6.4.1 Synthesis and characterization of non-ionic thermoresponsive co-polymer microgels

Non-ionic thermoresponsive microgels were synthesized using the semi-batch surfactant-free emulsion polymerization. Different non-ionic co-monomers, which are acrylamide, 2-hydroxyethyl methacrylate and poly (ethylene glycol) methyl ether acrylate, were chosen in this study. The chemical structures of NP and the non-ionic co-monomers are shown in Figure 6.1.

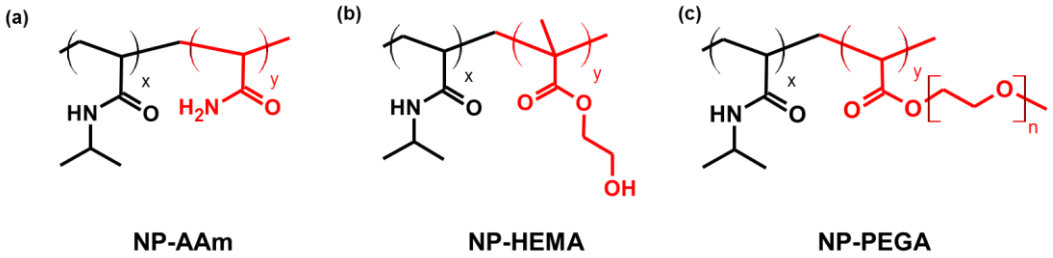

Figure 6.1 The chemical structures of non-ionic thermoresponsive copolymer microgels for FO draw agents: (a) NP-AAm, (b) NP-HEMA and (c) NP-PEGA.

Fourier transform infrared (FTIR) spectroscopy was used to confirm the incorporation of non-ionic co-monomers in copolymer microgels. Figure 6.2a shows the FTIR spectra for different non-ionic co-polymer microgels. The bands at 3282 cm^{-1} in all non-ionic microgels are due to N-H stretching from N-isopropylacrylamide while the broad adsorption band in the range of 3200 – 3600 cm^{-1} for NP95-HEMA5 microgel confirms the presence of hydroxyl group in this microgel [28]. The bands at 1726 cm^{-1} in NP95-HEMA5 and NP95-PEGA5 microgels correspond to ester carbonyl groups in HEMA and PEGMA co-monomer [28, 29]. Figure 6.2b shows the FTIR spectra for NP-AAm microgels at different AAm

feeding ratios. The amide I band at 1633 cm^{-1} is due to carbonyl stretching and the amide II band at 1530 cm^{-1} is due to NH plane bending from N-isopropylacrylamide. All the NP-AAm microgels show N-H stretching band between 3200 cm^{-1} and 3600 cm^{-1}. Although there is no clear spectrum difference between NP microgel and NP-AAm microgel due to the overlap amide I and amide II bands from both monomers, the amide I band and amide II band have stronger adsorption as the concentration of AAm increases.

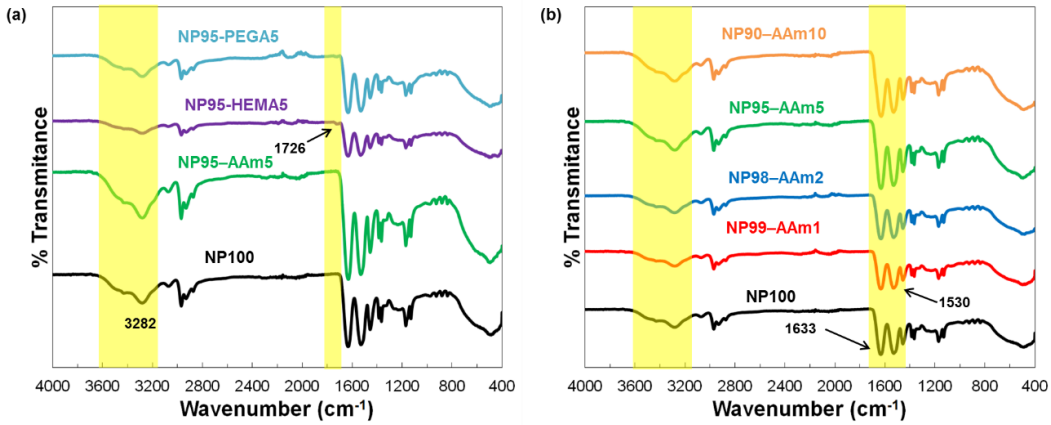

Figure 6.2 FTIR spectra of (a) different non-ionic thermoresponsive copolymer microgels and (b) NP-AAm microgels at different comonomer feeding ratios.

Dynamic light scattering (DLS) was used to determine the swelling ratio of each microgel by measuring the change of microgel hydrodynamic diameters with temperatures. Figure 6.3a and Figure 6.3b show the hydrodynamic diameter profiles for different non-ionic copolymer microgels and different NP-AAm microgels, respectively. Copolymerizing NP with different non-ionic co-monomers slightly shifts the volume phase transition temperature (VPTT) of the microgels depending on the solvation behavior of comonomers as shown in Figure 6.3a. A slight increase in VPTT is observed in NP95-AAm5 microgel due to the contribution of hydrophilic

acrylamide [30] while the decrease in VPTT is observed in NP95-HEMA5 and NP95-PEGA5. The influence of acrylamide hydrophilicity on VPTT is also observed for NP-AAm microgels as shown in Figure 6.3b. NP-AAm microgels with acrylamide feed ratio up to 5 wt% shows the continuous increase in their VPTTs while still maintaining sharp phase transition. The phase transition becomes broad for the NP90-AAm10 due to decrease in thermo sensitivity caused by the contribution of hydrophilic acrylamide functional group [31] and the VPTT increases to 36 ºC. The details of the VPTTs for these microgels are summarized in Table 6.4 (Supporting Information).

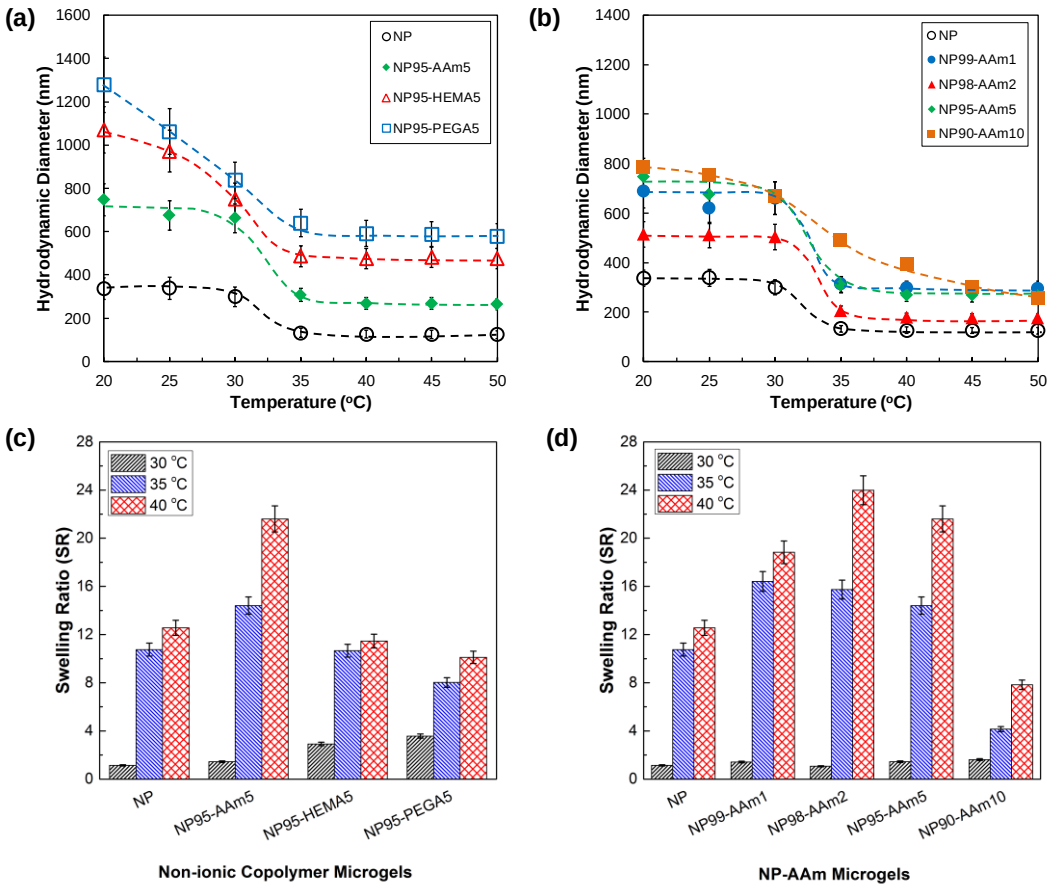

Figure 6.3 Hydrodynamic diameters *vs.* temperatures for: (a) non-ionic thermoresponsive copolymer microgels and (b) different feeding ratios of acrylamide. Swelling ratios at

different temperatures for: (c) non-ionic thermoresponsive copolymer microgels and (d) different feedings ratio of acrylamide.

The swelling ratios of different non-ionic copolymer microgels at different temperatures near their VPTTs are shown in Figure 6.3c. Incorporating acrylamide as a comonomer significantly improves the swelling ratio of the microgel while other comonomers reduce the swelling ratios due to their more hydrophobic properties than acrylamide. Figure 6.3d shows the effect of acrylamide feeding ratio on the swelling ratios of NP-AM microgels near their VPTTs. Increasing the feeding ratio of acrylamide beyond 5 wt% significantly reduces the swelling ratio of the microgels due to the possible formation of intermolecular hydrogen bonding between primary amide from acrylamide and secondary amide from N-isopropylacrylamide which results in reduced the availability of acrylamide groups to attract water molecules [32, 33].

6.4.2 Water flux and water content profiles of non-ionic thermoresponsive copolymer microgels

Incorporation of different non-ionic comonomers into N-isopropylacrylamide-based microgels alters the profiles of water flux and water content of the microgels as shown in Figure 6.4. The NP microgel shows the longest equilibrium swelling time (90 min) and the lowest water flux among other non-ionic microgels. On the other hand, NP95-AAm5 microgel has the shortest equilibrium swelling time (40 min) and the highest water flux due to the contribution of hydrophilic acrylamide. In addition, this microgel also reveals the highest water content compared to other non-ionic microgels. While NP95-HEMA5 and NP95-PEGA5 have longer swelling time than NP95-AAm5, their equilibrium swelling times are shorter than NP microgel. The

equilibrium swelling times for NP95-HEMA5 and NP95-PEGA5 are 55 min and 50 min, respectively. The water contents of both microgels are less than NP microgel consistent with their lower swelling ratios compared to NP microgel as shown in Figure 6.3c.

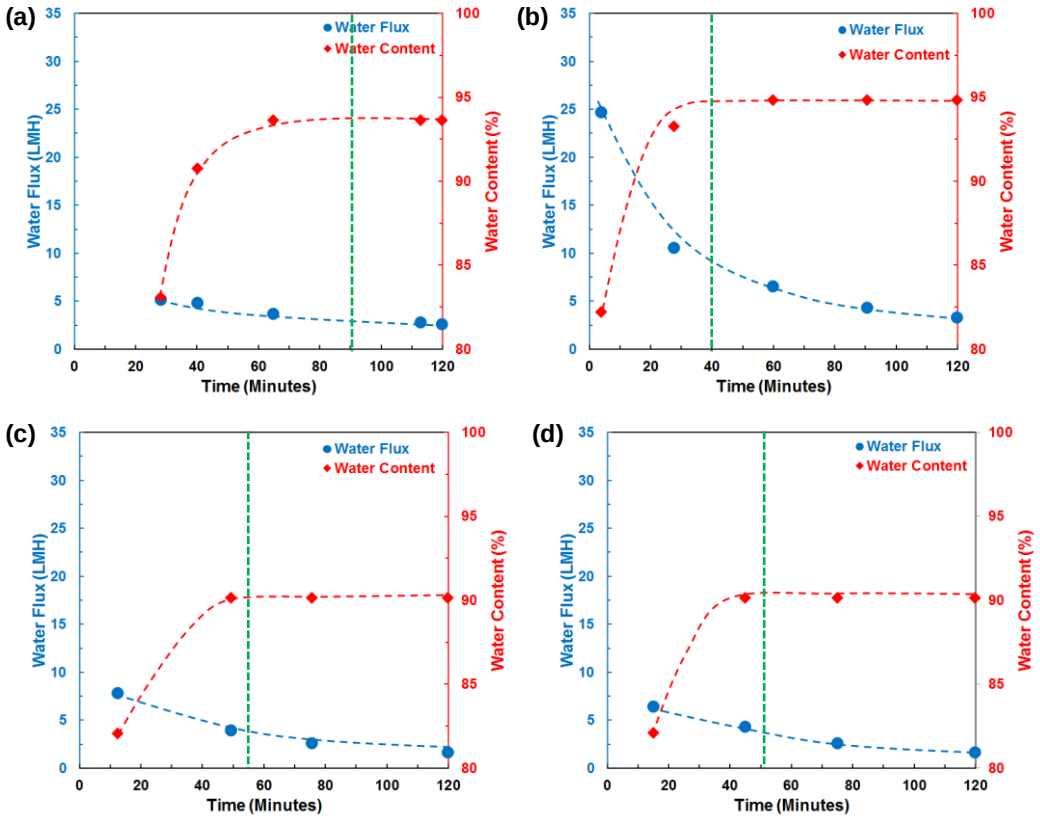

Figure 6.4 Water flux and water content profiles of different non-ionic copolymer thermoresponsive microgels: (a) NP, (b) NP95-AAm5, (c) NP95-HEMA5 and (d) NP95-PEGA5, over a two-hour water absorption period. Feed solution is 2000 ppm NaCl and the room temperature was maintained at 20 ± 2 ºC. The green vertical lines indicate equilibrium swelling time.

Figure 6.5 shows the water flux and water content profiles of NP-AAm microgels with different acrylamide feed ratios. NP99-AAm1 microgel shows shorter equilibrium swelling time (80 min) and higher water content than NP microgel in

Figure 6.4a due to the contribution of hydrophilic acrylamide. As the acrylamide feeding ratio increases, the equilibrium swelling time becomes shorter due to strong solvation of the microgels. The shortest equilibrium swelling time was observed in NP90-AAm10 microgel (35 min). However, its equilibrium water content is slightly less than other NP-AAm microgels due to the reduced swelling ratio as observed in Figure 6.3d.

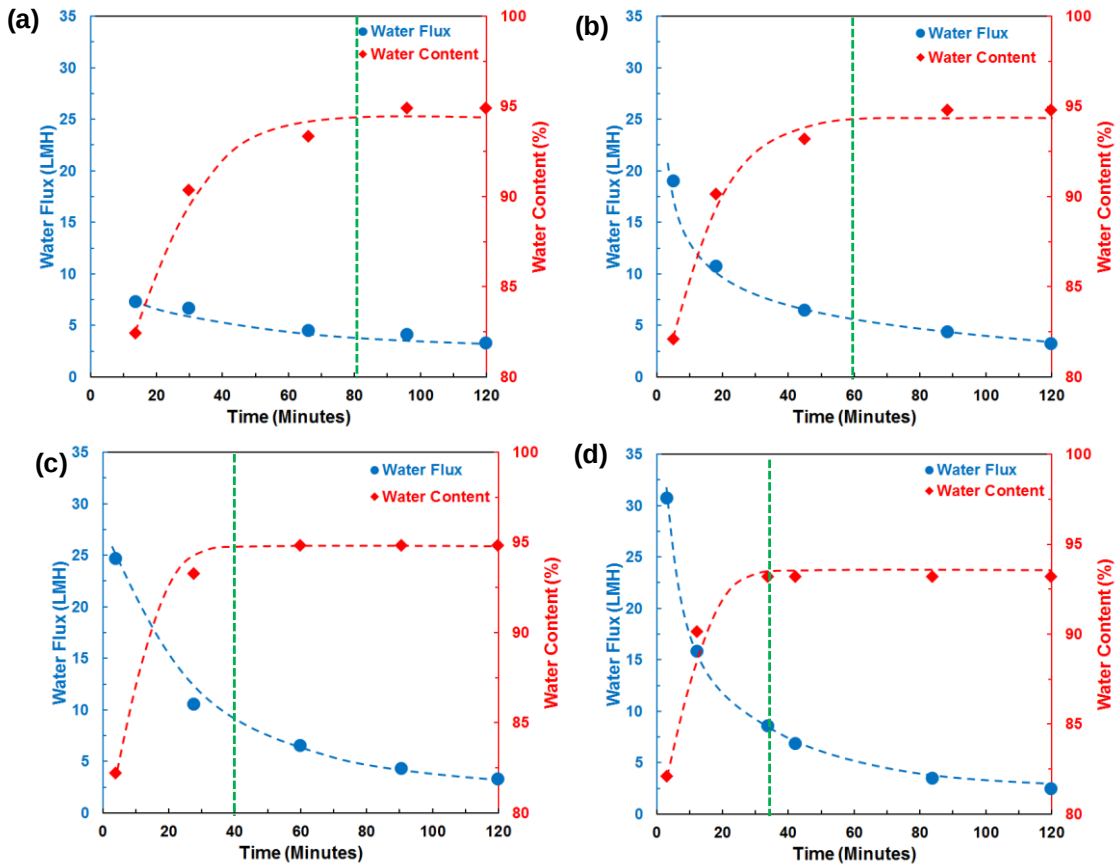

Figure 6.5 Water flux and water content profiles of NP-AAm microgels with different acrylamide concentration: (a) NP99-AAm1, (b) NP98-AAm2, (c) NP95-AAm5 and (d) NP90-AAM10, over a two-hour water absorption period. Feed solution is 2000 ppm NaCl and the room temperature was maintained at 20 ± 2 °C. The green vertical lines show equilibrium swelling time.

6.4.3 Initial water flux and water recovery of non-ionic copolymer microgels

The initial water flux and water recovery for different non-ionic copolymer microgels and different concentration of acrylamide are shown in Figure 6.6. NP microgel shows the lowest water flux among other non-ionic copolymer microgels. The water flux for NP microgel is 5.1 LMH and the water recovery is 83.3%. The water flux is improved to 24.7 LMH when NP95-AAm5 is used as draw agent for FO process due to hydrophilic nature of acrylamide. However, the water recovery slightly decreases to 78.7% compared to NP microgel. The water flux for NP95-HEMA5 and NP95-PEGA5 (7.8 LMH and 6.4 LMH) are lower than that of NP95-AAm5 due to amphiphilic characteristics of the co-monomers while the water recovery for both microgels are higher than that of NP and NP95-AAm5 microgels. The water recovery for NP95-HEMA5 and NP95-PEGA5 are 88.9 % and 89.1 %, respectively. Although there is an increase in microgel hydrophilicity such as in NP95-AAm5, the water recovery is not greatly compromised as observed in ionic microgels [27, 34]. This might be due to the absence of ionic interaction between water and ionic functional group in the microgels. The interaction between water and hydrophilic functional groups is mainly dominated by hydrogen bonding interaction which is relatively weak compared to ionic interaction in ionic microgels. As a result, most water can be recovered when the temperature of the microgels is brought to above the VPTT.

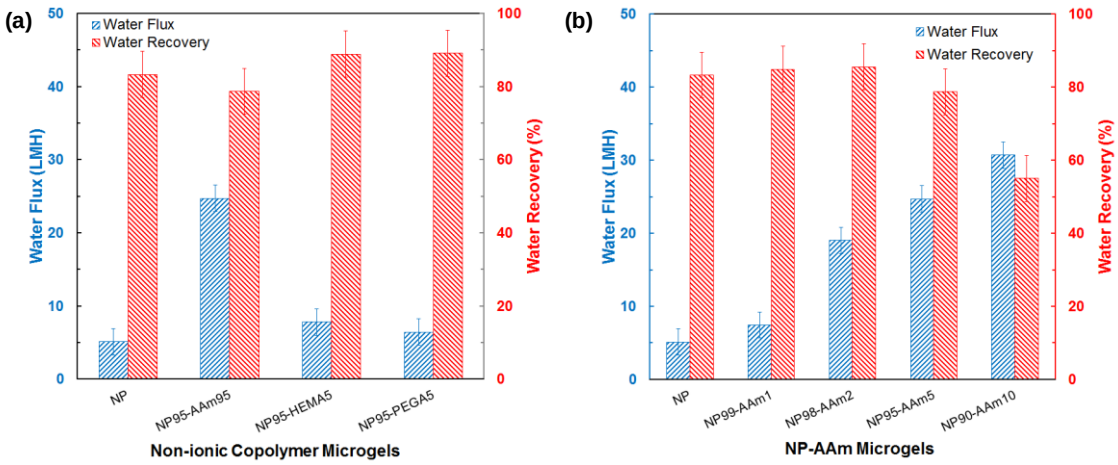

Figure 6.6 Initial water flux and water recovery for: (a) different non-ionic thermoresponsive microgels and (b) different NP-AAm microgels. Membrane orientation is AL-DS. Feed solution is 2000 ppm NaCl. Temperature of the feed solution is 20 ± 2 ºC.

As the NP95-AAm5 microgel has better water flux while maintaining relatively high water recovery, further investigation on effect of acrylamide concentration on water flux and water recovery during FO process is shown in Figure 6.6b. NP99-AAm1 microgel has higher water flux (7.4 LMH) and higher water recovery (84.8%) than NP microgel. The water flux and water recovery is further improved for NP98-AAm2 microgel. The water flux and water recovery for this microgel are 19 LMH and 85.5 %, respectively. Further increase in water flux (24.7 LMH) is observed in NP95-AAm5 while the water recovery starts to decrease to 78.7 %. The highest water flux is achieved for NP90-AAm10 and the water recovery significantly drops to 55%. This observation is in agreement with our previous work and other results where the introduction of ionic moieties or hydrophilic functional group will increase the water flux but decrease the water recovery in hydrogel or microgel-based FO desalination [27, 34].

6.4.4 Apparent overall water flux of non-ionic thermoresponsive copolymer microgels

Apparent water flux measures the overall performance of microgel-driven FO desalination by taking account equilibrium swelling time and water recovery time. In addition, this parameter provides an insight on the water flux that can be generated after water recovery process [34]. The apparent water fluxes of non-ionic microgels used in this work are shown in Figure 6.7. NP microgel has the lowest apparent flux (0.8 LMH) among other non-ionic copolymer microgels. NP-AAm microgels show enhanced apparent flux due to its faster equilibrium swelling time and high swelling ratios with NP95-AAm5 has the best apparent water flux (6.1 LMH). Although NP90-AAm10 has the highest initial water flux and the fastest equilibrium swelling time, the amount of water recovered is lower than NP95-AAm5. As a result, NP90-AAm10 has a lower apparent flux than NP95-AAm5. The apparent fluxes for NP95-HEMA5 and NP95-PEGA5 are higher than that of NP microgel but lower than NP95-AAm5 due to their relatively low initial water flux of NP microgel. The detailed apparent water flux for each microgel can be seen in Table 6.5 (Supporting Information).

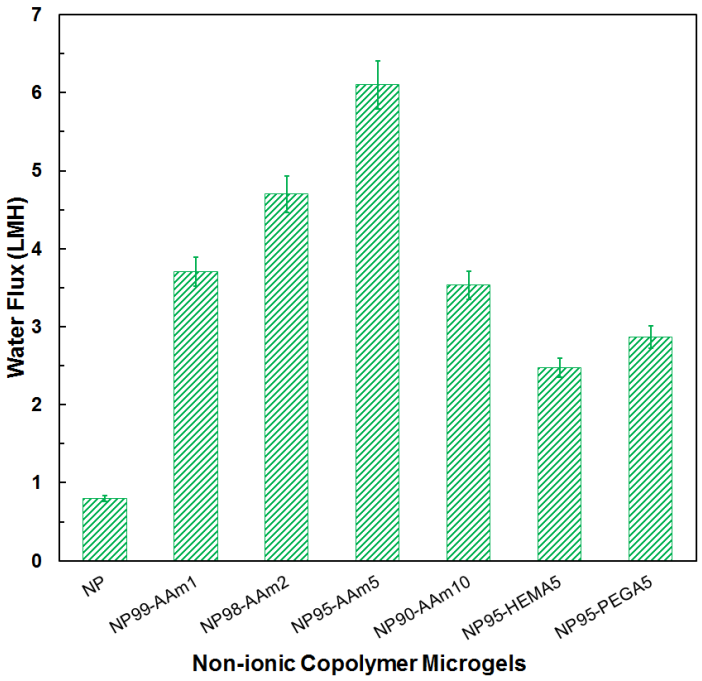

Figure 6.7 Apparent water flux for different non-ionic thermoresponsive copolymer microgels and different feeding ratio of acrylamide.

6.4.5 Analysis of Hansen solubility parameters of non-ionic thermoresponsive copolymer microgels

Designing thermoresponsive microgels as the FO draw agents requires understanding of the degree of solvation of particular monomer and comonomer and Hansen solubility parameter approach can be used to predict the interaction between polymer and solvent [35-38]. In this study, the Hansen solubility parameter for each monomer and comonomer was calculated using the Hoftyzer – Van Krevelen method based on group contribution analysis [39]. Hansen solubility parameter consists of the dispersion, δ_d, the polarity, δ_p, and the hydrogen bonding, δ_h, parameters. Table 6.2 shows the calculated individual Hansen solubility parameters.

Table 6.2 Hansen solubility parameters of water and non-ionic monomer/comonomer predicted using Hoftyzer – Van Krevelen method in $(MPa)^{1/2}$

Chemical Species	δ_d	δ_p	δ_h	δ_{total}
Water*	18.1	12.9	15.5	27.1
NP	16.7	7.8	7.0	19.7
AAm	14.6	12.2	12.9	23.0
HEMA	14.5	5.8	14.9	21.6
PEGA	15.7	2.9	8.8	18.2

*The values were obtained from ref. 17

The small difference between the total Hansen solubility parameter, δ_{total}, for water and a monomer indicates the monomer has good water solubility while the large difference of δ_{total} the monomer has less affinity towards water molecules. Acrylamide has the smallest difference in δ_{total} while PEGA has the largest difference in δ_{total}. This finding is consistent with the highest initial water flux generated by NP95-AAm5 and the lowest initial water flux generated by NP95-PEGA5. In addition, the VPTTs of NP95-HEMA5 and NP95-PEGA5 shown in Figure 6.3a are slightly lower than NP95-AAm5 indicating these copolymer microgels were more hydrophobic than NP95-AAm5 [40, 41].

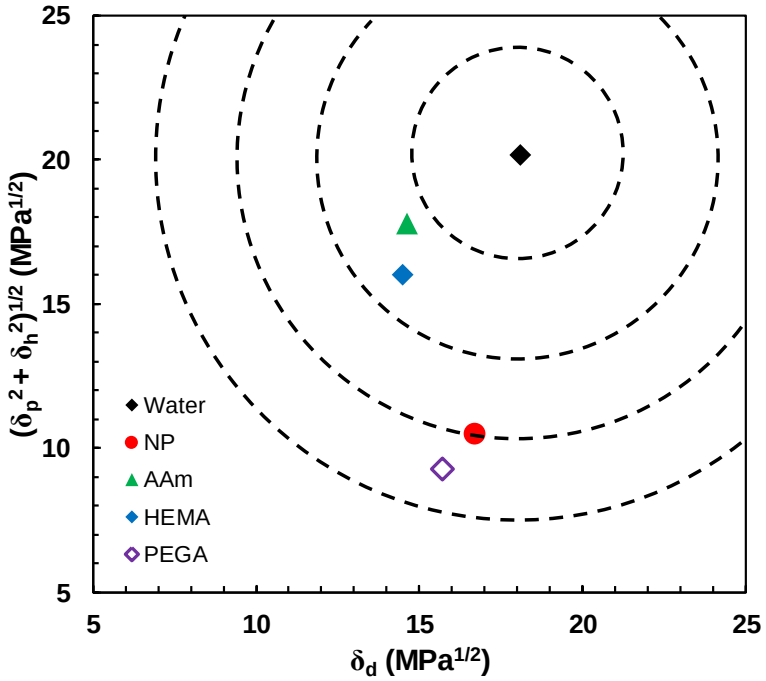

Figure 6.8 The plot of Hansen solubility parameter of δ_d vs. $(\delta_p^2 + \delta_h^2)^{1/2}$ showing the water affinity towards NP monomer and other non-ionic comonomer. The Hansen solubility parameters of monomers were calculated using Hoftyzer – Van Krevelen method. The dotted lines are a measure of the radial distance from water.

Plotting δ_d vs. $(\delta_p^2 + \delta_h^2)^{1/2}$ of Hansen solubility parameters shows the relative radial distance between water molecules and the monomer/comonomer [36]. The short distance from water means strong interaction between water molecules and the monomers. Acrylamide has the closest position to water molecules while poly (ethylene glycol) methyl ether acrylate has the furthest distance to water molecules as shown in Figure 6.8. The solubility distance parameters can be calculated using Equation 6.12-6.14 (Supporting information) and are summarized in Table 6.3.

Table 6.3 The solubility distance parameter (Ra), relative energy difference (RED) parameter and the cohesion energy densities (H) parameter of monomer/co-monomer with water

Monomer/Co-monomer – Water	Ra	RED	H
NP – Water	10.3	0.74	0.55
AAm – Water	7.5	0.54	0.29
HEMA – Water	10.1	0.73	0.53
PEGA – Water	12.9	0.93	0.86

The cohesion energy density (H) and relative energy difference (RED) provide a further insight on how strong the interaction between water molecules and the monomers. The small values of these parameters mean good monomer – water interaction. The value of cohesion energy density must be less than 1 for given polymer – solvent system to be soluble. As shown in Table 6.3, acrylamide has the smallest values of RED and H while poly (ethylene glycol) methyl ether acrylate has the largest values of both parameters. The values of these parameters are consistent with the performance of non-ionic copolymer microgels shown in Figure 6.6.

6.5 Conclusions

Thermoresponsive microgels copolymerized with different non-ionic comonomers (acrylamide, 2-hydroxy ethyl methacrylate and poly (ethylene glycol) methyl ether acrylate) have been prepared using surfactant-free emulsion polymerization and applied as FO draw agents. The hydrophilicity of comonomers affects the water flux, water recovery and equilibrium swelling time in FO process. These copolymer microgels showed enhanced water recovery compared to NP microgel and previously synthesized ionic copolymer microgels due to the weak hydrogen-bonding

interaction between water and the hydrophilic group of these non-ionic copolymer microgels. NP-AM microgel with 5 wt% acrylamide feeding ratio has the best overall performance among other microgels due to its optimized hydrophilicity and hydrophobicity. This results in high water flux and water recovery with fast equilibrium swelling time. The theoretical analysis of Hansen solubility parameters of each comonomer is also consistent with experimental water flux and water recovery data. This analysis will be useful for optimization of microgel materials to improve FO desalination performance.

6.6 Acknowledgement

The authors would like to thank the financial support from the Australian Research Council (DP110102877). YH would like to appreciate the support of Adelaide Graduate Research Scholarships (AGRS).

6.7 References

1. Lee, S.; Boo, C.; Elimelech, M.; Hong, S., Comparison of fouling behavior in forward osmosis (FO) and reverse osmosis (RO). *Journal of Membrane Science* **2010,** *365*, (1-2), 34-39.
2. Noh, M.; Mok, Y.; Lee, S.; Kim, H.; Lee, S. H.; Jin, G.-w.; Seo, J.-H.; Koo, H.; Park, T. H.; Lee, Y., Novel lower critical solution temperature phase transition materials effectively control osmosis by mild temperature changes. *Chemical Communications* **2012,** *48*, (32), 3845-3847.
3. Nakayama, D.; Mok, Y.; Noh, M.; Park, J.; Kang, S.; Lee, Y., Lower critical solution temperature (LCST) phase separation of glycol ethers for forward osmotic control. *Physical Chemistry Chemical Physics* **2014,** *16*, (11), 5319-5325.

4. Ge, Q. C.; Chung, T. S., Hydroacid complexes: a new class of draw solutes to promote forward osmosis (FO) processes. *Chemical Communications* **2013,** *49*, (76), 8471-8473.

5. Ling, M. M.; Chung, T.-S.; Lu, X., Facile synthesis of thermosensitive magnetic nanoparticles as "smart" draw solutes in forward osmosis. *Chemical Communications* **2011,** *47*, (38), 10788-10790.

6. Guo, C. X.; Zhao, D.; Zhao, Q.; Wang, P.; Lu, X., Na(+)-functionalized carbon quantum dots: a new draw solute in forward osmosis for seawater desalination. *Chem Commun (Camb)* **2014,** *50*, (55), 7318-21.

7. Nguyen, H. T.; Chen, S.-S.; Nguyen, N. C.; Ngo, H. H.; Guo, W.; Li, C.-W., Exploring an innovative surfactant and phosphate-based draw solution for forward osmosis desalination. *Journal of Membrane Science* **2015,** *489*, 212-219.

8. Zhong, Y.; Feng, X.; Chen, W.; Wang, X.; Huang, K. W.; Gnanou, Y.; Lai, Z., Using UCST Ionic Liquid as a Draw Solute in Forward Osmosis to Treat High-Salinity Water. *Environ Sci Technol* **2016,** *50* (2), 1039-45.

9. Cai, Y.; Shen, W.; Wei, J.; Chong, T. H.; Wang, R.; Krantz, W. B.; Fane, A. G.; Hu, X., Energy-efficient desalination by forward osmosis using responsive ionic liquid draw solutes. *Environmental Science: Water Research & Technology* **2015,** *1*, (3), 341-347.

10. Orme, C. J.; Wilson, A. D., 1-Cyclohexylpiperidine as a thermolytic draw solute for osmotically driven membrane processes. *Desalination* **2015,** *371*, 126-133.

11. Stone, M. L.; Rae, C.; Stewart, F. F.; Wilson, A. D., Switchable polarity solvents as draw solutes for forward osmosis. *Desalination* **2013,** *312*, 124-129.

12. Shaffer, D. L.; Werber, J. R.; Jaramillo, H.; Lin, S.; Elimelech, M., Forward osmosis: Where are we now? *Desalination* **2015,** *356*, 271-284.

13. Ge, Q.; Su, J.; Amy, G. L.; Chung, T.-S., Exploration of polyelectrolytes as draw solutes in forward osmosis processes. *Water Research* **2012,** *46*, (4), 1318-1326.

14. Tian, E.; Hu, C.; Qin, Y.; Ren, Y.; Wang, X.; Wang, X.; Xiao, P.; Yang, X., A study of poly (sodium 4-styrenesulfonate) as draw solute in forward osmosis. *Desalination* **2015,** *360*, 130-137.

15. Gwak, G.; Jung, B.; Han, S.; Hong, S., Evaluation of poly (aspartic acid sodium salt) as a draw solute for forward osmosis. *Water Research* **2015,** *80*, 294-305.

16. Brazel, C. S.; Rosen, S. L., *Fundamental Principles of Polymeric Materials*. Wiley: 2012.

17. Hansen, C. M., *Hansen Solubility Parameters: A User's Handbook, Second Edition*. CRC Press: 2007.

18. Li, D.; Zhang, X.; Yao, J.; Simon, G. P.; Wang, H., Stimuli-responsive polymer hydrogels as a new class of draw agent for forward osmosis desalination. *Chemical Communications* **2011,** *47*, (6), 1710-1712.

19. Li, D.; Zhang, X.; Yao, J.; Zeng, Y.; Simon, G. P.; Wang, H., Composite polymer hydrogels as draw agents in forward osmosis and solar dewatering. *Soft Matter* **2011,** *7*, (21), 10048-10056.

20. Cai, Y.; Shen, W.; Loo, S. L.; Krantz, W. B.; Wang, R.; Fane, A. G.; Hu, X., Towards temperature driven forward osmosis desalination using Semi-IPN hydrogels as reversible draw agents. *Water Research* **2013,** *47*, (11), 3773-3781.

21. Razmjou, A.; Simon, G. P.; Wang, H. T., Effect of particle size on the performance of forward osmosis desalination by stimuli-responsive polymer hydrogels as a draw agent. *Chemical Engineering Journal* **2013,** *215*, 913-920.

22. Razmjou, A.; Barati, M. R.; Simon, G. P.; Suzuki, K.; Wang, H., Fast Deswelling of Nanocomposite Polymer Hydrogels via Magnetic Field-Induced Heating for Emerging FO Desalination. *Environmental Science & Technology* **2013,** *47*, (12), 6297-6305.

23. Lyon, L. A.; Serpe, M. J., *Hydrogel Micro and Nanoparticles*. Wiley: 2012.

24. Zhang, X.-Z.; Yang, Y.-Y.; Chung, T.-S., The Influence of Cold Treatment on Properties of Temperature-Sensitive Poly(N-isopropylacrylamide) Hydrogels. *Journal of Colloid and Interface Science* **2002,** *246*, (1), 105-111.

25. Zeng, Y.; Qiu, L.; Wang, K.; Yao, J.; Li, D.; Simon, G. P.; Wang, R.; Wang, H., Significantly enhanced water flux in forward osmosis desalination with polymer-graphene composite hydrogels as a draw agent. *Rsc Advances* **2013,** *3*, (3), 887-894.

26. Razmjou, A.; Liu, Q.; Simon, G. P.; Wang, H., Bifunctional Polymer Hydrogel Layers As Forward Osmosis Draw Agents for Continuous Production of Fresh Water Using Solar Energy. *Environmental Science & Technology* **2013,** *47*, (22), 13160-13166.

27. Hartanto, Y.; Yun, S.; Jin, B.; Dai, S., Functionalized thermo-responsive microgels for high performance forward osmosis desalination. *Water Research* **2015,** *70*, 385-393.

28. Ramírez-Jiménez, A.; Alvarez-Lorenzo, C.; Concheiro, A.; Bucio, E., Radiation-grafting of 2-hydroxyethylmethacrylate and oligo (ethylene glycol) methyl ether methacrylate onto polypropylene films by one step method. *Radiation Physics and Chemistry* **2012,** *81*, (1), 27-32.

29. Zhang, X.; Zhou, L.; Zhang, X.; Dai, H., Synthesis and solution properties of temperature-sensitive copolymers based on NIPAM. *Journal of Applied Polymer Science* **2010,** *116*, (2), 1099-1105.

30. Zhang, J.; Pelton, R., The surface tension of aqueous poly(N-isopropylacrylamide-co-acrylamide). *Journal of Polymer Science Part A: Polymer Chemistry* **1999,** *37*, (13), 2137-2143.

31. Wang, Q.; Zhao, Y.; Xu, H.; Yang, X.; Yang, Y., Thermosensitive phase transition kinetics of poly(N-isopropylacryl amide-co-acrylamide) microgel aqueous dispersions. *Journal of Applied Polymer Science* **2009,** *113*, (1), 321-326.

32. Yildiz, B.; Işik, B.; Kiş, M., Thermoresponsive poly(N-isopropylacrylamide-co-acrylamide-co-2-hydroxyethyl methacrylate) hydrogels. *Reactive and Functional Polymers* **2002,** *52*, (1), 3-10.

33. Yıldız, B.; Işık, B.; Kış, M., Synthesis and characterization of thermoresponsive isopropylacrylamide–acrylamide hydrogels. *European Polymer Journal* **2002,** *38*, (7), 1343-1347.

34. Cai, Y.; Wang, R.; Krantz, W. B.; Fane, A. G.; Hu, X. M., Exploration of using thermally responsive polyionic liquid hydrogels as draw agents in forward osmosis. *RSC Advances* **2015,** *5*, (118), 97143-97150.

35. Brandrup, J.; Immergut, E. H.; Grulke, E. A., *Polymer Handbook*. Wiley: 1999.

36. Gu, M.; Kilduff, J. E.; Belfort, G., High throughput atmospheric pressure plasma-induced graft polymerization for identifying protein-resistant surfaces. *Biomaterials* **2012,** *33*, (5), 1261-1270.

37. Leung, M. H. M.; Harada, T.; Dai, S.; Kee, T. W., Nanoprecipitation and Spectroscopic Characterization of Curcumin-Encapsulated Polyester Nanoparticles. *Langmuir* **2015,** *31*, (42), 11419-11427.

38. Ravindra, R.; Krovvidi, K. R.; Khan, A. A., Solubility parameter of chitin and chitosan. *Carbohydrate Polymers* **1998,** *36*, (2–3), 121-127.

39. Van Krevelen, D. W.; Te Nijenhuis, K., Chapter 7 - Cohesive Properties and Solubility. In *Properties of Polymers (Fourth Edition)*, by, D. W. V. K.; Nijenhuis, K. T., Eds. Elsevier: Amsterdam, 2009; pp 189-227.

40. Liu, H. Y.; Zhu, X. X., Lower critical solution temperatures of N-substituted acrylamide copolymers in aqueous solutions. *Polymer* **1999,** *40*, (25), 6985-6990.

41. Nichifor, M.; Zhu, X. X., Copolymers of N-alkylacrylamides and styrene as new thermosensitive materials. *Polymer* **2003,** *44*, (10), 3053-3060.

6.8 Supporting Information

Table 6.4 Synthesis and characterization of non-ionic thermoresponsive copolymer microgels

Nomenclature	Monomer Content in Feed (g)		MBA (g)	KPS (g)	VPTT* (ºC)
	NIPAM	Co-monomers			
NP	3.0	-	0.03	0.03	32.5
NP99-AM1	2.97	0.03	0.03	0.03	33
NP98-AM2	2.94	0.06	0.03	0.03	34
NP95-AM5	2.85	0.15	0.03	0.03	34
NP90-AM10	2.7	0.3	0.03	0.03	36
NP95-HM5	2.85	0.15	0.03	0.03	30
NP95-PEGA5	2.85	0.15	0.03	0.03	28

*Determined from the tangent line of the inflexion point of the hydrodynamic diameter *vs.* temperature curves

Table 6.5 Summary of initial water flux, water recovery and apparent water flux for various non-ionic thermoresponsive copolymer microgels

Microgels	Initial Water Flux (LMH)	Water Recovery (%)	Apparent Water Flux (LMH)
NP	5.1	83.3	0.8
NP99-AM1	7.4	84.8	3.7
NP98-AM2	19	85.5	4.7
NP95-AM5	24.7	78.7	6.1
NP90-AM10	30.7	55.0	3.5
NP95-HM5	7.8	88.9	2.5
NP95-PEGA5	6.4	89.1	2.9

6.8.1 Hansen solubility parameter using Hoftyzer – Van Krevelen method based on group contribution analysis

The solubility distance parameters in Hansen solubility sphere, relative energy difference (RED) and ratio of cohesion energy densities (H), can be calculated using the following equations:

$$(Ra)^2 = 4(\delta_{d2} - \delta_{d1})^2 + \left(\delta_{p2} - \delta_{p1}\right)^2 + (\delta_{h2} - \delta_{h1})^2 \quad \text{Eq. 6.12}$$

$$RED = \frac{Ra}{Ro} \quad \text{Eq. 6.13}$$

$$H = \frac{RA}{R_M} \quad \text{Eq. 6.14}$$

6.8.1.1 N-Isopropylacrylamide

Density: 1.1 g/cm^3

Molecular weight: 113.2

Table 6.6 Solubility parameter component from group contributions analysis for poly (N-isopropylacrylamide)

Group	Amount	F_{di} $(MJ/m^3)^{1/2}.mol^{-1}$	F_{pi}^2 $(MJ/m^3).mol^{-2}$	E_{hi} $J.mol^{-1}$
-CH_3	2	840	0	0
-CH_2-	1	270	0	0
>CH-	2	160	0	0
-CO-	1	290	592,900	2,000
-NH-	1	160	44,100	3,100
Σ		1,720	637,000	5,100

6.8.1.2 Acrylamide

Density: 1.13 g/cm^3

Molecular weight: 71.1

Table 6.7 Solubility parameter component from group contributions analysis for polyacrylamide

Group	Amount	F_{di} $(MJ/m^3)^{1/2}.mol^{-1}$	F_{pi}^2 $(MJ/m^3).mol^{-2}$	E_{hi} $J.mol^{-1}$
$-CH_2-$	1	270	0	0
>CH-	1	80	0	0
-CO-	1	290	592,900	2,000
$-NH_2$	1	280	0	8,400
Σ		920	592,900	10,400

6.8.1.3 2-hydroxyethyl methacrylate

Density: 1.073 g/cm^3

Molecular weight: 130.1

Table 6.8 Solubility parameter component from group contributions analysis for poly (2-hydroxyethyl methacrylate)

Group	Amount	F_{di} $(MJ/m^3)^{1/2}.mol^{-1}$	F_{pi}^2 $(MJ/m^3).mol^{-2}$	E_{hi} $J.mol^{-1}$
$-CH_3$	1	420	0	0
$-CH_2-$	3	810	0	0
>C<	1	-70	0	0
-COO-	1	390	240,100	7,000
-OH	1	210	250,000	20,000
Σ		1,760	490,100	27,000

6.8.1.4 Poly (ethylene glycol) methyl ether acrylate

Density: 1.09 g/cm^3

Molecular weight: 480

Table 6.9 Solubility parameter component from group contributions analysis for poly (ethylene glycol) methyl ether acrylate

Group	Amount	F_{di} $(MJ/m^3)^{1/2}.mol^{-1}$	F_{pi}^2 $(MJ/m^3).mol^{-2}$	E_{hi} $J.mol^{-1}$
$-CH_3$	1	420	0	0
$-CH_2-$	19	5,130	0	0
>CH-	1	80	0	0
-COO-	1	390	240,100	7,000
=C<	1	70	0	0
-O-	9	900	1,440,000	27,000
Σ		6,990	1,680,100	34,000

Chapter 7. Conclusions and Future Research Directions

7.1 Summary

The overall objective of this thesis is to advance the development of microgel-based FO draw agent by investigating the effect of different thermoresponsive copolymer microgels as FO draw agents on the water flux and water recovery performance of microgel-driven FO desalination process. The thesis focuses on N-isopropylacrylamide-based microgels copolymerized with different comonomer materials.

Chapter 2 summarizes recent development of various synthetic materials as draw agents for FO desalination process. This chapter also highlights polymer-based materials might become a good candidate for high performance FO draw agents due to the high osmotic pressure that can be generated by these materials. Literature review in applying thermoresponsive hydrogels as FO draw agents is presented and it indicates further work to improve the performance of these hydrogels is needed. Furthermore, brief thermodynamic of polymer dissolution is presented that explains the reason of lower energy consumption during water recovery process when polymers are used as FO draw agents.

Based on the literature survey in Chapter 2, we propose thermoresponsive microgels as FO draw agents in Chapter 3. Water flux up to 23.8 LMH and water recovery up to 55 % can be achieved depending on the concentration of acrylic acid in the microgels. The large improvement of water flux and water recovery can be

related to the large surface area of the microgels which enhances the contact between microgel particles and membrane surfaces.

From the previous chapter, we find that adding a weak acidic comonomer such as acrylic acid largely improved the water flux performance during water drawing process. As a result, further investigation on the effect of different acidic comonomers is presented in Chapter 4. We find that copolymer microgel with itaconic acid as a comonomer has the best overall performance among other acidic copolymer microgels. The water flux and water recovery of this copolymer microgel are 44.8 LMH and 47.2%, respectively. In addition, the apparent water flux of this microgel is 3.1 LMH.

In Chapter 5, we further our work by investigating the effect of different cationic copolymer microgels on the water flux and water recovery performance in FO process. The copolymer microgel with 2-diethylamino ethyl methacrylate as a comonomer has the best performance among other cationic copolymer microgels. The microgel also shows improved performance compared with previously synthesized acidic microgels. The water flux and water recovery of this microgel are 45.6 LMH and 44.8 %, respectively. The apparent flux is 5.5 LMH with faster equilibrium swelling time (30 minutes) than acidic copolymer microgels. In addition, the analysis of Hansen solubility parameters is introduced to predict the solvation behaviors of the cationic comonomers which have large impact on the performance of cationic copolymer microgels as FO draw agent.

In Chapter 6, we make further improvement on the water recovery performance by copolymerizing N-isopropylacrylamide with different non-ionic comonomers. The copolymer microgel of N-isopropylacrylamide and acrylamide has the best

performance among other non-ionic copolymer microgels. The water flux and water recovery of this microgel are 24.7 LMH and 78.7 %, respectively while the apparent flux is 6.1 LMH.

In summary, the performance of thermoresponsive copolymer microgel as FO draw agent largely depends on the solvation degree and the dissociation constants (pK_a) of the comonomer materials. Suitable amount of comonomer must be incorporated to achieve balanced performance in water flux and water recovery which will lead to optimum overall performance of microgel-driven FO desalination. Table 7.1 summarizes the best performance of synthesized thermoreponsive copolymer microgels presented in this thesis.

Table 7.1 Summary of the FO performance of thermoresponsive copolymer microgels

Copolymer microgels	Water flux (LMH)	Water recovery (%)	Apparent flux (LMH)
Anionic (MCG-NP-IA)	44.8	47.2	3.1
Cationic (MCG-NP-DEAEMA)	45.6	44.8	5.5
Non-ionic (MCG-NP-AAm)	24.7	78.7	6.1

7.2 Future directions

Although the work presented in this thesis has significantly advanced the performance of thermoresponsive microgel-based FO draw agents for desalination application in laboratory scale, the work summarized in the following section can be carried out in the future to further improved the performance of water drawing and

releasing capabilities of the copolymer microgels and to make this technology practical in industrial setting:

1. Different monomers showing thermoresponsive properties can be used instead of N-isopropylacrylamide to improve the swelling ratio of the microgel which will lead to better overall performance.
2. Ternary copolymer microgels involving thermoresponsive moiety, ionic comonomers and non-ionic comonomer can be used to further improve the hydrophilic – hydrophobic balance which will also lead to better overall performance.
3. Further experimental work on the effect of salt concentration, microgel loading, operational temperature, membrane orientation, pH of the feed solution can be done to optimize the process conditions. The results can be fed back to the material design which will lead to optimized performance of microgel-driven FO desalination system.
4. The process design of this thermoresponsive microgel-driven FO desalination system which allows the process to be operated in continuous manner should be further researched to make the system practical in industrial setting.

List of Publications and Conferences

1. **Hartanto, Y.**, Yun, S., Jin, B., Dai, S. "Functionalized thermo-responsive microgels for high performance forward osmosis desalination", *Water Res.*, ***2015**, 70, pp 385-393*.
2. **Hartanto, Y.**, Zargar, M., Wang, H., Jin, B., Dai, S. "Thermoresponsive Acidic Microgels as Functional Draw Agents for Forward Osmosis Desalination", *Environ. Sci. Technol.*, ***2016**, 50 (8), pp 4221–4228*.
3. **Hartanto, Y.**, Zargar, M., Jin, B., Dai, S. "Thermoresponsive Cationic Copolymer Microgels as High Performance Draw Agents in Forward Osmosis Desalination", *In Revision for Journal of Membrane Science*.
4. **Hartanto, Y.**, Zargar, M., Jin, B., Dai, S. "Non-ionic Thermoresponsive Copolymer Microgels as Draw Agents for Enhanced Water Recovery in Forward Osmosis Desalination", *In Preparation*.
5. **Hartanto, Y.**, Jin, B., Dai, S. "Emerging Draw Solute Materials in Forward Osmosis Desalination: Recent Development and Challenge", *In Preparation*.
6. **Hartanto, Y.**, Jin, B., Dai, S. "Thermo-responsive microgel as draw agent for forward osmosis brackish water desalination", *2nd International Conference on Desalination using Membrane Technology*, Singapore, 2015. (Oral Presentation)
7. **Hartanto, Y.**, Jin, B., Dai, S. "Thermo-responsive microgels with novel functional co-monomer for enhanced water recovery process in forward

osmosis desalination", *2nd International Conference on Desalination using Membrane Technology*, Singapore, 2015. (Poster Presentation)

8. Zargar, M., **Hartanto, Y.**, Jin, B., Dai, S. "Thin Film Nanocomposite Membranes: Which Medium to Choose for Nanoparticle Integration", *The 12th International Conference on Membrane Science and Technology (MST 2015)*, Tehran (Iran), 2015.